UNIVERSITÀ DEGLI STUDI DI TRIESTE

XXVIII CICLO DEL DOTTORATO DI RICERCA IN BIOMEDICINA MOLECOLARE

OCT4 promotes high-grade serous ovarian cancer aggressiveness through pRB inactivation and enhancement of genomic stability

Settore scientifico disciplinare **BIO/13**

DOTTORANDO

ELISA COMISSO

COORDINATORE

PROF. GUIDALBERTO MANFIOLETTI

SUPERVISORE DI TESI

DR. ROBERTA BENETTI

ANNO ACCADEMICO 2014/2015

UNIVERSITÀ DEGLI STUDI DI TRIESTE

XXVIII CICLO DEL DOTTORATO DI RICERCA IN BIOMEDICINA MOLECOLARE

OCT4 promotes high-grade serous ovarian cancer aggressiveness through pRB inactivation and enhancement of genomic stability

Settore scientifico disciplinare **BIO/13**

DOTTORANDO

ELISA COMISSO

COORDINATORE

PROF. GUIDALBERTO MANFIOLETTI

SUPERVISORE DI TESI

DR. ROBERTA BENETTI

ANNO ACCADEMICO 2014/2015

To my family...

ABSTRACT

OCT4 (*POU5F1*) is a member of the POU family of transcription factors and is known to play a crucial role in the maintenance of self-renewal and pluripotency in Embryonic Stem Cells (ESCs). Nowadays, several studies highlight the importance of OCT4 expression in tumors in order to maintain the tumorigenic stem cell-like features. Despite the essential role of OCT4 during embryogenesis and reprogramming of somatic cells, its exact role in tumorigenesis is still not well defined. In this thesis we found that OCT4 drives the expression of Nuclear Inhibitor of Protein Phosphatase type 1 (NIPP1) and Cyclin F (CCNF) that together inhibit Protein Phosphatase 1 (PP1) in High-Grade Serous Ovarian Cancer (HG-SOC). This causes pRB hyper-phosphorylation, accelerated cell proliferation and increased *in vitro* tumorigenicity of ovarian cancer cells. In parallel, OCT4 and NIPP1/CCNF drive the expression of the central Chromosomal Passenger Complex (CPC) components, Borealin, Survivin and the mitotic kinase Aurora B, that are essential for the maintenance of genomic stability. CPC, in fact, promoting the "centrosomes clustering mechanism" and the correction of microtubule-kinetochore attachments errors, leads to increased mitotic stability. Loss of *OCT4* or *NIPP1/CCNF* results in severe mitotic defects, multipolar spindles and supernumerary centrosomes, finally leading to the induction of senescence and apoptosis. Importantly, activation of these parallel pathways leads to a dramatically reduced overall survival of HG-SOC patients. In conclusion we demonstrate that OCT4 increases HG-SOC aggressiveness through two parallel pathways: inactivation of the Retinoblastoma tumorsuppressor pathway and enhancement of mitotic fidelity in cancer cells, highlighting an unknown role of OCT4 as central regulator of genomic stability and pRB tumorsuppressor pathway activity. Thus, targeting the OCT4-NIPP1/CCNF-PP1-pRB pathway could be a promising strategy to manage and treat specifically an aggressive subpopulation of HG-SOC.

TABLE OF CONTENTS

1. INTRODUCTION 1
1.1 Ovarian cancer 1
1.1.1 Ovarian cancer incidence in Europe 1
1.1.2 Histopathology classification 2
1.1.3 The origin and pathogenesis of Epithelial Ovarian Cancer 3
1.1.4 High-grade serous carcinomas (HG-SOC) 4
1.1.5 Symptoms and diagnosis 6
1.1.6 Treatments 7
1.1.7 Recurrent disease 9
1.1.8 Metastasis and ovarian "cancer stem cell hypothesis" 9
1.2 OCT4 (octamer-binding transcription factor 4) 12
1.2.1 OCT4 in tumor progression and chemoresistance 14
1.2.2 OCT4 and ovarian cancer 15
1.2.3 OCT4 based therapy 17
1.3 Retinoblastoma protein (pRB) 19
1.3.1 Cell cycle regulation 20
1.3.2 Post-translational modification 22
1.3.3 Senescence and apoptosis 23
1.3.4 Genomic stability regulation 23
1.3.5 Tumor suppressive functions 26
1.4 Protein Phosphatase 1 (PP1) 28
1.4.1 pRB regulation through PP1 29
1.4.1.1 Nuclear Inhibitor of PP1 (NIPP1) 29
1.4.1.2 Cyclin F (CCNF) 30
1.4.2 OCT4-pRB axis in mouse Embryonic Stem Cells (mESCs) 30
1.5 Genomic stability in tumors 32
1.5.1 Centrosome amplification 32
1.5.1.1 Centrosome clustering mechanism 35

1.5.2 Chromosomal Passenger Complex (CPC) 38
1.5.2.1 CPC functions in kinetochore-microtubule attachments 40
1.5.2.2 CPC and centrosome clustering mechanism 43
1.5.2.3 CPC and cancer 44
2. AIM OF THE THESIS 45
3. RESULTS 47
3.1 The OCT4-NIPP1/CCNF-PP1 axis mediates pRB hyper-phosphorylation and poor survival in High-Grade Serous Ovarian Cancer (HG-SOC) 47
3.2 The OCT4-NIPP1/CCNF-PP1-pRB axis promotes cell proliferation and tumorigenic potential 53
3.3 The OCT4-NIPP1/CCNF-PP1-pRB axis promotes mitotic progression 60
3.4 The OCT4-NIPP1/CCNF-PP1 axis ensures mitotic fidelity by driving the expression of Chromosomal Passenger Complex (CPC) 64
3.5 OCT4-CCNF/NIPP1-PP1 axis is essential to ensure CPC function 70
3.6 OCT4-CCNF/NIPP1-PP1-pRB axis correlates with CPC activation and poor prognosis in HG-SOC patients 78
3.7 Final model 83
4. CONCLUSIONS AND DISCUSSION 85
5. MATERIALS AND METHODS 90
6. REFERENCES 100

1. INTRODUCTION

1.1 Ovarian cancer

1.1.1 Ovarian cancer incidence in Europe

Ovarian cancer is the 5th most frequent cancer in Europe for females and the 13th most common cancer overall, with about 65600 new cases diagnosed and 42000 new deaths in 2012 **(Fig. 1.1)** (Ferlay J. et al., 2013).

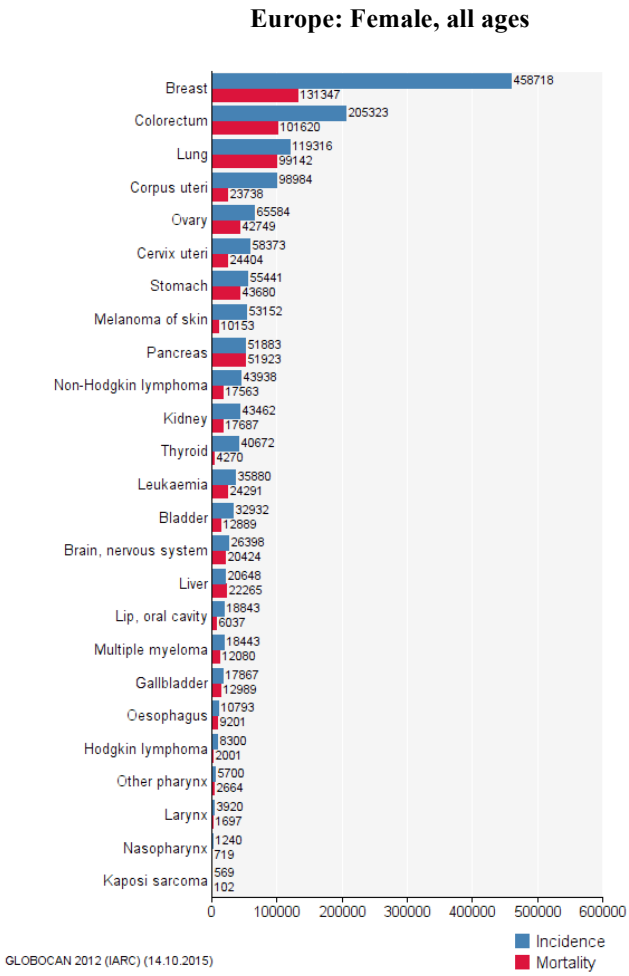

Figure 1.1. Incidence and mortality of European females at all ages (available from: http://globocan.iarc.fr, accessed October 2015).

The reasons for this high death rate are the absence of specific signs and symptoms in most cases, the lack of specific screening techniques and the extremely metastatic nature of the disease. This means that most women were diagnosed with an advanced metastatic stage of the disease. Two thirds of ovarian cancer cases are diagnosed in women after the age of 55 years old. In addition, the presence of breast or ovarian cancer in a first-degree relative triples the risk. The risk is increased among carriers of a *BRCA* gene mutation. For *BRCA1* mutation the lifetime risk is between 39 to 46% and for *BRCA2* mutation the risk is around 12 to 20%. Women who have used oral contraceptives, have been pregnant or have breastfed, are associated with a decreased risk of ovarian cancer onset (Clarke-Pearson D. L., 2009). Due to modern management a large number of women reach a complete remission. However, most of those with an advanced disease will develop chemoresistant recurrence within 18 months. Chemoresistance and metastases are the main problems to overcome in the management of ovarian cancer.

1.1.2 Histopathology classification

The World Health Organization (WHO) classified ovarian neoplasms according to the most probable tissue of origin. Three main types were classified as surface epithelial, germ cell and sex cord-stromal (Chen V. W. et al., 2003). Almost 10 years ago a new classification was proposed that separated epithelial ovarian cancers, the most frequent types, into type I and II tumors (Shih I. M. et al., 2004). Type I tumors are composed of low-grade serous ovarian carcinoma (LG-SOC), low-grade endometrioid, clear cell, mucinous and transitional (Brenner) carcinomas **(Fig. 1.2)**. These tumors develop slowly and are confined to the ovary. They lack mutations of TP53 and exhibit a share lineage with the corresponding benign cystic neoplasm, often through an intermediate (borderline tumor) step, supporting the tumor progression model. In contrast, type II tumors, are highly aggressive, evolve rapidly and almost always are present in advanced stages. Typically, they have spread the ovary at the time of diagnosis. Type II tumors are composed by high-grade serous ovarian carcinoma (HG-SOC), undifferentiated carcinoma and malignant mixed mesodermal tumors (carcinosarcoma) **(Fig. 1.2)**. They

display TP53 mutations in over 80% of cases and rarely harbour the mutations that are found in the type I tumors (Kurman R. J. and Shih I.-M., 2010). Currently based on immunohistochemistry, histopathology and molecular genetic analysis, epithelial ovarian carcinomas are classified in: HG-SOC (70%), endometrioid carcinomas (EC, 10%), clear-cell carcinomas (CCC, 10%), mucinous carcinomas (MC, 3%) and LG-SOC (< 5%) (Prat J., 2012).

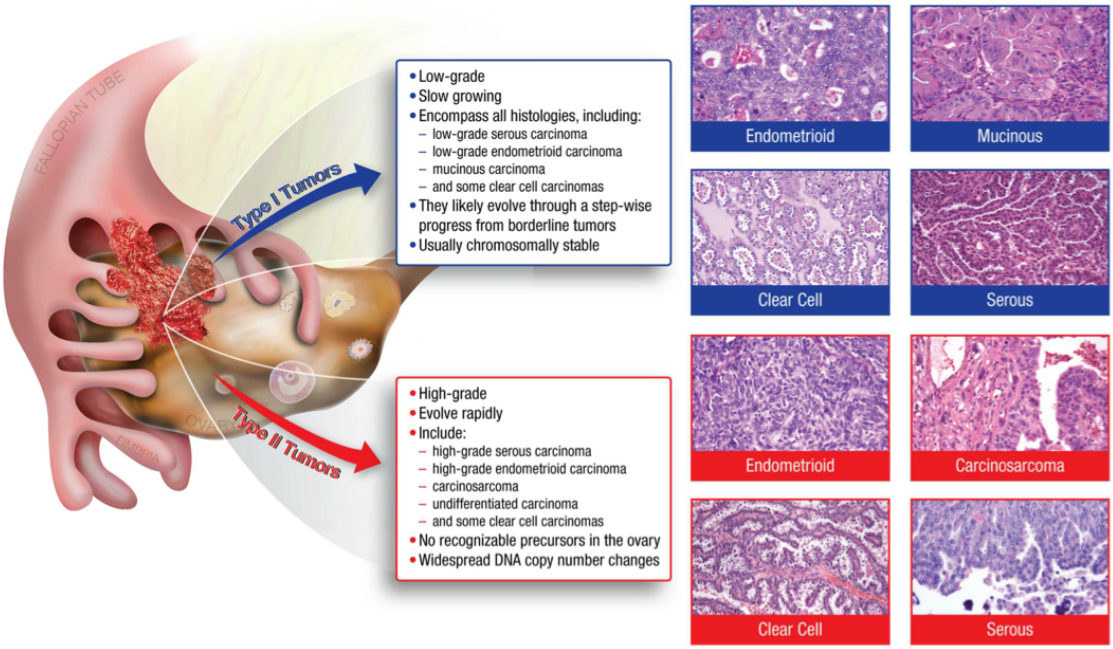

Figure 1.2. Histologic subtypes of ovarian cancer. Type I tumors are low-grade and are characterized by slow proliferation that typically arise from well-recognized precursors lesions (borderline tumors). These tumors develop from the ovarian surface epithelium, inclusion cysts or endometriosis. In contrast, Type II tumors are high-grade and characterized by a rapid proliferation (Jones P. M. and Drapkin R., 2013).

1.1.3 The origin and pathogenesis of Epithelial Ovarian Cancer

Epithelial ovarian cancer (EOC) is the most frequent type of cancer (90%) (Ledermann J. A. et al., 2013). The origin and pathogenesis of epithelial ovarian cancer have puzzled researchers for decades. Therefore, the cell of origin of ovarian cancer has been long debated. Currently there are three main views of ovarian carcinogenesis. The traditional view has been that the tumors are all derived from the ovarian surface epithelium (mesothelium), and that subsequent metaplastic changes lead to the development of different cell types (serous, endometrioid, clear cell, mucinous and transitional cell – Brenner). However, normal ovary does not contain these types of cells. For this reason,

the second theory proposes that tumors with a müllerian phenotype (serous, endometrioid and clear cell) are derived from müllerian-type tissue and not from mesothelium. These tissues give rise to cysts in paratubal and paraovarian locations (considered a "secondary müllerian system") and, according to this theory, ovarian tumors will develop from these cysts. When the tumor expands and destroys ovarian tissue it seems to have arisen in the ovary. The limitations of the first two theories regard the fact that mesothelium bears no resemblance to serous, endometrioid, mucinous, clear cell or transitional (Brenner) carcinomas and that precursor lesions resembling these carcinomas have rarely been reported in paratubal and paraovarian cysts. For these reasons, recently, a new theory argues that ovarian carcinomas arise from high-grade "serous tubal intraepithelial carcinomas" (STICs) in the fallopian tube, which then spread to the ovary. Currently, the most persuasive evidence suggests that the vast majority of what seems to be primary ovarian cancers derives from the fallopian tube and endometrium, thus not directly from the ovary (Kurman R. J. and Shih I.-M., 2010). Several studies confirmed that *in situ* early invasive tubal carcinomas occurred in women with a genetic predisposition for the development of ovarian cancer (Callahan M. J. et al., 2007; Carcangiu M. L. et al., 2004; Shaw P. A. et al., 2009). Is it possible that ovarian carcinomas might develop as a result of implantation of malignant cells from the tubal carcinoma to the ovary (Vang R. et al., 2013).

1.1.4 High-grade serous carcinomas (HG-SOC)

High-grade serous carcinomas (HG-SOC) are the most common ovarian cancer. The majority of patients were diagnosed with an advance stage of the disease (about 80%) and tumors confined to the ovary at diagnosis are uncommon (< 10%) (Prat J., 2012). The observation that high-grade carcinomas showed mucosal tubal involvement including "serous tubal intraepithelial carcinoma" (STIC) (Kindelberger D. W., 2007), gave strong support to the proposal that STICs may be the cause of ovarian high-grade serous carcinoma (Kurman R. J. and Shih I.-M., 2010). Depending on whether there is a mutation of KRAS/BRAF/ERBB2 or TP53, a low or high-grade serous carcinoma develops **(Fig. 1.3)**.

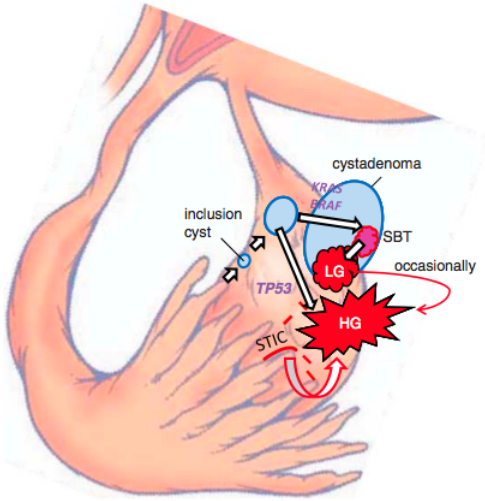

Figure 1.3. Proposed mechanisms for the development of low-grade and high-grade serous carcinoma. 1) Normal tubal epithelium could implant on the ovary to form an inclusion cyst. According to the specific mutation, a low or high-grade serous carcinoma develops. Low-grade serous carcinoma often develops from serous borderline tumor, which arises from serous cystadenoma. 2) Malignant cells that spread from serous tubal intraepithelial carcinoma (STIC) could implant on the ovarian surface resulting in the development of high-grade serous carcinoma (Kurman R. J. and Shih I.-M., 2010).

From a molecular point of view almost 100% of HG-SOC harbour a TP53 mutation (Ahmed A. A. et al., 2010). Integrated genomic analysis of ovarian cancer in several hundred tumors, further identifies somatic mutations in NF1, BRCA1, BRCA2 and CDK12. Importantly, homologous recombination repair of DNA damage is defective in 50% of HG-SOC and NOTCH and FOXM1 signalling are implicated in the pathophysiology of serous tumors **(Fig 1.4)** (Bell D. et al., 2011).

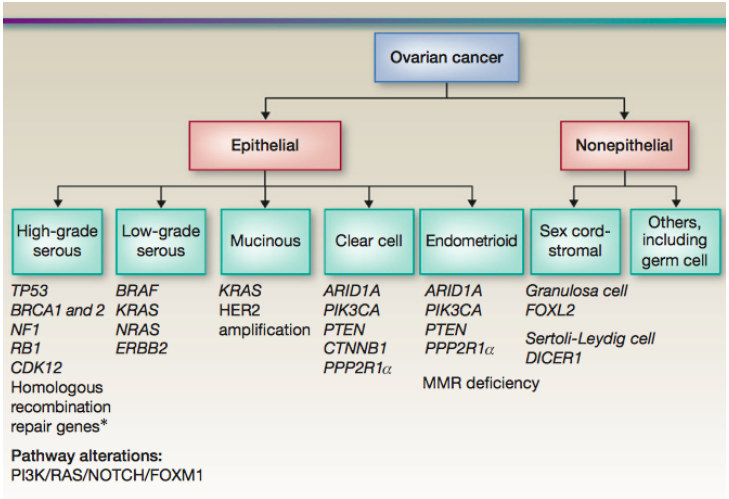

Figure 1.4. Mutations and molecular alterations of epithelial ovarian carcinoma subtypes (Banerjee S. and Kaye S. B., 2013).

It is important to note that 67% of HG-SOC display altered signalling pathway of pRB due to amplification or upregulation of cyclins and CDKs, that lead to its enzymatically inactivation, whereas only 2% specimens carry mutations to *RB1* gene **(Fig. 1.5)** (Bell D. et al., 2011).

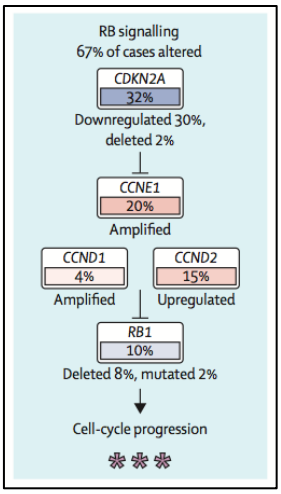

Figure 1.5. pRB altered pathway in high-grade serous ovarian cancer (Jayson G. C. et al., 2014).

1.1.5 Symptoms and diagnosis

Early detection is the key to the treatment of ovarian cancer. However, patients frequently are diagnosed in a late stage. In fact, ovarian cancer has often been called the "silent killer" because its symptoms are predominantly present in advanced stages when chance of cure is poor. However, a prospective case-control study found that 95% of women with ovarian cancer reported symptoms prior to diagnosis, with the most common are abdominal (77%), gastrointestinal tract (70%), pain (58%), constitutional (50%), urinary (34%) and pelvic (26%) (Goff B. A. et al., 2004), indicating they are not necessarily gynaecological in nature. The UK National Institute for Health and Clinical Excellence (NICE) has recommended that patients, especially those older than 50 years old, who develop symptoms like irritable bowel syndrome should undergo measurement

of serum cancer antigen 125 (CA-125) concentration as a second screening. Of notice, it remains unclear whether ovarian cancer screening reduces mortality. Thus, routine screening of the general population for ovarian cancer is not recommended (Clarke-Pearson D. L., 2009). For women in whom fertility is no longer an issue, risk-reducing salpingo-oophorectomy is the most useful strategy. Younger women can decide for annual screening by pelvic ultrasound, although in a recent trial screening for CA-125 and transvaginal ultrasound compared with usual care did not reduce ovarian cancer mortality. In addition, diagnostic evaluation following a false-positive screening test was associated with complications (Buys S. S. et al., 2011).

1.1.6 Treatments

Treatment of ovarian cancer combines surgical cytoreduction of the tumor mass with cytotoxic chemotherapy. The main purposes of surgery are to provide a histopathological diagnosis, to remove the bulk of the tumor and to establish the FIGO stage (International Federation of Gynecology and Obstetrics staging systems). Surgery includes a total hysterectomy, bilateral salpingo-oophorectomy, debulking and omentectomy. Importantly, retrospective randomized studies suggest that minimum residual disease after surgery is associated with longer survival (du Bois A. et al., 2009). When surgical debulking is not feasible at diagnosis neoadjuvant (preoperative) chemotherapy is widely accepted. In this case, debulking surgery is performed after three of the six cycles of chemotherapy (Jayson G. C. et al., 2014). For advanced stage disease drugs containing platinum have been the standard of care for almost 40 years. A study published in 1996 found that incorporation of paclitaxel into first-line therapy improves the duration of progression-free survival (PFS) and overall survival (OS) in women with incompletely resected stage III and IV ovarian cancer (McGuire W. P. et al., 1996). Currently, three-weekly cycles of the less toxic carboplatin is given in combination with paclitaxel or docetaxel (Vasey P. A. et al., 2004). Attempts to improve the efficacy of the treatment adding a third cytotoxic compound were not successful. Thus, the standard of care for the past 20 years has remained carboplatin and paclitaxel. Recent positive randomized trials are becoming an option for first-line chemotherapy of advance ovarian cancer **(Fig. 1.6).** The anti-endothelial growth factor (VEGF) antibodies improve the PFS (Burger et al., 2011; Perren et al., 2011;

Aghajanian et al., 2012; Pujade-Lauraine et al., 2012) as well as a Japanese study, which showed that fractionating paclitaxel into a dose-dense weekly schedule, improves significantly the PFS and OS (Katsumata N. et al., 2009).

	Findings
Armstrong,2006[54]	Intraperitoneal chemotherapy improves PFS and OS but is toxic
Katsumata, (JGOG) 2009[55]	Dose dense paclitaxel improves PFS and OS incurred from first line therapy in Japanese patients; confirmatory trials in USA and Europe are in progress
Burger, 2011,[56] and Perren, 2011[57]	Anti-VEGF antibody-containing regimens improve PFS in the first-line treatment setting
Aghajanian, 2012,[58] and Pujade-Lauraine, 2012[59]	Anti-VEGF antibody-containing regimens improve PFS in the platinum sensitive and resistant setting
Ledermann, 2012[60]	PARP inhibitors improve PFS in high-grade serous ovarian cancer

PFS= progression-free survival. OS=overall survival. PARP=poly (ADP-ribose) polymerase.

Figure 1.6. Key recent positive phase 3 clinical-trials (Jayson G. et al., 2014).

Another trial, in which chemotherapy was intraperitoneal delivered, showed significantly improved survival but the general uptake was poor and cause neurological and gastrointestinal toxic effects (Armstrong D. et al., 2006).

Ovarian cancer that harbour *BRCA1* and *2* mutations often show an increased chemosensitivity to platinum and other DNA damaging agents corresponding with a longer survival compared to women with sporadic ovarian cancer. The mechanism depends on the crucial role of BRCA proteins in homologous recombination. In fact, in patients with homologous recombination deficiency, there is an increase dependence on the poly (ADP-ribose) polymerase (PARP) single-strand repair pathway. For this reason PARP inhibitors induce significant tumor lethality, because cells are no more able to repair spontaneously DNA damage. Clinical benefits in terms of PFS have been seen with olaparib, a PARP inhibitor, when used as maintenance therapy after platinum-based treatment with few toxic effects even after prolonged administration (Ledermann J. et al., 2012).

1.1.7 Recurrent disease

Today, all Epithelial Ovarian Cancers (EOCs) are treated with the same approach of debulking surgery and chemotherapy, carboplatin and paclitaxel, for six cycles. The outcome is approximately the same and depends on the quality of the debulking and the responsiveness to platinum. Despite an 80% of patients respond to therapy, less than 20% of women will be cured, and most will eventually recur. Currently, patients with recurrent disease are usually incurable (Verschraegen C. et al., 2015). In addition, there are increasing body of evidences that current combined surgical-chemotherapy approaches have reached a plateau of efficacy. The median progression free survival (PSF) of advanced ovarian cancer is about 18 month. However, after first-line chemotherapy (that lasts 4-5 months) the patient develops a recurrent platinum-sensitive disease (platinum-free interval of 6-12 months) (Jayson G. C. et al., 2014). This recurrence disease is best treated with a combination of platinum-containing drugs such as carboplatin with paclitaxel, gemcitabine or pegylated liposomal doxorubicin (Parmar M. K. et al., 2003; González-Martín A. J. et al., 2005; Pfisterer J. et al., 2006; Pujade-Lauraine E. et al., 2010). Nevertheless, as a rule, the intervals between recurrences become progressively shorter, until platinum sensitivity is lost (platinum-resistant disease). Typically, platinum-containing chemotherapy continues until the patient develops a platinum-resistant disease, that is define as progression within 6 months of the last platinum-containing regimen (Jayson G. C. et al., 2014).

1.1.8 Metastasis and ovarian "cancer stem cell hypothesis"

Ovarian cancer can be considered as a semi-solid malignant disease because disseminates within the peritoneal fluid as single cells, aggregates of some cells or even small spheroids inside the peritoneal cavity (Zeimet A. G., 2012). It is important to note that for ovarian cancer, unlike other cancers, no anatomical barrier surrounds the ovaries to widespread metastasis throughout the peritoneal cavity. Secondary tumor implants block lymphatic vessels inhibiting the outflow of ascites fluid that leaks from disordered tumor vessels (Bast R. C. Jr. et al., 2009; Shield K. et al., 2009). Indeed, distinct from other tumors, EOC metastasis occurs as cancer cells are shed from the ovary and form multicellular aggregates or spheroids in ascites suspension, before adhering to the

peritoneal surface (forming numerous nodules) and establishing a secondary tumor **(Fig. 1.7)**.

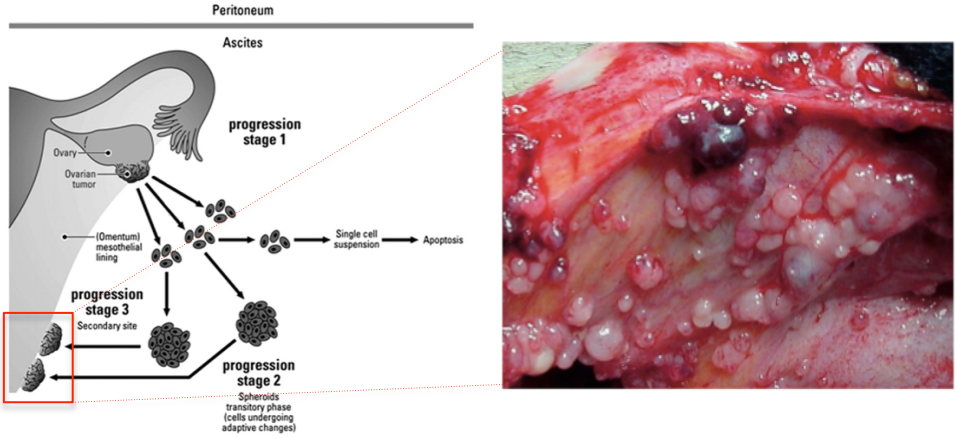

Figure 1.7. Model of ovarian cancer progression (left) and typical peritoneal dissemination in advanced ovarian cancer (right). Multiple tumor spheroids can be seen either floating or embedded in the peritoneal cavity during primary debulking surgery. Adapted from Shield K. et al., 2009 and Zeimet A. G. et al., 2012.

Within a given tumor there are distinct cell populations with different capacities to grow, survive, metastasize and resist to chemotherapy. One model that has emerged in tumor biology is the "Cancer Stem Cell Hypothesis" (CSC) (Medema J. P., 2013). The CSC theory hypothesize that the progression and recurrence of cancers are due to a small population of CSCs within a tumor, which causes tumor progression and relapse following recurrent disease (Vermeulen L. et al., 2012). Ovarian cancer has been postulated to imitate the CSC model (Aguilar-Gallardo C. et al., 2012; Curley M. D. et al., 2011; Ahmed N. et al., 2013). If it is assumed that ovarian cancer is a CSC-model disease we can hypothesized that hundreds of tumor spheroids existing in the peritoneal cavity of advance-stage patients may have originated from a small population of ovarian CSCs with tumorigenic potential (Zeimet A. G. et al., 2012). It can be therefore assumed that the highest concentration of CSCs in ovarian cancer exist within the free-floating tumor spheroids contained in the ascites of advanced-stage EOC patients. The concentration of CSCs has been shown to enhance in the ascites of chemoresistant recurrent EOC patients compared to untreated chemonaive ones (Latifi A. et al., 2012). In addition, spheroids found in ascites are capable of tumorigenesis *in vitro* and have a

reduced response to chemotherapeutic drugs *in vitro* (Burleson K. M. et al., 2006; L'Esperance S. et al., 2008; Zhang S. et al., 2008; Latifi A. et al., 2012). It is not surprising that spheroids present in malignant ascites may represent a significant drawback to efficacious treatment of late stage EOC. This can be the result of chemoresistant CSCs in ascites, which remain undetected as residual tumor cells after chemotherapy and progressively increase in number with consecutive cycle of treatments **(Fig. 1.8 and Paragraph 1.1.7)** (Zeimet A. G. et al., 2012). Experimentally, *in vitro* enrichment and propagation of CSCs were achieved by growing cells in a non-adherent condition in the form of spheres (Abubaker K. et al., 2013; Latifi A. et al., 2011).

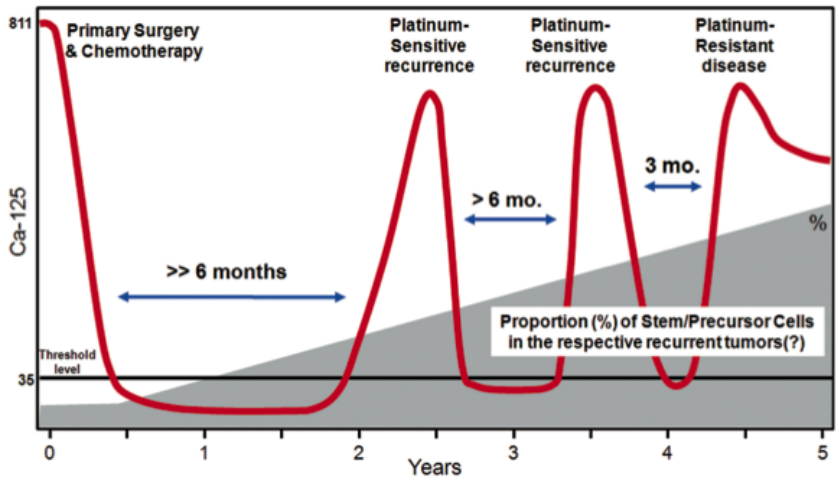

Figure 1.8. Classical clinical course with recurrences of advance-stage ovarian cancer and the hypothetical increase in the numbers of cancer stem cells (Zeimet A. G. et al., 2012).

1.2 OCT4 (octamer-binding transcription factor 4)

OCT transcription factors are crucial developmental regulators from the maintenance of embryonic pluripotent state to terminal differentiation. OCT proteins are a subclass of the POU (Pit-1, Oct1/2, Unc-86) family of transcription factors that recognize the "octamer motif", an 8 bp consensus sequence [ATGC(A/T)AAT], and its variants (Bodner M. et al., 1988; Ingraham H. A. et al., 1988; Kemler I. et al., 1989).

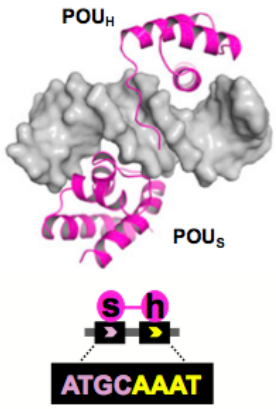

Figure 1.9. The POU family of transcription factors are characterized by the presence of an homeodomain (POU_H, of about 60 amino acid) joined by a flexible linker to a second, independently folded DNA-binding domain termed the POU-specific domain (POU_S) (Herr W. et al., 1988; adapted from Tantin D., 2013).

As illustrated for Oct1, the 5' ATGC motif associates with the POU-specific domain (POU_S), while the 3' half-site associates with the POU homeodomain (POU_H) **(Fig. 1.9)**. The octamer motif is found in the regulatory regions of both ubiquitous and tissue-specific target genes.

The human *OCT4* gene is located on chromosome 6p21.3 (Krishnan R. R. et al., 1995). OCT4 gene originates three transcript variants (*OCT4A*, *OCT4B* and *OCT4B1*) that are characterized by different 5' termini and identical 3' termini. *OCT4A* transcript consists of exons 1, 2b, 2d, 3, and 4, among which exon 1 is present only in *OCT4A* variant. In contrast, *OCT4B* transcript is truncated without exon 1. *OCT4B1* transcript is similar to *OCT4B* but it has an additional exon 2c. *OCT4* gene has been considered to contain four exons. In fact, exons 2a, 2b, 2c, and 2d are part of the entire exon 2 in which several alternative splicing sites are located **(Fig. 1.10)**.

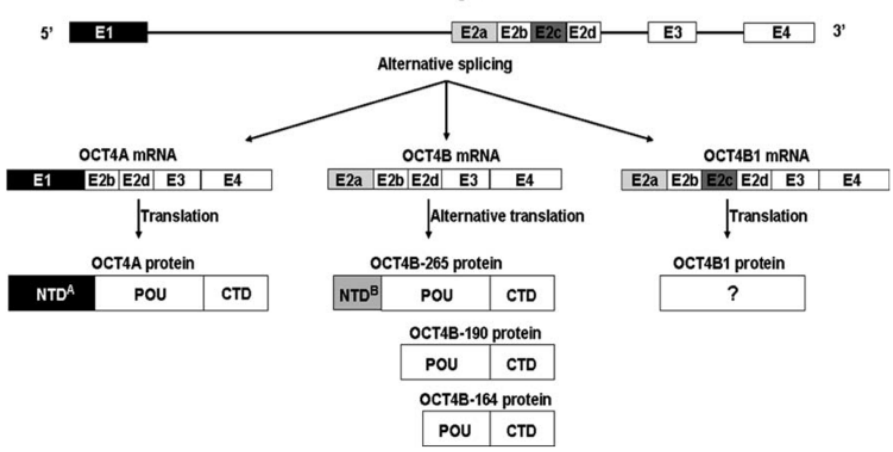

Figure 1.10. *OCT4* gene generates three transcripts and four protein isoforms. Different colored boxes indicate the different regions of *OCT4* isoforms, while white boxes indicate the identical regions. Abbreviations: NTD, N-transactivation domain; CTD, C-transactivation domain; POU, a bipartite DNA binding domain (Wang X. and Dai J., 2010).

OCT4A protein is expressed in the early mammalian embryo and in the germline. Within the early embryo OCT4A is expressed in pluripotent cells of the blastocyst inner cell mass (ICM) and epiblast, which will create all the cells of the embryo. OCT4-deficient embryos fail to establish pluripotency because, instead of forming an ICM, differentiate into trophectoderm and fail normal implantation (Nichols J. et al., 1998). This suggests that the accurate level of OCT4A protein expression in embryonic stem cells (ESCs) is crucial to maintain lineage-specific ESC differentiation and distinct developmental fates. OCT4A is also expressed in embryonic stem cells (ESCs) derived from the ICM, and has been shown to induce reprogramming of differentiated cells to induced pluripotent stem cells (iPSs), either alone or in combination with other factors (Takahashi K. and Yamanaka S., 2006; Okita K. and Yamanaka S., 2010; Kim J. B. et al., 2009).

OCT4B mRNA encodes three isoforms by alternative translation initiation at AUG and CUG start codons, respectively. The protein products are OCT4B-265, OCT4B-190 and OCT4-164. The OCT4B-190 and OCT4B-256 proteins have been discovered to play a function after heat shock and oxidative stress treatment, and to be upregulated under genotoxic stress, respectively (Wang X. et al., 2009, Gao Y. et al., 2012).

No protein products of OCT4B1 mRNA have been discovered yet, but a study revealed that *OCT4B1* could be spliced into *OCT4B* and produce the three isoforms: OCT4-265, OCT4B-190 and OCT4B-164 (Gao Y. et al., 2010). In addition, there are evidences that

point out also to its role in stemness (Papmichos S. I. et al., 2009).

Liedtke et al. (Liedtke S. et al., 2007 and 2008) and de Jong et al. (de Jong et al., 2006) have emphasized that nonspecific primers for real-time PCR and Affymetrix probe can result in false-positive artifacts and misinterpretations due to *OCT4* variants and its pseudogenes. Thus, it is recommended to discriminate *OCT4* variants to take into account that exon 1 is unique in *OCT4A* transcript. Accordingly, it seems that the best approach is to design specific primers for *OCT4A* transcript in exon 1 to distinguish *OCT4A* from *OCT4B* and *OCT4B1* variants, excluding all pseudogenes of OCT4 (reviewed in Wang X. and Dai J., 2010). In addition, the primers should be intron spanning to avoid PCR amplification from *OCT4* genome sequence.

1.2.1 OCT4 in tumor progression and chemoresistance

Gidkel S. et al. observed the first evidence of the role of OCT4 in cellular transformation in 2003 (Gidkel S. et al., 2003). The authors observed that ectopic dose-dependent expression of OCT4 increases the malignant potential of ESCs. Until now several malignant neoplasms have been found to express OCT4 and correlate with tumor grade and disease progression (Zhao P.-P. et al., 2012; Zhang X. et al., 2010; Huang P. et al., 2012; Rijlaarsdam M. A. et al., 2011; Lin H. et al., 2014; Kong D. et al., 2014; Li Z. et al., 2014; Jóźwicki W. et al., 2014). In addition, compared to tumors with low OCT4 expression, high levels of OCT4 have been associated with metastasis and shorter patients survival rates (He W. et al., 2012; Chen Z. et al., 2012; Karoubi G. et al., 2009; Liu T. et al., 2014; Li N. et al., 2015; Yin J. Y. et al., 2015). A study published in 2011 found that lentiviral ectopic expression of OCT4 in primary breast cancer cells led to the selection of tumor-initiating cells that developed high-grade poorly differentiated breast carcinomas when injected in nude mice (Beltran A. S. et al., 2011). Further evidences show that OCT4 expression has been associated with the maintenance and enhancement of CSC-like characteristics (Chen Y.-C. et al., 2008; Kim R. J. et al., 2011) and highlight the importance of OCT4 expression in tumors in order to maintain cancer-stem cell like features. It is also believed that OCT4 plays a key role in the survival of a population of CSCs with drug resistance phenotype. To support this notion, OCT4 overexpressing liver cancer cells were found to be more resistant to cisplatin and doxorubicin treatment compared to control cells both *in vitro*

and *in vivo* (Wang X. Q. et al., 2010). Furthermore, short-term single treatment of chemotherapy results in the enrichment of ovarian cancer stem cell-like cells and OCT4 that led to an increased tumor progression (Abubaker K. et al., 2013). Additional findings associate OCT4 with cisplatin resistant cancer cells with an increase ability to metastasize and to be more tumorigenic in both oral and drug resistant prostate cancer cells (Tsai L. L. et al., 2011; Linn D. E. et al., 2011). Importantly, knocking down *OCT4* expression by specific small hairpin (sh) RNA reduce the growth of drug-resistant cells *in vitro* and *in vivo*, suggesting that OCT4 expression in cancer cells is also essential for acquiring and maintaining a drug-resistant phenotype. OCT4 is also found to inhibit apoptosis in cancer cells by different possible mechanisms (Wang Y. D. et al., 2013; Hu T. et al., 2008). Altogether, these evidences point out to the importance of OCT4 in tumor initiation and progression toward chemoresistant disease.

1.2.2 OCT4 and ovarian cancer

The first description of OCT4 in ovarian cancer was in ovarian dysgerminoma, a tumor derived from undifferentiated germ cells (Cheng L. et al., 2004). Later on, OCT4 was found to be expressed in immature teratoma of the ovary (Abiko K. et al., 2010), in serous and mucinous epithelial ovarian cancer (Zhang J. et al., 2010). In the latter study and in another very recently published, OCT4 expression was shown to be significantly increased from normal surface ovarian surface epithelium/Fallopian tube epithelium, to benign/borderline tumors to high-grade serous carcinomas, highlighting the association between OCT4 with tumor initiation and progression of serous ovarian cancer (Zhang J. et al., 2010; Samardzija C. et al., 2015). The involvement of OCT4 in EOC cancer stem cells (CSCs) was firstly demonstrated in 2005 when a single tumorigenic clone was isolated from the ascites of a patient with advanced EOC using serial dilution (Bapat S. A. et al., 2005). Subsequently, CSCs have been isolated from ovarian tumors and cell lines based on their ability to efflux the DNA binding dyes (Hu L. et al., 2010; Vathipadiekal V. et al., 2012). It is supposed that CSCs are responsible for chemoresistance and relapse in tumors. The evidence for such properties of CSCs of EOC derived from the findings that show recurrent chemoresistant ovarian tumor cells to be enriched in CSC-like cells and stem cell pathways, indicating that CSCs of the ovary may contribute to the progression of the disease (Latifi A. et al., 2012; Hu L. et

al., 2010; Abubaker K. et al., 2013; Samardzija C. et al., 2015). Ovarian cancer currently is considered a CSC-model disease in which CSCs are the cells responsible for the generation of hundreds of tumor spheroids/multicellular aggregates present in the peritoneal cavity of advance-stage patients (Zeimet A. et al., 2012). Considering the role of OCT4 as pluripotent regulator in developing embryo, the core of cancer spheroids would resemble the inner cell mass (ICM) containing chemoresistant CSC-like cells that are able to evade chemotherapy, undergoing self-renewal and reform a secondary tumor **(Fig. 1.11)**. The model speculates that cancer cells from primary tumor (ovary) can spread into the peritoneum. Core cells expressing OCT4 in the ascites microenvironment will survive chemotherapy treatment and will serve as a niche for regenerating cells. The surviving spheroids are supposed to be the main cause of recurrence and treatment failure (Samardzija C. et al., 2012).

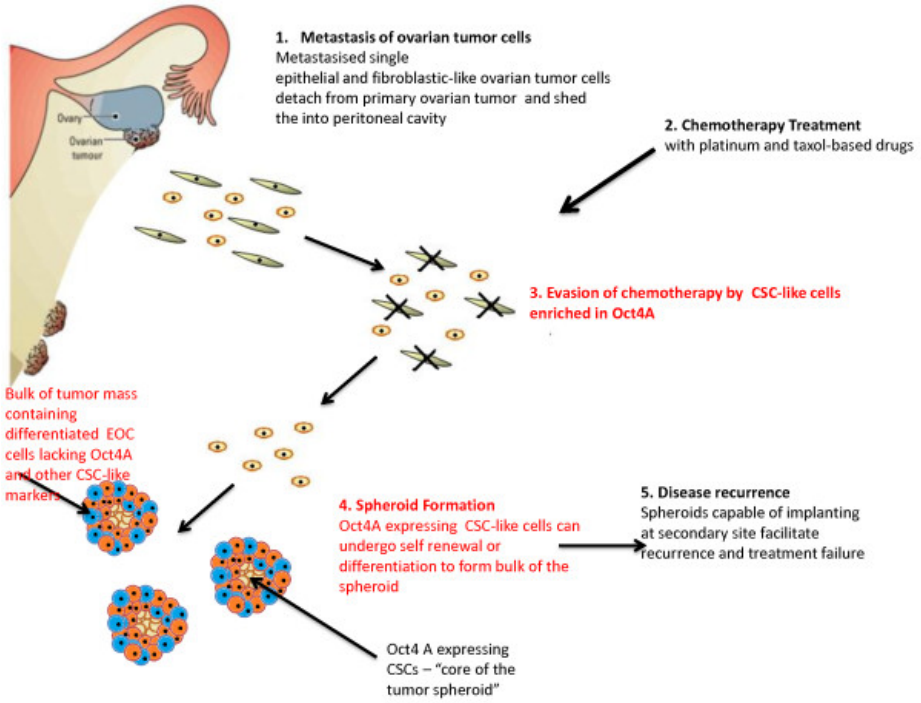

Figure 1.11. Propose model for the role of OCT4 expressing spheroids in ovarian cancer evolution and progression (Samardzija C. et al., 2012).

1.2.3 OCT4 based therapy

The implication of the CSCs model in cancer therapy is of remarkable importance. This because targeting only the progeny and not CSCs would prevent tumor eradication and promote chemoresistance. The model proposed in **Fig. 1.12** is based on the assumption that OCT4 is able to render cells capable of long term survival through ongoing self-renewal, tumorigenicity and chemoresistance, which would contribute to EOC recurrence. To support this hypothesis, it is reported that OCT4 knockdown in mice *in vivo* reduce significantly the tumor mass, tumor size and invasiveness in mice, which resulted in an increase of survival rates compared with control mice (Samardzija C. et al., 2015). Since OCT4 is expressed at low levels in normal somatic tissues, its specific targeting may be a promising strategy to target CSCs in EOC, preventing tumor progression, chemoresistance and recurrence. One possibility is to inhibit the upstream targets of OCT4 such as WNT, AKT and TGF-beta that may lead to the specific death of OCT4 expressing CSCs. It is also possible to target OCT4 by microRNAs (miRNA) that are responsible for its regulation in ovarian cancer progression and chemoresistance. Until now, at least two miRNAs have been identified to target specifically OCT4 in cancer. In fact, miR-145 up-regulation promotes differentiation in human endometrial carcinoma cells (Wu Y. et al., 2011). We recently discovered that miR-335 targets OCT4 in mouse embryonic stem cells (mESCs) (Schoeftner S. and Scarola M. et al., 2013). In line with our findings, miR-335 functions as tumor suppressor in pancreatic cancer repressing OCT4 (Gao L. et al., 2014). A miRNA-based therapy using miRNA substitutes and antagonists will become available during the next few years. microRNA-based therapeutics are a great goal in cancer therapy since it would correct the aberrant microRNA transcription levels of CSCs.

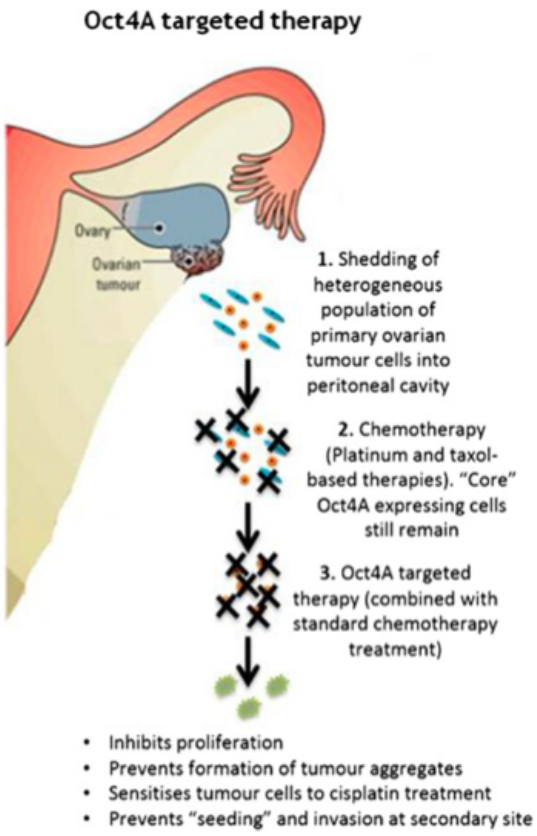

Figure 1.12. Model of OCT4 targeted therapy. OCT4-expressing ascites tumor cells would be targeted by OCT4-specific therapy in combination with standard chemotherapy. This results in decrease cancer cell survival and limited formation of aggregates/spheroids, avoiding tumor recurrence (Samardzija C. et al., 2015).

1.3 Retinoblastoma protein (pRB)

pRB (Retinoblastoma protein) is the first tumorsuppressor to be identified and cloned (1986-1987) (Friend S. H. et al., 1986; Lee W. H. et al., 1987; Fung Y. K. et al., 1987). In 1971 Knudson A. G. Jr. hypothesize that mutations on both *RB1* alleles would cause its inactivation and originate retinoblastoma ("two-hit hypothesis") (Knudson A. G. Jr., 1971). Hereditary retinoblastoma is caused by a germ line transmission of a single mutation in one *RB1* allele and the subsequent loss of the second *RB1* allele in somatic retina cells. Typically, hereditary retinoblastoma arises early compared to sporadic retinoblastoma in which both inactivated alleles are located in somatic retina cells. pRB is one of the members of a family of three proteins that include p107 and p130 (*RBL1* and *RBL2*, respectively) (Hannon G. J. et al., 1993; Ewen M. E. et al., 1991). These proteins are called "pocket proteins" because all three family members contain a conserved domain referred to as the "pocket" that interacts with the LXCXE motif (Leu-x-Cys-x-Glu), known to mediate the interaction with viral oncoproteins (Dick F. A., 2007). Pocket proteins are crucial for cell proliferation. Therefore, deregulation of cell cycle control in cancer requires the inactivation of their growth regulatory function.

Human *RB1* consists of 928 amminoacids and shares structural proprieties with p107 and p130. The most extensive sequence homology lies in the well-conserved "small pocket" region, which is composed by A and B domain, separated by a flexible spacer region **(Fig.1.13)**. The "small pocket" is the minimal fragment of pRB that is capable of interacting with viral oncoproteins, such as E1A and SV40 large T antigen (Hu Q. J. et al., 1990). These viral proteins contain the LXCXE motif that is essential for a stable interaction with RB family proteins (DeCaprio J. A. et al., 1988; Dyson N. et al., 1992).

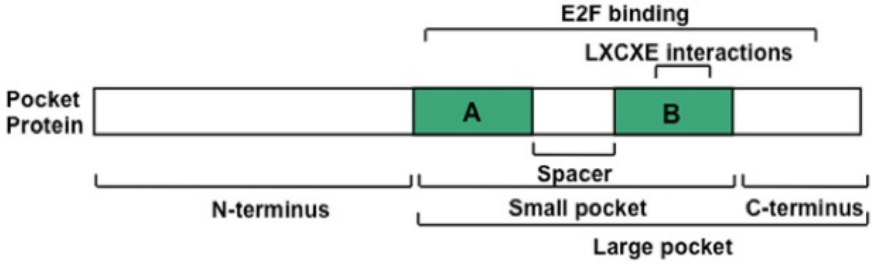

Figure 1.13. The main characteristic of RB-family proteins is the pocket domain. The "small pocket" is defined as the minimal domain necessary to bind to viral oncoproteins. The "large pocket" is the minimal growth-suppressing domain that is capable to bind E2F transcription factors and also viral proteins (Henley S. A. and Dick F. A., 2012).

Many other proteins interact with pRB with the LXCXE domain, such as histone deacetylase HDAC-1 and HDAC-2, and BRG1 of the chromatin remodeling complex SWI/SNF (Harbour J. W. and Dean D. C., 2000). Since these proteins possess chromatin-regulating activity are thought to negatively regulate transcription. LXCXE motif is the most characterized but is not certainly the unique one. The combination of the small pocket and the C-terminal domain has been called the "large pocket" **(Fig. 1.13)**. This pocket domain is sufficient to interact with E2F family of transcription factors and suppress their transcription (Hiebert S. W. et al., 1992; Qin X. Q. et al., 1992). Two unique features of pRB, that are missing in p107 and p130 proteins, are a docking site used only by E2F1, and a short region in the C-terminus that is competitively occupied by cyclin/cyclin dependent kinases (CDKs) or protein phosphatase 1 (PP1) **(Fig. 1.14)**.

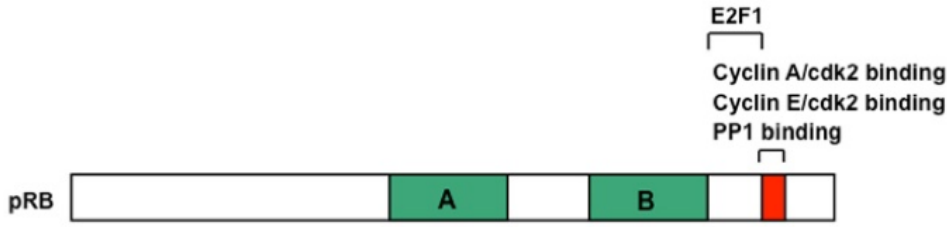

Figure 1.14. Features of pRB at C-terminus domain that binds to E2F1 and cyclins/cyclins dependant kinases or protein phosphatase 1 (PP1) (Henley S. A. and Dick F. A., 2012).

1.3.1 Cell cycle regulation

pRB was discovered to be phosphorylated in synchrony with the cell cycle (Buchkovich K. et al., 1989; Chen P. L. et al., 1989; DeCaprio J. A. et al., 1989), suggesting that pRB may be a cell cycle regulator. This hypothesis was initially supported by the observations that exogenous unphosphorylated pRB could block cells in the G1 phase of the cell cycle (Goodrich et al. D. W., 1991; Connell-Crowley L. et al., 1997), and that

pRB knockdown leads to a faster G1/S transition (Herrera R. E. et al., 1996). The first pRB partner to be discovered was E2F1 transcription factor (Helin K. et al., 1992; Kaelin W. G. Jr. et al., 1992; Shan B. et al., 1992). There are eight E2F family members and only E2Fs 1-5 are capable of binding to pocket proteins (Classon M. et al., 2002). The unphosphorylated form of pRB, the active form, are capable to bind E2Fs transcription factor blocking their ability to activate transcription necessary for the transition from G1 to S phase. This transcriptionally repression of E2F mediated by pRB is considered the major mechanism to control cell cycle. In fact, pRB has a key role in the regulation of the checkpoint G1-S in mammals. As shown in **Fig. 1.15**, mitogenic signals stimulate the expression of cyclin D and a parallel increase in cyclin-dependent kinase 4 (CDK4) and CDK6 activity. These factors initiate pRB phosphorylation (inactivation), which is increased by the activity of CDK2-cyclin A/E complexes. pRB phosphorylation disrupts its association with E2F transcription factor. This allows the expression of genes that enable progression through S-phase and mitosis (Morris E. J. and Dyson N. J., 2001). At the end of mitosis, during the transition to G1 phase, pRB is dephosphorylated through the action of phosphatases. Importantly, several anti-mitogenic signals have a role in preventing pRB phosphorylation by limiting the activity of CDKs (Knudsen E. S. and Knudsen K. E., 2008).

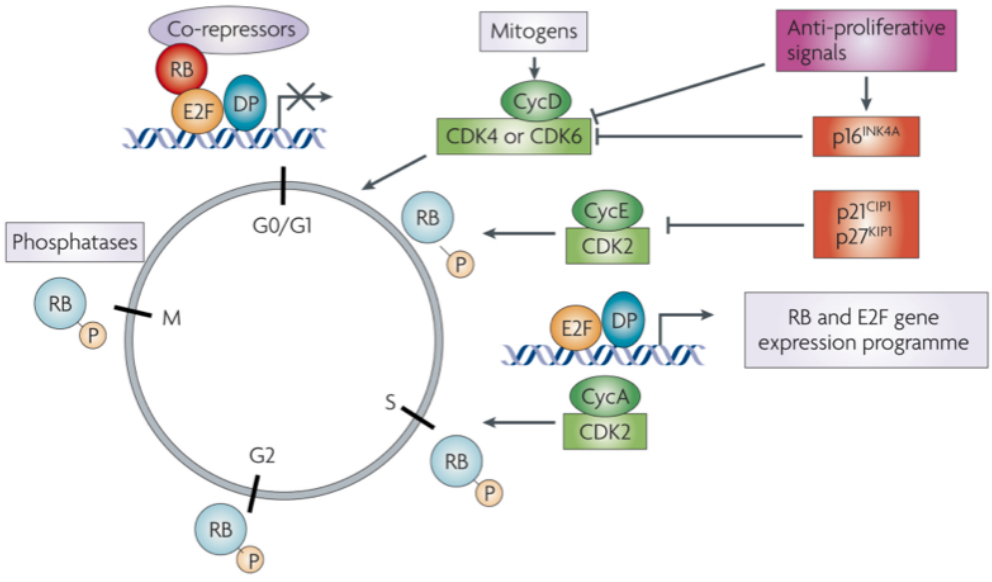

Figure 1.15. Cell cycle regulation mediated by pRB (Knudsen E. S. and Knudsen K. E., 2008).

Unphosphorylated pRB is able to bind E2Fs and recruits enzymes capable to modify chromatin, repressing transcription (Trimarchi J. M. and Lees J. A., 2002). In conclusion, the absence of proliferative stimuli renders pRB the main restrain to cellular division.

1.3.2 Post-translational modification

Regulation of pRB structure and functions are extremely complex because of several post-translational modifications on the protein, such as phosphorylation, acetylation and sumoylation (Burkhart D. L. and Sage J., 2008). Phosphorylation is the most studied modification on pRB. There are 16 known phosphorylation sites mediated by Cyclin Dependent Kinases (CDKs) on pRB that occur in a site-specific manner (Connell-Crowley et al., 1997) **(Fig. 1.16)**. As described before, pRB is hypo and hyper-phosphorylated in synchrony with the cell cycle.

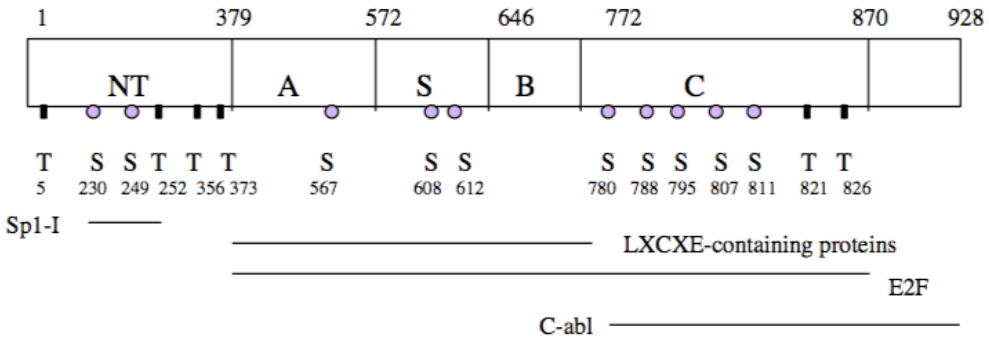

Figure 1.16. Structure of pRB with its consensus sites for CDKs mediated phosphorylation (adapted from Tamrakar S. et al. 2000).

Phosphorylation is firstly regulated through cyclins degradation during cell cycle and CDKs inhibitors. $p16^{INK4a}$, a member of INK inhibitors, is responsible for the specific inhibition of CDK4, which mediates pRB phosphorylation (Huschtscha L. I. and Reddel R. R., 1999). In addition, phosphorylation levels depend on the synergic activity of kinases and phosphatases, which in turn remove charged phosphate groups.

1.3.3 Senescence and apoptosis

Senescence is the permanent arrest of cell cycle (even though cells are metabolic active), induced by several cellular stresses and telomeric shortening, with the establishment of typical flat and large morphology and the expression of specific senescent markers. Cellular senescence is an *in vivo* suppressor of cancer initiation as a result of oncogenic stress. Senescence signals that engage the classical p16–pRB pathway generally do so by inducing the expression of p16, preventing pRB phosphorylation and inactivation. In this condition, pRB ceases cell proliferation by suppressing the activity of E2F, limiting cell-cycle progression (Campisi J. and D'Adda di Fagagna F., 2007). In addition, RB family controls telomere length and mediate the induction of senescence in this condition (Garcia-Cao M. et al., 2002). For these reasons pRB loss could bypass cellular senescence after oncogenic stresses are induced. It has also been shown that E2Fs deregulation in RB-knockout mice induces apoptosis (Trimarchi J. M. and Lees J. A., 2002). This induction in strictly associated with post-translational modification changes on E2F1 that allow it to respond to DNA damage and induce cell death (Munro S. et al., 2012). In particularly, pRB binding and inhibition to E2F1 has been interpreted as a mean to block apoptosis.

1.3.4 Genomic stability regulation

More recently, it has emerged that pRB does not only play a role in cell cycle progression, but has multiple functions in differentiation during embryogenesis and in adult tissues, and, most importantly, in the maintenance of genomic stability. In fact, pRB is considered a transcriptional co-factor that can bind multiple factors, antagonizing or enhancing its functions. In addition, pRB is an adaptor for the recruitment of chromatin remodeling enzymes, controlling target genes and modifying the structure at chromosomic level (Burkhart D. L. and Sage J., 2008). Several studies reported that pRB inactivation or its acute loss enhances genomic instability. These genomic changes include endoreduplication, increases in ploidy, high rate of chromosomal segregation errors, supernumerary centrosomes, centromeric defects and formation of micronuclei (Amato A. et al., 2009; Coschi C. H. et al., 2009; Hernando E.

et al., 2004; Iovino F. et al., 2006; Isaac C. E. et al., 2006; Manning A. L. et al., 2010; Mayhew C. N. et al., 2007; Srinivasan S. V. et al., 2007). The reason for these changes is that the inactivation of pRB or its acute loss leads to defects during mitosis.

Different mechanisms are able to sense improper connection of microtubules to kinetochores as well as the tension across sister-kinetochores. The proper bidirectional attachment of both kinetochores of the duplicated chromatids to microtubules from opposing spindle poles is termed amphitelic, whereas syntelic and monotelic attachments describe erroneous attachment states **(Fig. 1.17)**. These errors are efficiently sensed by the Spindle Assembly Checkpoint (SAC).

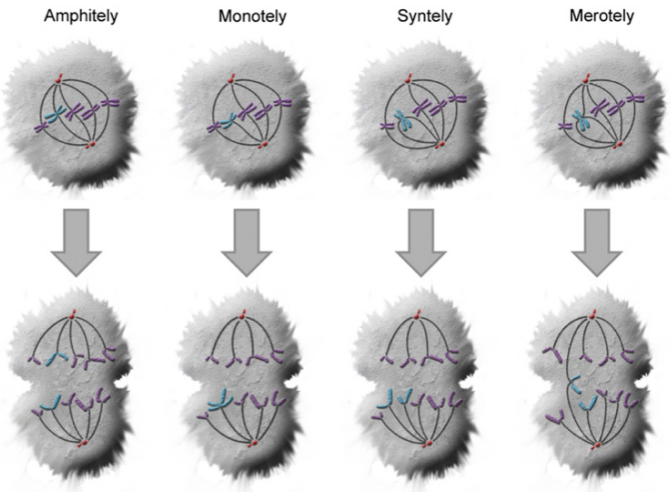

Figure 1.17. Correct and incorrect microtubule-kinetochore attachments. Amphitely is the situation in which all sister-kinetochores are correctly attached to microtubules from opposite poles. Monotelic attachment is the attachment to only one kinetochore/sister chromatid of a chromosome, whereas the second kinetochore is not attached to microtubules. In syntelic attachments both sister-kinetochores from a single chromosome are connected to microtubules from only one spindle pole. Both monotely and syntelic attachments activates the spindle assembly checkpoint (SAC) which delays anaphase onset until all chromatids are properly connected with the spindle. On the contrary merotely does not activate SAC. In this case all kinetochores are attached to microtubules but single kinetochores are connected to microtubules from both spindle poles (Anderhub S. J. et al., 2012).

Cells with Chromosomal INstability (CIN) often display lagging chromosomes and anaphase bridges (Gascoigne K. E. et al., 2008). These phenotypes are frequently caused by another incorrect microtubule-kinetochore attachment type, namely merotely. This error arises when one kinetochore is attached to microtubules from both spindle poles and is not sensed by the SAC because the attachments develop sufficient tension

between sister kinetochores **(Fig. 1.17)**. Attachment of microtubules to kinetochores is a highly dynamic process which depends on spatial proximity between kinetochores and microtubules nucleating from centrosomes (Mitchison T. J. et al., 1985) and is strictly regulated by a set of proteins to avoid incorrect attachments. It is well known that merotelic attachments promote whole chromosome missegregation that are found in chromosomally unstable tumor cell lines, resulting in aneuploidy. There are evidences that suggest that pRB loss of function leads to CIN in cancer by promoting merotelic kinetochore attachment. In fact, several studies highlight that loss of pRB leads to a defective loading of condensin II and cohesin specifically at centromeric region of mitotic chromosomes, compromising centromere structure and function, leading to merotelic errors (Manning A. L. et al., 2010; Coschi C. H. et al., 2010; van Harn T. et al., 2010). pRB has been also shown to have an impact on genome stability through other mechanisms that are dependent or independent by E2Fs **(Fig. 1.18)**. The first one relies on E2F target gene overexpression of "Mitotic Arrest Deficient 2" (MAD2), as a consequence of pRB loss, that causes lagging chromosomes. These errors can be due to overactive spindle assembly checkpoint or from an inability to resolve merotelic microtubule attachments to sister chromatids (Schvartzman J. M. et al., 2011; Kebeche L. and Compton D. A., 2012). Another consequence of E2F deregulation followed pRB loss is the abnormal low nucleotide pools and replication stress (Bester A. C. et al., 2011), which ultimately cause aneuploidy. The second mechanism is E2F-independent and is due to heterochromatin regulation. pRB is a regulator of heterochromatin at centromeres with a role in chromosome structure and attachments to spindle microtubules. Consequently, loss of pRB leads to missegregation of chromosomes and aneuploidy (Gonzalo S. et al., 2005). All together, maintenance of genome stability through the regulation of pericentromeric heterochromatin could contribute to pRB tumor suppressor activity.

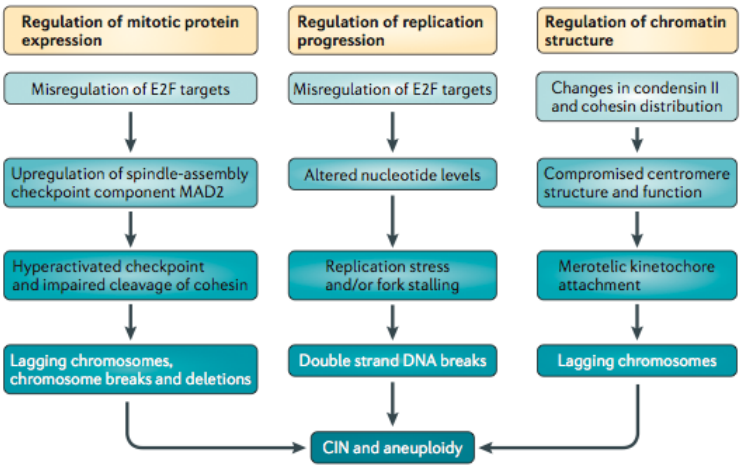

Figure 1.18. Three different mechanisms by which pRB pathway disruption can promote chromosome segregation errors, chromosome instability (CIN) and aneuploidy (Manning A. L. and Dyson J. D., 2012).

1.3.5 Tumor suppressive functions

pRB pathway is inactivated by different mechanisms in cancer that include both RB mutation/deletion and its enzymatic inactivation. As mentioned before, mutation of RB gene is the initial event of familiar and sporadic retinoblastoma. pRB deficiency it is also the cause of osteosarcoma in children and, in adults, it is responsible for cervical carcinoma and squamous carcinoma of the oral cavity through pRB inactivation by E7 oncoproteins of papillomavirus (HPV) (Doorbar J., 2006; Perez-Ordonez B. et al., 2006). The same mechanism could involve also liver malignancy with viral etiology (Munakata T. et al., 2004). In addition, pRB is inactivated in 90% of human small cell lung carcinoma (SCLC) (Meuwissen R. et al., 2003). Of notice, the enzymatic inactivation of pRB is a phenomenon observed in nearly 70% of a subtype of HG-SOC cancer, instead mutations in this gene occur only in 2% of the patients (Bell D. et al., 2011). G1-S transition is one of the thorniest phase of the cell cycle because from it depends cell proliferation. Cells in which such control is lost succumb to neoplastic transformation with uncontrolled proliferation, even though proliferative signals are missing. In addition to its role as a negative regulator of the G1-S transition, pRB has also been found to promote cellular differentiation, modulate cell fate decision, be important for oncogene-induced senescence and affect cellular sensitivity to apoptosis (reviewed in Burkhart D. L. and Sage J., 2008).

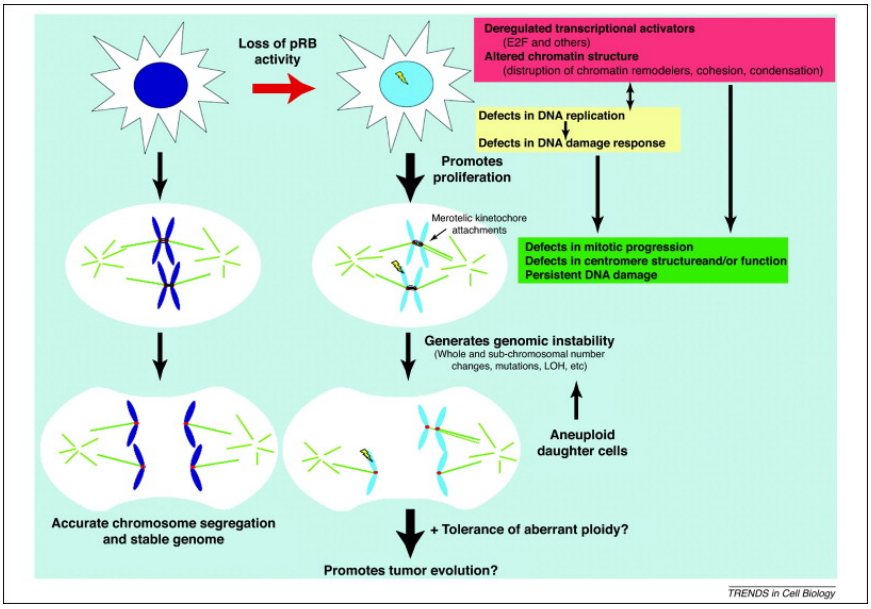

Figure 1.19. Role of pRB in maintenance of genomic stability (Manning A. L. and Dyson N. J., 2011).

It is not clear which of the functions of pRB are the most important for its tumor suppression activity. Certainly CIN and aneuploidy have crucial roles in tumorigenesis and evolution of cancer cells. Given the important changes seen in pRB-deficient cells (paragraph 1.3.4) it seems that pRB contribution in maintaining genome stability is critical for its tumor suppressive activity **(Fig. 1.19)**.

1.4 Protein Phosphatase 1 (PP1)

Reversible protein phosphorylation is a molecular switch by which organisms regulate physiological processes. These important functions are regulated not only by kinases through phosphorylation but also by phosphatases through dephosphorylation. This post-translational modification is the addition or removal of a negatively charged phosphate that can modify the structural conformation of a target protein and/or its interactions with other proteins. Thus, phosphorylation alters protein activity, function, stability and localization. Given the importance of this modification it is believed that it may cause cancer. However, the majority of oncogenes identified thus far encode for protein kinases. Even though, the growing body of evidence on the role of protein phosphatase in tumorigenesis, strongly highlight the importance of such a protein as a new therapeutic target. Protein Phosphatase 1 (PP1) is a member of the PPP family of serine/threonine phosphoprotein phosphatases (Cohen P. T. W. et al., 1997). This phosphatase act as a holoenzyme composed of a catalytic subunit (PPP1C or PP1) and a regulatory subunit (known as PPP1R or PIP - PPP1 interacting protein). PP1 was identified in the early 1940s as the enzyme responsible for the conversion of "phosphorylase a" to "phosphorylase b" (Cohen P. T. W. et al., 1997), but later it has been shown to play a role in several important functions such as cell division, apoptosis, protein synthesis and cytoskeletal reorganization. In mammals, there are three genes encoding for PPP1C (PPP1CA, PPP1CB and PPP1CC). Splicing events on each of those transcripts generate three isoforms of *PPP1CA* (PP1α1, α2 and α3), one for *PPP1CB* (PP1β/δ) and two splicing variants for *PPP1CC* (PP1γ1 and PP1γ2) (Gregório L. K. et al., 2014). Since PPP1C catalytic subunit isoforms are similar sequences and specificity to their substrate, it is believed that are mainly the regulatory subunits, with which PPP1C interacts, that control the specificity and diversity of PPP1C. These regulatory subunits (PPP1 interacting proteins – PIPs) have different effects on PP1 modulating its activity, target protein and substrates (Bollen M. et al., 2001). PP1 holoenzymes are composed by a highly conserved catalytic subunit complexed with one or two variable regulatory subunits.

1.4.1 pRB regulation through PP1

One of the physiological substrates of PP1 is pRB. Of notice, in the M-G1 transition, pRB is dephosphorylated by PP1, returning to its active, growth-suppressive hypo-phosphorylated state (Vietri M. et al., 2006). PP1 is capable of de-phosphorylate pRB at Ser^{249}, Thr^{356}, Ser^{608}, Ser^{788}, Ser^{795}, Ser^{807} and Thr^{826} (Tamrakar S. et al., 2000).
One of the first identified inhibitor of PP1 is the "Nuclear inhibitor of PP1" (NIPP1 or PPP1R8 – Protein Phosphatase 1 regulatory subunit 8) (Beullens M. et al., 1992; Van Eynde A. et al., 1995). The NIPP1-mediated inhibition of PP1, that dephosphorylates pRB, is considered a cell cycle-regulated mechanism (Van Eynde A. et al., 2004). Recently, it has been discovered that Cyclin F (CCNF) is involved in the maintenance of pRB in its hyper-phosphorylated form at G1/S and G2/M transition (Sissons J. et al., 2004). In accordance to Campbell P. A., Cyclin F could degrade PP1 through its E3 ubiquitin ligase (Campbell P. A. et al., 2007). NIPP1 and CCNF are briefly described below.

1.4.1.1 Nuclear Inhibitor of PP1 (NIPP1)

The first identification of the Nuclear Inhibitor of PP1 (NIPP1) dates back in 1992 when it was discovered in bovine thymus nuclei as a potent inhibitor of the protein Ser/Thr phosphatase PP1 (Beullens M. et al., 1992). Subsequently, it became clear that NIPP1 is key for several other functions. In fact, NIPP1 is considered a scaffold protein since it interacts with several proteins to carry out its functions. NIPP1 is involved at least in three important cellular processes: transcription, development and splicing. Firstly, NIPP1 is a transcriptional repressor since it interacts with two proteins of the Polycomb repressive complex 2 (PRC2), EED and EZH2 (Jin Q. et al., 2003; Roy N. et al., 2007). Secondly, NIPP1 expression is found necessary for embryonic development because NIPP1-/- embryos showed lethality with retarded growth at embryonic day 6.5 (onset of gastrulation) and impaired proliferation (Van Eynde A. et al., 2004). Finally, NIPP1 is linked with spliceosomes and "speckles" that are splicing factor storage sites (Boudrez A. et al., 2000). In particular, in this context NIPP1 is crucial for a late assembly of spliceosome (Beullens M. and Bollen M., 2002).

1.4.1.2 Cyclin F (CCNF)

Cyclin F (also known as Fbxo1) is the founding member of the F-box protein family and is essential for mouse development (Bai C. et al., 1996; Tetzlaff M. T. et al., 2004). Elledge et al. identified a functional domain called "F-box" domain (Bai C. et al., 1996). Indeed, cyclin F is also known as F-box only protein 1 (Fbxo1). In addition to an F-box domain, cyclin F contains a cyclin box domain, but, in contrast to typical cyclins, it does not bind/activate any cyclin-dependent kinases (CDKs) (Bai C. et al., 1996; D'Angiolella V. et al., 2010; Fung T. K. et al., 2002; Tetzlaff M. T. et al., 2004). The F-box domain is required for binding to Skp1, a component of the SCF ubiquitin ligase machinery, that in turn recruits Cul1 to assemble a functional SCF complex. The complex recruits the E2 for ubiquitylation of target substrates (Cardozo T. et al., 2004). Recent work, found that cyclin F localizes to both the centrosomes and the nucleus. During G2, centrosomal cyclin F targets CP110 for proteasome-mediated degradation to limit centrosome duplication to once per cell cycle (D'Angiolella V. et al., 2010).

1.4.2 OCT4-pRB axis in mouse Embryonic Stem Cells (mESCs)

In 2013 our group discovered a new axis connecting the stemness factor OCT4 and the tumor suppressor pRB in mouse embryonic stem cells (mESCs) (Schoeftner S. and Scarola M. et al., 2013). Particularly, we demonstrated that OCT4 controls the cell cycle program of self-renewing mESCs by protecting pRB from de-phosphorylation by the Protein Phosphatase 1 (PP1) complex. Mechanistically, OCT4 transcriptionally activates CCNF (Cyclin F) and NIPP1, two potent inhibitors of PP1, which becomes unable to de-phosphorylate pRB, leading to its hyper-phosphorylated form **(Fig. 1.20)**. Cell cycle control of mESCs differs significantly from somatic cells. mESCs, in fact, display shorter G1 phase and a predominant presence of hyper-phosphorylated pRB (inactive form) (Savatier P. et al., 1994). This means that E2F-dependent genes are transcribed independently from cell cycle progression (Stead E. et al., 2002; White J. et al., 2005). Therefore, this unusual cell cycle regulation is considered crucial for the stemness maintenance of mESCs, avoiding cellular differentiation and specification. There are evidences that the accumulation of the hypo-phosphorylated form of pRB is

associated with the acquisition of the ability to differentiate in several lineages (Orford K. W. and Scadden D. T., 2008) and with loss of stemness (Galderisi U. et al., 2006). We found that at the onset of mESCs differentiation, transcriptional repression of OCT4 causes the collapse of the OCT4-pRB self-renewal axis, leading to a rapid de-phosphorylation of pRB, the exit from self-renewal, and the establishment of a cell cycle program of differentiated cells.

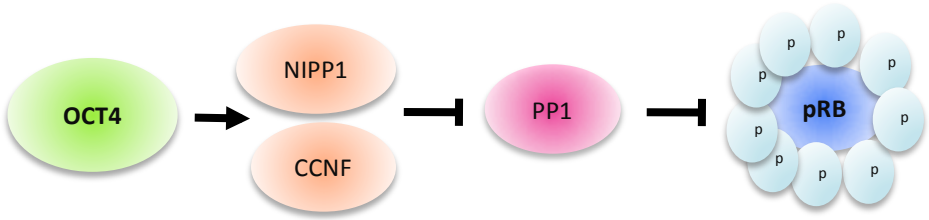

Figure 1.20. Schematic representation of the OCT4-pRB axis discovered in mouse embryonic stem cells (mESCs) (adapted from Schoeftner S. and Scarola M. et al., 2013).

1.5 Genomic stability in tumors

Genomic instability is a common feature of almost all human cancers. In fact, cancer is an evolutionary multistep process that emerges from non-lethal mutations that interfere with critical genes, leading to unregulated growth. There are different forms of genomic instability. These include microsatellite instability, increased frequencies of base-pair mutations and epigenetic changes (Negrini S. et al., 2010; Easwaran H. et al., 2014). However, the most frequent form is called chromosomal instability (CIN), which is defined as the high rate by which chromosome structure and number changes in cancer cells compared to normal cells (Negrini S. et al., 2010). An abnormal number of chromosomes (aneuploidy) was firstly described by Leo Hansemann in 1890 as the first identified hallmark of cancer cells (Hansemann L., 1890; Hanahan D. and Weinberg R. A., 2011). In its work Hansemann reported the recurrent presence of asymmetric and multipolar mitosis in carcinoma tissue (Hansemann L., 1890; Hansemann L., 1891). These pioneering observations prompted Theodore Boveri, who observed the presence of supernumerary centrosomes and abnormal mitotic figures in sea urchin embryos, to postulate his theory that centrosomal defects might cause aneuploidy and cancer (Boveri T., 1914).

1.5.1 Centrosome amplification

Centrosomes are organelles that are the main microtubule-organizing centers of most animal cells (Azimzadeh J. et al., 2007; Bornens M. et al., 2002; Bornens M. et al., 2012). They are of crucial importance for the assembly of the mitotic spindle and subsequent cell division, controlling several interphase and mitotic microtubule-dependent processes (Azimzadeh J. et al., 2007; Bornens M. et al., 2002; Bornens M. et al., 2012, Mahen R. and Venkitaraman A. R., 2012; Bettencourt-Dias M. et al., 2007). Centrosomes consist of two orthogonally arranged, barrel-shaped centrioles, which are embedded in the so-called pericentriolar material (PCM) **(Fig. 1.21)**. The PCM contains proteins required for microtubule anchorage and nucleation (Doxsey S. J. et al., 1994; Stearns T. et al., 1991). Contrary to the view that PCM is considered an amorphous

material, using super-resolution microscopy, several groups have found that the PCM is a highly ordered structure, the components of which occupy spatial domains around centrioles by using a concentric toroidal distribution (Fu J. and Glover D. M., 2012; Lawo S. et al., 2012; Mennella V. et al., 2012).

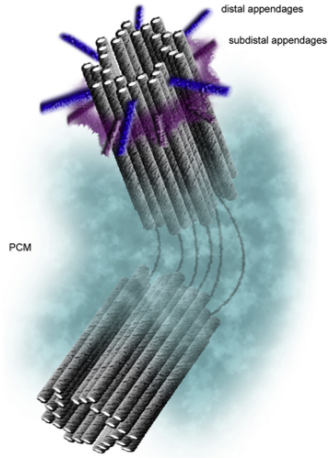

Figure 1.21. Centrosome structure. One centrosome is composed by two centrioles (made up by nine microtubules triplets), embedded in the pericentriolar material (PCM) (Anderhub S. J. et al., 2012).

Generally, during mitosis, there is a bipolar spindle generated by two opposite centrosome, each of which contains a pair of centrioles. These two centrioles usually display an orthogonal orientation and are tightly connected. At the end of mitosis, this association is lost during a process called centriole disorientation or disengagement (Kuriyama R. and Borisy G. G., 1981) **(Fig. 1.22)**. Subsequently, centriole duplication occurs during S phase, therefore, normally, cells in G1 phase harbour a single centrosome with connected centrioles. Centrosomes duplicated precisely once per cell cycle, as DNA replication, ensuring correct segregation of duplicated chromosomes. This event is characterized by the formation of procentrioles at the proximal end of each parental centriole. These structures then elongate until they reach their maximal length. Only at the transition from G2 to M phase there is the complete maturation of centrosomes due to the exchange of several PCM components and the recruitment of additional γ-tubulin ring complexes. These changes are essential for the increased microtubule-nucleating activity. Activation of microtubule-dependent motor proteins leads to centrosomes separation from each other and causes the formation of the two spindle poles **(Fig. 1.22)**. Finally, each daughter cell inherits one centrosome (Reviewed in Nigg E. A., 2002).

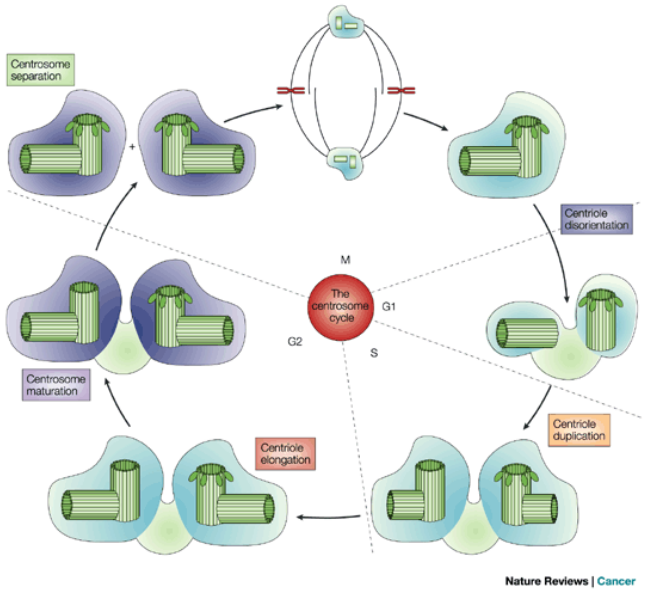

Figure 1.22. Centrosome duplication is coordinated with cell-cycle progression, during S phase, and the duplicated centrosomes are linked together until late G2 phase. At this point they separate to define the opposite spindle poles for mitotic spindle assembly. At the onset of mitosis, the PCM surrounding the centrioles dramatically increases in size and acquires the ability for microtubule nucleation and anchoring (centrosome maturation) (Nigg E. A., 2002).

Although the centrosome number is tightly regulated, solid as well as hematologic malignancies often harbour incorrect centrosome numbers (Anderhub S. J. et al., 2012). Interestingly, centrosome abnormalities were found to occur also in ovarian tumors. For this reason centrosome dysfunction may be an early event in ovarian carcinogenesis and could be involved in ovarian tumor progression (Hsu L.-C. et al., 2005).

Various mechanisms have been described to lead to centrosome amplification. Centriole overduplication and *de novo* formation results in increased number of extra centrioles, whereas cell fusion, mitotic skipping and cleavage failure lead to a duplicated DNA and centrosome numbers. Both overduplication and *de novo* centriole formation take place during S-phase whereas cleavage failure and mitotic skipping occur in mitosis (Anderhub S. J. et al., 2012).

Importantly, supernumerary centrosomes can lead to the formation of multipolar mitotic spindles, an abnormal mitotic arrangement which is believed to result in chromosome missegregation and aneuploidy (Anderhub S. J. et al., 2012). Extra centrosomes might be of advantage or disadvantage for tumorigenesis; on one hand, multiple centrosomes promote aneuploidy and enhance tumorigenesis, on the other hand, give rise to mitotic spindle multipolarity and high-grade genomic instability that lead to cell death. The

latter possibility might be detrimental for cell proliferation owing to mitotic arrest and failed cytokinesis (Fukasawa K., 2007; Ganem N. J. et al., 2009).

1.5.1.1 Centrosome clustering mechanism

The presence of more than two centrosomes within a cell could be the cause of spindle multipolarity during mitosis, increasing the number of spindle poles to which chromosomes can become attached. The outcome is the formation of more than two daughter cells that may be unviable because of the massive chromosomal loss (high-grade aneuploidy). Interestingly, however, cancer cells frequently harbour an increase number of centrosomes and still survive. In order to do that, cancer cells use multiple mechanisms to avoid spindle multipolarity. One such mechanism, termed centrosomal clustering, can prevent multipolar spindle formation by grouping the supernumerary centrosomes into two groups through the regulation of microtubule integrity, motor proteins (such as dynein and kinesin) and the SAC (Basto R. et al., 2008; Kwon M. et al., 2008; Quintyne N. J.et al., 2005; Yang Z. et al., 2008) **(Fig. 1.23)** (see paragraph 1.5.2.2). Centrosome clustering allows the formation of a 'pseudo-bipolar' mitotic spindle, which prevents multipolarity. Studies about clustering mechanism discovered the formation of a transient multipolar spindle intermediate before centrosome clustering mechanism activates (Ganem N. J. et al., 2009; Silkworth W. T. et al., 2009). During this brief multipolar state, there is an accumulation of merotelic kinetochore–microtubule attachments, which are not well recognized by the SAC mechanism (Ganem N. J. et al., 2009; Ogden A. et al., 2012). For this reason, when centrosome clustering works correctly, "low-grade" (viable cells) missegregation occurs and this minor aneuploidy is a characteristic that drives malignancy and tumor evolution (Holland A. J. et al., 2009). Several demonstrations indicate that centrosome amplification is an early event in carcinogenesis, because is an event present in precancerous and preinvasive lesions (D'assoro A. B. et al., 2002; Nigg E. A., 2006). On the contrary, in the absence of clustering, supernumerary centrosomes lead to the formation of multipolar mitosis, which may induce aneuploidy of a critically high grade. Cells in multipolar state may also arrest in mitosis and die through other mechanisms (Ganem N. J. et al., 2009). This type of error can threaten genomic

integrity and promote “high-grade” CIN because it causes both numerical and structural abnormalities (Guerrero A. A. et al., 2010).

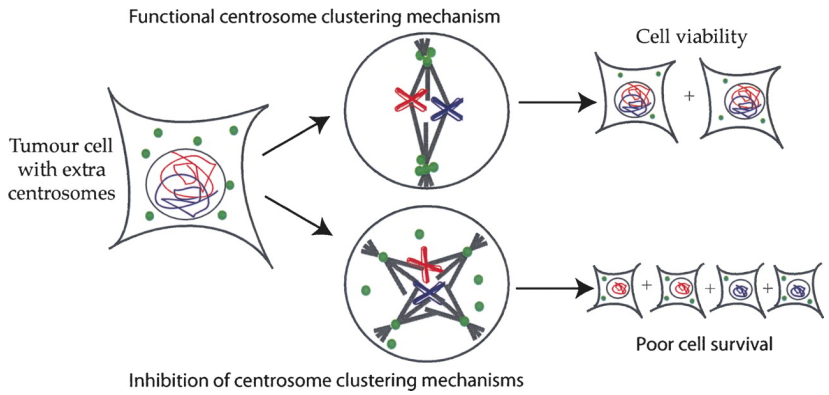

Figure 1.23. Centrosome clustering mechanism. Inhibition of centrosome clustering mechanisms may result in multipolar spindle assembly and abnormal cell division, leading to the production of low-viable progeny (Gergely F. and Basto R., 2008).

A model to explain this mechanism is to consider that the incorrect attachment between kinetochores and microtubules activates the SAC, which cause a mitotic delay (Basto R. et al., 2008; Chiroli E. et al., 2009; Foley E. A. and Kapoor T. M., 2013). During this period, the motor proteins generate forces to drive the extra centrosomes into two distinct groups (Kwon M. et al., 2008; Quintyne N. et al., 2005). Finally, the centrosomal clustering corrects the kinetochore–microtubule attachment errors to inactivate the SAC and induces spindle bipolarity (Fukasawa K., 2007; Marthiens V. et al., 2012).

Whereas cancer cells with extra centrosomes depend on clustering for survival, it is unnecessary to healthy human cells with normal centrosome number. Since clustering occurs specifically in cancer cells, the targeted inhibition of centrosome clustering mechanism is an opportunity for nontoxic chemotherapy. As shown before, clustering may provide survival advantages and promote malignancy through the acquisition of CIN via merotelic microtubule–kinetochore attachment and chromosomes missegregation (Ganem N. J. et al., 2009; Silkworth W. T. et al., 2009). Since multipolar mitosis induces “high-grade” spindle abnormalities that lead to lethality, declustering of supernumerary centrosomes to acquire multipolarity should specifically target cancer cells, unlike classical chemotherapy, without affecting healthy tissues. To

discover compounds that might inhibit centrosome clustering mechanism several molecules were screen for their ability to cause multipolarity in cancer cells harbouring extra centrosomes. One of these drugs is Griseofulvin, that is a nontoxic antifungal agent able to induce declustering in different human cancer cell lines in a concentration-dependent manner (Rebacz B. et al., 2007). Importantly, it suppresses proliferation of tumor cells at doses that are nontoxic to nontransformed cells. The antiproliferative effect of griseofulvin is due to its antimitotic action and its ability to induce declustering. The precise mechanism by which Griseofulvin realize declustering remains largely unknown but it is supposed to limit microtubule dynamicity and prevent clustering ability leading to declustering (Panda D. et al., 2005). Another drug, bromonoscapine, a derivative of the nontoxic, cough-suppressant drug, attenuates microtubule dynamic without impacting on their ultrastructure inducing centrosome declustering and multipolar mitosis formation (Karna P et al., 2011). The mechanism by which bromonoscapine attenuates microtubule dynamicity is currently under investigation. A third class of compounds is found to impact on centrosome clustering and is composed by some phenanthrene-derived poly-ADP-ribose polymerase (PARP) inhibitors (Castial A. et al., 2011). PARP-1 has a complex role in cancer since its expression is upregulated in different human tumors (Miwa M. and Masutani M., 2007) but downregulated in others (Tong W. M. et al., 2007). Treatment of tumors harbouring centrosome amplification with a phenanthrene-derived PARP-1 inhibitor induces clustering inhibition, spindle multipolarity and death by mitotic catastrophe (Castiel A. et al., 2011). Importantly, treatment of normal proliferating cells has no effect on spindle morphology, centrosome integrity, mitosis, or cell viability (Castiel A. et al., 2011). Considering that griseofulvin, bromonoscapine and PARP-1 inhibitors induce declustering, these drugs might have a great potential for cancer cell-specific chemotherapy. Contrary to classical chemotherapy, which leads to cell toxicity, declustering agents might overcome these side effects since declustering itself should not have any impact on normal cells, thus providing cancer cell-specific action. Considering the high frequency of amplified centrosomes in cancer cells, agents that induce spindle multipolarity might be a promising strategy as a non-toxic chemotherapeutics (Krämer A. et al., 2011). Importantly, the molecular mechanisms behind their functions remain yet to be determined.

1.5.2 Chromosomal Passenger Complex (CPC)

Chromosomal Passenger Complex (CPC) is an important complex since it regulates crucial events during mitosis, such as chromosome segregation and cytokinesis. It localizes to chromosomes during early mitosis and transfer to the spindle midzone during late mitosis (Earnshaw W. C. and Barnat R. L., 1991). CPC is composed by the enzymatic component Aurora B and the three regulatory and targeting components INCENP (Inner CENtromere Protein), Survivin (BIRC5) and Borealin (CDCA8) **(Fig. 1.24)** (Ruchaud S. et al., 2007; van der Waal M. S. et al., 2012). Importantly, the different CPC localization during mitosis ensures correct substrates phosphorylation. This process is essential in many functions such as chromosome condensation, correction of kinetochore–microtubule attachments errors, activation of the Spindle Assembly Checkpoint (SAC) and cytokinesis. If INCENP, Survivin, Borealin or Aurora B function and/or localization are altered, proper cell division is compromised (Adams R. R. et al., 2001a; Carvalho A. et al., 2003; Honda R. et al., 2003; Gassmann R. et al., 2004; Vader G. et al., 2006).

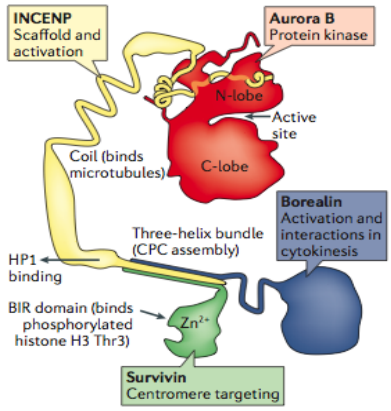

Figure 1.24. The Chromosomal Passenger Complex (CPC) components. A representation of the CPC, which is composed by Aurora B, Inner Centromere Protein (INCENP), Survivin and Borealin (Carmena M. et al., 2012).

CPC components are briefly shown below. **Inner CENtromere Protein (INCENP)** was the first member of the complex to be identified (Cooke C. A. et al., 1987).

INCENP functions as a scaffold protein that interacts with Aurora-B, Survivin and Borealin (Adams R. R. et al., 2000; Gassmann R. et al., 2004; Wheatley S. P. et al., 2001; Bolton M. A. et al., 2002; Chen J. et al., 2003). The C-terminus of INCENP is involved in the binding and regulation of Aurora B. **Survivin (BIRC5)** is a conserved member of the inhibitor of apoptosis protein (IaP) family and contains a single baculovirus IaP repeat (bIR) domain that serves for the dimerization of Survivin (Chantalat L. et al., 2000; Verdecia M. A. et al., 2000). Survivin can bind the other three components and is phosphorylated by Aurora B (Carvalho A. et al., 2003; Wheatley S. P. et al., 2004). **Borealin (CDCA8)** is phosphorylated by Aurora B *in vitro* (Gassmann R. et al., 2004) and it is regulated by phosphorylation at multiple sites (Hayama S. et al., 2007; Jelluma N. et al., 2008; Kaur H. et al., 2010; Date D. et al., 2012). **Aurora B (AURKB)** is a Ser/Thr kinase that is conserved from yeast to mammals (Terada Y. et al., 1998; Chan C. S. and Botstein D., 1993). Aurora B activation is a gradual and continuous process. First of all, Aurora B binds the IN box of INCENP, which activates low levels of kinase activity. This enables Aurora B to phosphorylate a C-terminal TSS (Thr-Ser-Ser) motif in INCENP (Honda R. et al., 2003; Bishop J. D. and Schumacher J. M., 2002) and the Thr232 in the T-loop of its kinase domain, resulting in its full activation (Sessa F. et al., 2005).

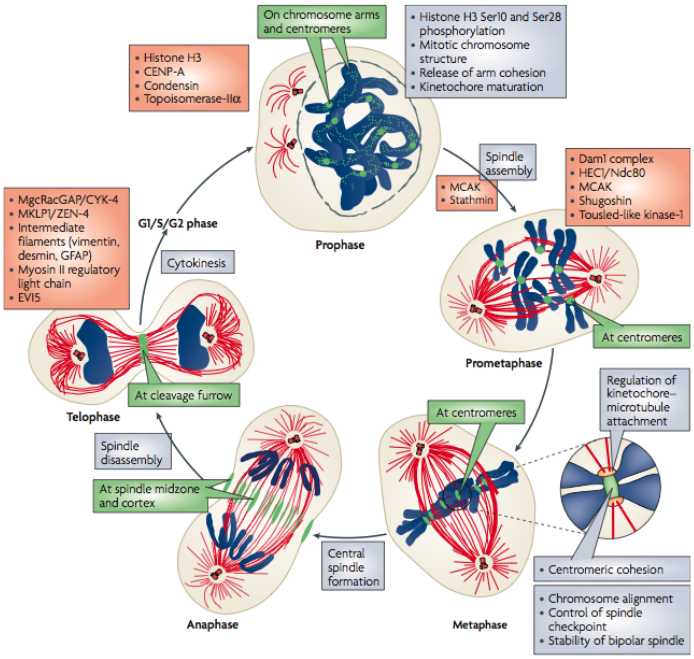

Figure 1.25. Localization and functions of Chromosomal Passengers Complex. Scheme of CPC localization (green), functions (grey boxes) and main targets (red boxes) during mitosis (Ruchaud S. et al., 2007).

During prophase CPC is localized on chromosome arms where it phosphorylates histone H3 on Serine 10 and 28 (Ser10 and Ser28) **(Fig. 1.25)**. Subsequently, on prometaphase and metaphase chromosomes it accumulates at centromeres. In this location CPC is essential for the correct formation of a bipolar spindle and its stability. Effectively, the CPC has a role in centromeric cohesion and in the correction of kinetochore–microtubule attachments errors. Moreover, in anaphase, the CPC translocates to the spindle midzone and at the cortex in which it has a role in the formation of the central spindle. Finally, in telophase, the CPC is enriched at the cleavage furrow and at the midbody, where it is involved in cytokinesis (Ruchaud S. et al., 2007).

1.5.2.1 CPC functions in kinetochore-microtubule attachments

As described before, Aurora B and CPC components localize at centromere until anaphase onset. Nicklas R. B. et al. provided direct evidence that attachments are stabilized through tension across the centromere (Nicklas R. B. and Koch C. A., 1969; Nicklas R. B. and Ward S. C., 1994). Studying budding yeast mutants with increased ploidy it was shown that Ipl1 (an homologues of Aurora B) promotes the turnover of attachments in the absence of tension (Tanaka T. U. et al., 2002). In addition, Aurora B inactivation by its inhibitors leads to stabilization of incorrect attachments (Hauf S. et al., 2003; Ditchfield C. et al., 2003). On the contrary, activation of Aurora B by removing the inhibitor activity leads to correction of attachment errors by destabilizing incorrect attachments (Lampson M. A. et al., 2004). These studies demonstrate that Aurora B phosphorylates kinetochore substrates in the absence of tension to destabilize incorrect attachments and allow the formation of new ones. Based on Nicklas R. B. experiments, phosphorylation of Aurora B substrate depends to tension. In line with this hypothesis it was found that the ability to sense tension relies on the spatial localization of Aurora B in close proximity to its substrates at the outer kinetochore. These observations suggest that a correct bi-oriented kinetochores separates Aurora B at the inner centromere from its outer kinetochore substrates, making the kinase less able to

phosphorylate and destabilize its substrates (Tanaka T. U. et al., 2002; Cimini D. et al., 2006; Andrews P. D. et al., 2004) **(Fig. 1.26)**.

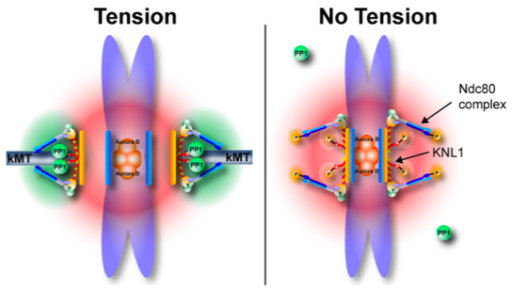

Figure 1.26. Model for the generation of a phosphorylation gradient. Aurora B is activated (dark red circles) at the inner centromere by auto-phosphorylation. In the low-tension state (incorrect attachments), Aurora B phosphorylates its substrates whereas in the high-tension state (correct attachments), Aurora B is spatially separated from its substrates. In contrast to Aurora B, recruitment of Protein Phosphatase 1 (PP1) to the outer kinetochore produces a counteracting gradient of dephosphorylation (Liu D. et al., 2010).

Thus, a phosphorylation gradient is generated by concentration of Aurora B at the inner centromere **(Fig. 1.26)**. In low-tension state due to incorrect attachments, Aurora B phosphorylates KNL1 and NDC80, two kinetochore proteins, which lead to reduced binding of PP1 and microtubules to kinetochores. When tension is achieved in correctly bi-oriented kinetochores, Aurora B is spatially separated from kinetochores substrates, so KNL1 and NDC80 are dephosphorylated and the binding of PP1 and microtubules is increased, leading to microtubule-kinetochore attachment stabilization (Liu D. et al., 2010; Lampson M. A. et al., 2011).

The crucial functions of the CPC are directly associated to its localization. The normal changes in localization is key for regulating the orderly mitotic exit by suppressing Aurora B activity at the location where its functions are no longer needed while enhancing Aurora B activity at new locations in which it becomes essential. Microtubule-kinetochore correction is possible only if Aurora B is present at centromere and is activated. During late S phase, CPC is found on pericentromeric heterochromatin involving Heterochromatin Protein 1 (HP1) binding to INCENP (Cooke C. A. et al., 1987; Ainsztein A. M. et al., 1998; Nozawa R.-S. et al., 2010). Subsequently, the CPC enriches at the inner centromere after Aurora B phosphorylation on histone H3 Ser10

(H3-S10) that causes CPC dissociation from chromosome arm during metaphase to anaphase transition (Fischle W. et al., 2005; Hirota T. et al., 2005) **(Fig. 1.27)**. This process depends also from the interaction of Survivin and Borealin with centromere-specific histone markers created by other kinases (Kelly A. E. et al., 2010; Wang F. et al., 2010).

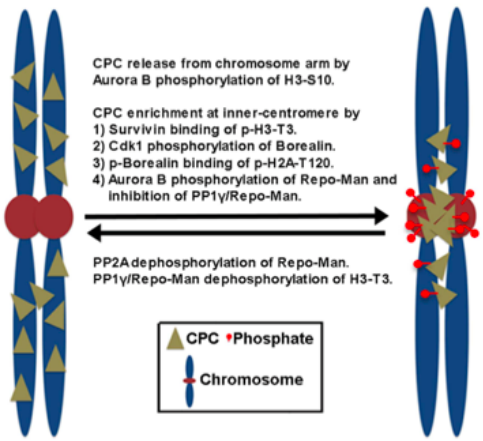

Figure 1.27. Mechanisms of CPC accumulation at the inner centromeres. Phosphorylation of histone H3 on Ser10 (H3-S10) mediated by Aurora B detaches the CPC from the chromosome arm leading to its enrichment at the inner centromeres. This also involves the interaction of Survivin and Borealin with the centromere-specific phosphorylated histone markers (p-H3-T3, p-H2A-T120) in this location. On the contrary, PP1γ/Repo-Man phosphatase dephosphorylates the histone makers at the chromosome arm (Kitagawa M. and Lee S. H., 2015).

Phosphorylation of Borealin and Survivin, through Cdk1 and Haspin kinase activity respectively, are key for their binding to the phosphorylated histone H2A on Thr120 (H2A-120) and phosphorylated histone H3 on Thr3 (H3-T3) (Kawashima S. A. et al., 2010; Tsukahara T. et al., 2010; Kelly A. E. et al., 2010; Wang F. et al., 2010). H2A-T120 and H3-T3 phosphorylation marks overlap at the inner centromeres, explaining how the CPC levels increases at this site (Yamagishi Y. et al., 2010). On the other hand, PP1 together with Repo-Man acts antagonistically to Haspin and dephosphorylates H3-T3 at the chromosome arm but not at the centromere. This because Aurora B phosphorylation of Repo-Man at centromere prevents PP1/Repo-Man recruitment at this location (Qian J. et al., 2013). These data demonstrate that Aurora B and PP1 opposing activities are crucial for the targeting of CPC from chromosome arm to centromere where its functions are needed for proper chromosome segregation.

1.5.2.2 CPC and centrosome clustering mechanism

As previously cited (see paragraph 1.5.1.1) several mechanisms are involved in the correct clustering of extra centrosomes **(Fig. 1.28)**.

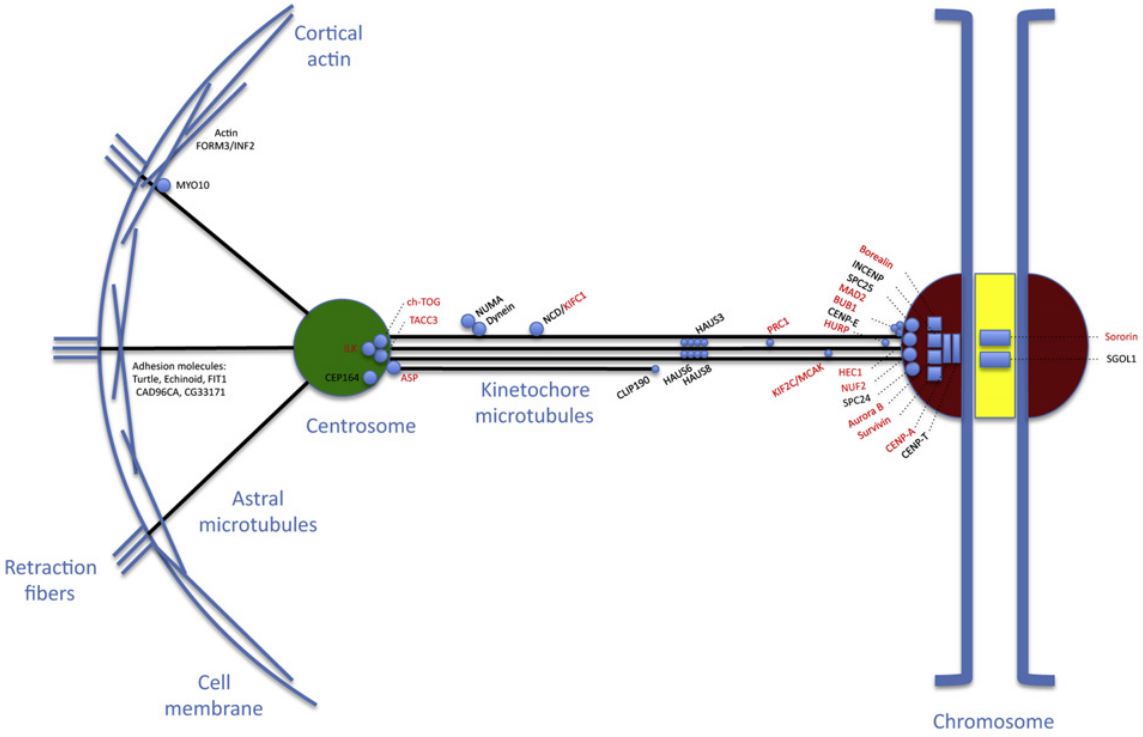

Figure 1.28. Proteins and mechanisms involved in centrosome clustering. Proteins colored in red are overexpressed in human cancer cells (Krämer A. et al., 2011).

An additional important mechanism relies on the activation of MAD2-dependent delay of anaphase onset, which is essential for a functional centrosome clustering and to prevent multipolar mitosis, in cell harbouring extra-centrosomes (Basto R. et al., 2008; Kwon M. et al., 2008; Yang Z. et al., 2008). MAD2 is an important component of the spindle assembly checkpoint (SAC) since it inhibits dissolution of sister chromatids until microtubule attachment at kinetochores is complete and spindle tension is established (Weaver B. A. et al., 2007). Thus, multipolarity is associated with incorrect kinetochore attachment or insufficient tension that activates the SAC leading to metaphase arrest. Interestingly, more recently other proteins involved in centrosome clustering were discovered using genome-wide RNAi screening in human cancer cells

with extra centrosomes. All CPC components, Aurora B, INCENP, Borealin and Survivin, were found to be involved in this process, suggesting a crucial role for such a complex in centrosome clustering (Leber B. et al., 2010). Since CPC activity at the kinetochore is necessary for the correction of merotelic kinetochore-microtubule attachments, which, as long as uncorrected, cause reduced spindle tension, it seems that spindle tension itself plays a crucial role in this process (Kwon M. et al., 2008; Leber B. et al., 2010). Effectively, chromatids attachments to microtubules of opposite spindle poles are obtained through a trial-and-error process in which the correct ones exert tension across the centromere, stabilizing kinetochore-microtubule interactions. On the other hand, incorrect attachments apply less tension and are destabilized, providing a new opportunity to bi-orient (Liu D. et al., 2009). Altogether, these findings confirm the idea that loss of centromere tension by different mechanisms results in centrosome declustering.

1.5.2.3 CPC and cancer

Several proteins of the CPC including Aurora B, Survivin and Borealin have been found to be overexpressed in several types of cancer (Carmena M. and Earnshaw W. C., 2003; Bischoff J. R. et al., 1998; Adams R. R. et al., 2001b; Altieri D. C., 2003; Chang J. L. et al., 2006; Hayama S. et al., 2006; Ferretti C. et al., 2010; Nguyen M.-H. et al., 2010; Tsou A. P. et al., 2003). In addition, an increased expression of Aurora B has been associated with tumor formation in mouse models (Diaz-Rodriguez E. et al., 2008; Nguyen H. G. et al., 2009). These observations and findings have already led to the development of specific and strong inhibitors of Aurora B kinase, which are currently in phase I and II clinical trials for several malignancies (Taylor S. and Peters J. M., 2008). Altogether, these data suggest that proteins involved in the “centrosome clustering mechanism” in cancer cells with extra centrosomes are often overexpressed in human cancers, suggesting that clustering of these centrosomes into a pseudo-bipolar spindle might be crucial for cancer cell survival and thus tumor progression.

2. AIM OF THE THESIS

Embryonic stem cells (ESCs) are of great interest as a model system for studying early developmental processes and because of their potential similarities with cancer. Recently we discovered a new connection between a stemness factor, Oct4, and a tumorsuppressor factor, pRb, in mouse ESCs (mESCs). We showed that Oct4 drives the expression of NIPP1 and CCNF, both efficient inhibitors of Protein Phosphatase 1 (PP1), the major pRb phosphatase in mESCs. Consequently, Oct4 expression protects hyper-phosphorylated pRb from dephosphorylation by PP1, resulting in its enzymatic inactivation. This leads to an accumulation of hyper-phosphorylated pRb that allows the maintenance of stemness features in mESCs (Schoeftner S. and Scarola M. et al., 2013).
Since stem cells and cancer cells share some properties related to self-renewal and problems during differentiation process, understanding the mechanisms that control self-renewal and pluripotency of ESCs could be useful in finding common pathways between ESCs and cancer, that will finally provide new inroads into the development of novel therapeutic treatments. Interestingly, human cancers with "embryonic stem cell signature" display common features with embryonic stem cells, such as self-renewal and the maintenance of an undifferentiated state, as well the expression of stemness marker genes OCT4, SOX2 and NANOG (Glinsky G. V., 2008; Kim J. and Orkin S. H. et al., 2011). Recently, several groups reported that expression signatures specific to ESCs are also found in many human cancers and in mouse cancer models, suggesting that these shared features might be crucial in cancer biology (Kim J. and Orkin S. H. et al., 2011).
Oct4 (Oct3/4 or POU5F1) is a member of the POU family of transcription factors and is known to play a crucial role in the maintenance of self-renewal and pluripotency in ESCs. Nowadays, several studies highlight the importance of sustaining OCT4 expression by tumors in order to maintain the tumorigenic stem cell-like characteristics. Despite the essential role of Oct4 during embryogenesis and reprogramming of somatic cells, its exact role in tumorigenesis is still not well defined. We consequently hypothesize that the OCT4-NIPP1/CCNF-PP1-pRB axis, found in an embryonic stem cell context, could have a role in specific subtype of human cancers with stemness

features, in maintaining tumour self-renewal and contribute to a poorer prognosis in ovarian cancer patients.

Therefore, the aim of this thesis work was to unveil the biological functions of the OCT4-NIPP1/CCNF-PP1-pRB axis in a cancer context and translate this pathway into clinical interest.

3. RESULTS

We recently demonstrated that OCT4 controls the cell cycle program of self-renewing mouse Embryonic Stem Cells (mESCs) by protecting tumor suppressor protein pRB from dephosphorylation by the Protein Phosphatase 1 (PP1) complex. Particularly, OCT4 drives the expression of two important inhibitors of PP1, NIPP1 and CCNF, leading to pRB hyper-phosphorylation, a crucial feature of mESCs that permits rapid cell divisions and the maintenance of self-renewal (Schoeftner S. and Scarola M. et al., 2013) **(Fig 3.1)**.

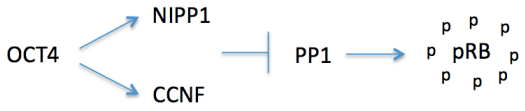

Figure 3.1. Working model. The pluripotency transcription factor OCT4 directly up-regulates the expression of NIPP1 and CCNF that inhibit protein phosphatase PP1 activity, resulting in pRB hyper-phosphorylation.

3.1 The OCT4-NIPP1/CCNF-PP1 axis mediates pRB hyper-phosphorylation and poor survival in High-Grade Serous Ovarian Cancer (HG-SOC)

Firstly, to understand the impact of the OCT4-NIPP1/CCNF-PP1-pRB axis in human cancer context, we screened a panel of human ovarian, prostate, non-small lung, osteosarcoma, breast and cervical cancer cell lines for the expression of the specific variant related to stemness *OCT4A* mRNA and we showed that ovarian cancer cell lines expressed the highest levels of this gene compared to other cancer cell lines **(Fig. 3.2A)**. Public gene expression data (Klijn C. et al., 2014) confirmed that ovarian cancer cell lines have the higher *OCT4* expression levels compared to cells from other cancer types **(Fig. 3.2B)**. As expected, consistent with their origin, embryonic carcinoma cells (NTERA2) show the highest *OCT4* expression **(Fig. 3.2C)**. Since OVCAR-3 cell line is a well-classified High-Grade Serous Ovarian Cancer (HG-SOC) (Mitra A. K. et al.,

2015), which reflects the most frequent type of ovarian malignancies, we decided to use this cell line as a model system to study the relevance of the axis in human cancer context.

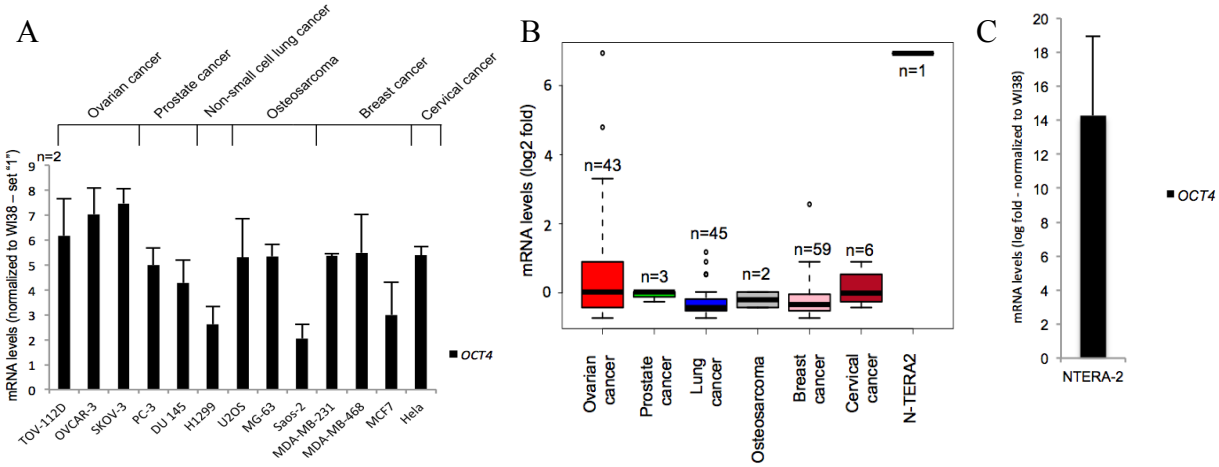

Figure 3.2. **(A)** Determination of *OCT4* (variant A) expression levels in human cancer cell lines. Left panel, mRNA quantification using specific *OCT4* variant 1 oligos by quantitative real-time PCR. *OCT4* levels were normalized against WI38 cells (values set "1"). **(B)** *OCT4* mRNA expression in cancer cell lines (public gene expression database, EGAS00001000610) (Klijn C. et al., 2014). **(C)** Quantitative real-time PCR analysis of *OCT4* mRNA levels in NTERA-2 cells. *OCT4* levels were normalized to human fibroblast cell line WI38 (value set "1"). n, number of independent experiments carried out; error bars indicate s.d.; a Student's t test was used to calculate significance values: *, $p < 0.05$; **, $p < 0.01$; ***, $p < 0.001$.

We confirmed in OVCAR-3 cell line the activity of the axis transfecting siRNA oligos against *OCT4* mRNA, that resulted in reduced expression of OCT4 target genes *NIPP1* and *CCNF* (**Fig. 3.3A**). This effect was recapitulated by contemporary knock-down of the OCT4 target genes *NIPP1/CCNF* (**Fig. 3.3A).** Same results were obtained using a different siRNA targeting another sequence of *OCT4* mRNA **(Fig. 3.3 B)**.

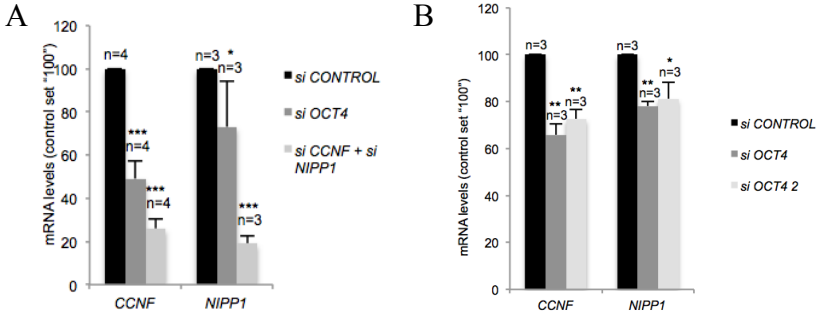

Figure 3.3. **(A)** Quantitative real-time PCR analysis of *CCNF* and *NIPP1* mRNA levels after transient knock-down of *OCT4* or *NIPP1*/*CCNF* in OVCAR-3 cells. Control siRNA value was set "100". Expression levels were normalized against *ACTIN*. **(B)** Real-time PCR analysis of *CCNF* and *NIPP1* expression of OVCAR-3 cells transiently transfected with two different siRNAs targeting *OCT4*. Control siRNA values were set "100". mRNA levels were normalized against *ACTIN*. n, number of independent experiments carried out; error bars indicate s.d.; a Student's t test was used to calculate significance values: *, $p < 0.05$; **, $p < 0.01$; ***, $p < 0.001$.

Importantly, pRB-T356 (target site of PP1) phosphorylation is reduced in *OCT4* or *NIPP1/CCNF* knock-down OVCAR-3 cells as well as using another siRNA targeting difference sequence on *OCT4* mRNA **(Fig. 3.4A and B)**. pRB-T356 phosphorylation was rescued by depleting *PP1β* in *OCT4* knock-down cells **(Fig. 3.4A)**. This demonstrates that the OCT4-NIPP1/CCNF-PP1 axis increases pRB phosphorylation status in OVCAR-3 cells by impairing PP1 function.

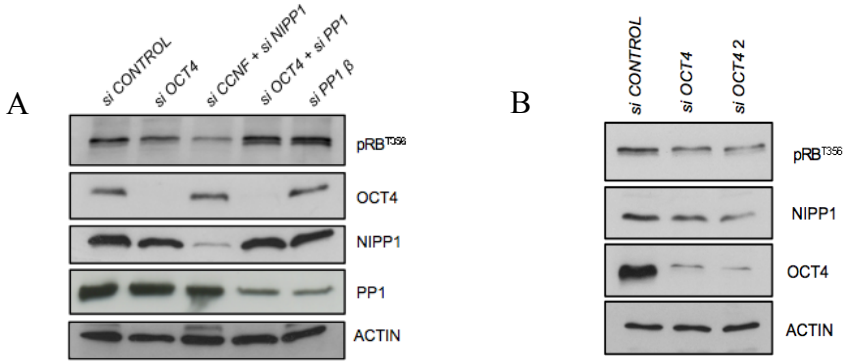

Figure 3.4. **(A)** Western blotting analysis of experimental cells using phospho pRB-T356, NIPP1 and OCT4 antibodies. ACTIN was used as a loading control. **(B)** Phospho pRB-T356, OCT4, NIPP1 and PP1 protein levels in OVCAR-3 transiently transfected with the indicated siRNAs oligos, as determined by western blotting. ACTIN was used as a loading control.

Performing immunofluorescence experiments we showed that OCT4 expression is extremely heterogeneous in OVCAR-3 cells **(Fig. 3.5)**.

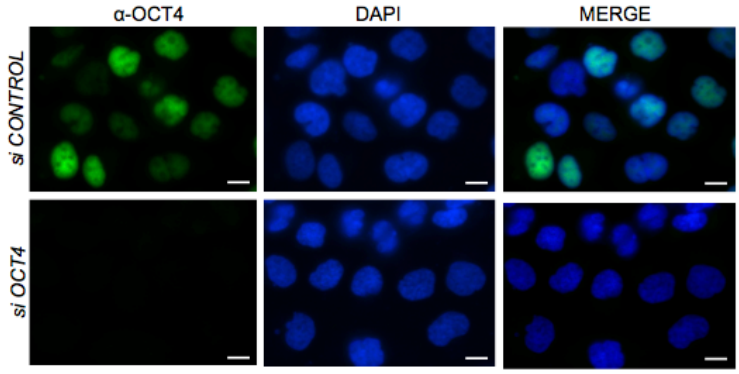

Figure 3.5. Immunofluorescence analysis of OCT4 expression in OVCAR-3 cell line 3 days after transfection of siRNA targeting *OCT4*.

A tumour mass is presumably composed by several types of cells that could express different endogenous OCT4 levels. These fluctuations could tightly modulate the activation of the axis and, therefore, influencing key features in EOC. This finding enables us to select three subclones, called hereafter subclone 11, 4 and 9, expressing low, intermediate and high OCT4 protein and mRNA levels, respectively **(Fig. 3.6A, B and C)**. Importantly, high endogenous levels of OCT4 are associated to increasing levels of NIPP1 and, therefore, of the hyper-phosphorylated form of pRB **(Fig. 3.6 A)**. This demonstrates that pRB phosphorylation levels are OCT4 dosage sensitive.

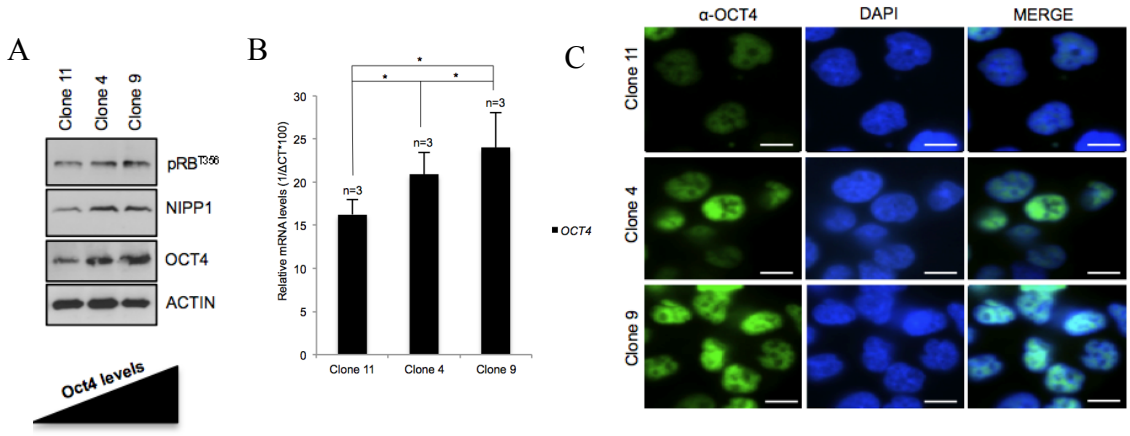

Figure 3.6. **(A)** Western blotting of phospho pRB-T356, OCT4, NIPP1 of OVCAR-3 subclones 11, 4 and 9. ACTIN was used as a loading control. **(B)** Relative *OCT4* mRNA levels (1/ΔCT*100) of OVCAR-3 subclones 11, 4 and 9 as determined by real-time PCR. mRNA levels were normalized against *ACTIN*. **(C)** Right panel, immunofluorescence of OCT4 of OVCAR-3 subclones 11, 4 and 9. n, number of independent experiments carried out; error bars indicate s.d.; a Student's t test was used to calculate significance values: *, $p < 0.05$; **, $p < 0.01$; ***, $p < 0.001$.

In line with our findings in the parental OVCAR-3 cell pool, we showed that knock-down of *OCT4* or *NIPP1/CCNF* results in decreased pRB-T356 phosphorylation in all OVCAR-3 subclones (**Fig. 3.7**). Of notice, again NIPP1 and pRB-T356 phosphorylation levels are dose-OCT4 dependent **(Fig. 3.7)**.

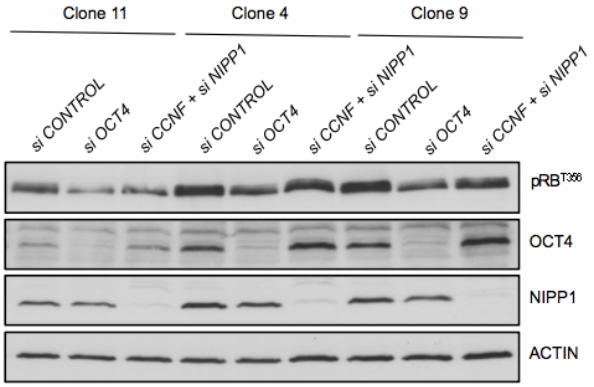

Figure 3.7. Western blotting of phospho pRB-T356, OCT4, NIPP1 in OVCAR-3 subclones 11, 4 and 9 after 3 days of transfection with the indicated siRNAs. ACTIN was used as a loading control.

Together, these data provide solid evidence that pRB phosphorylation levels are tightly controlled by the OCT4-NIPP1/CCNF-PP1-pRB axis in HG-SOC cells.

Using serous ovarian cancer data from the ovarian dataset derived from The Cancer Genome Atlas (TCGA) project we found a positive correlation between *NIPP1*/*CCNF* or *NIPP1*/*CCNF*/*OCT4* mRNA expression levels and pRB phosphorylation levels at the PP1 target sites pRB-S807 and pRB-T356, thus confirming our *in vitro* data (**Fig. 3.8A and B**).

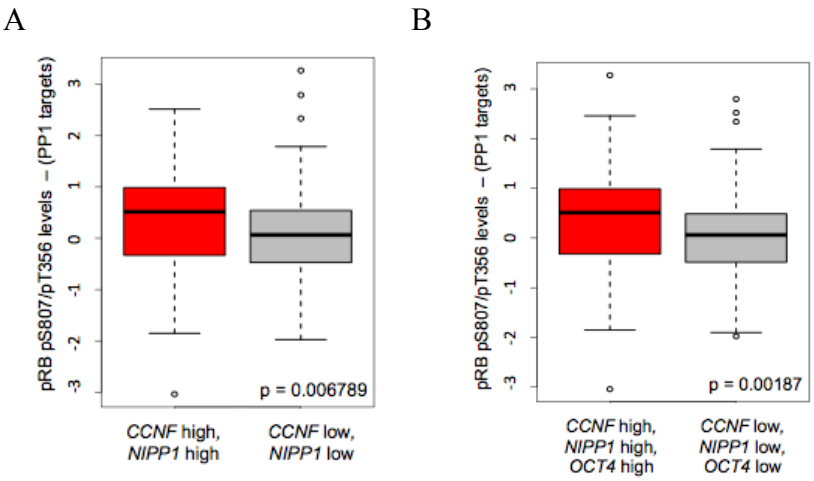

Figure 3.8. TCGA data set analysis correlating axis genes expression with phosphorylation levels at PP1 phosphorylation target sites in pRB-S807 and T356 (n=261). **(A)** Correlation of *NIPP1* and *CCNF* expression at the indicated PP1 phosphorylation target sites. **(B)** Correlation of *NIPP1*, *CCNF* and *OCT4* at the indicated PP1 phosphorylation target sites. Phosphorylation levels were normalized against overall amount of pRB protein levels. Each box signifies the upper and lower quartiles of data, the whiskers extend to the most extreme data points (minimum and maximum points); median is represented by a short line within the box. A Linear model regressions test was used to calculate significance values: *, $p < 0.05$; **, $p < 0.01$; ***, $p < 0.001$.

TCGA dataset also revealed that pRB- T356 and T807, another known PP1 target site, phosphorylation levels positively correlate with *RB1* mRNA expression levels in HG-SOC (p=0.03; **Fig. 3.9A**). This allowed us to create Kaplan-Meier survival curves using *RB1* mRNA expression as substitute marker for pRB phosphorylation levels. Importantly, we found that HG-SOC patients with increased *NIPP1/CCNF* expression display a significantly reduced overall survival (OS; p=0.008) that is even more significant when high *RB1* mRNA expression was added as additional parameter into the analysis (OS; $p=1.39e^{-05}$) (**Fig. 3.9B and C**). We conclude that the OCT4-NIPP1/CCNF-PP1 axis promotes the inactivation of the Retinoblastoma pathway, resulting in reduced HG-SOC patient overall survival.

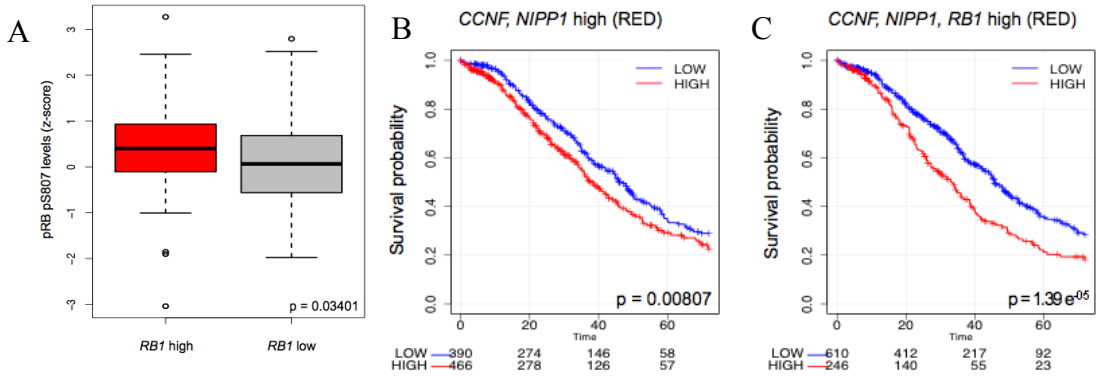

Figure 3.9. **(A)** TCGA data set analysis. *RB1* mRNA expression correlates with high phosphorylation at the PP1 target sites pRB (S807/T356). **(B)** Kaplan-Meier survival curve of overall survival (OS) for ovarian cancer patients who were classified according to the expression of *CCNF* and *NIPP1* genes. **(C)** Kaplan-Meier survival curve of OS according to the expression of *CCNF*, *NIPP1* and *RB1* genes. Due to the non-specificity of OCT4 probe we were not able to include OCT4 in Kaplan-Meier analysis. A Linear model regression test (A) and a Log-Rank test (B and C) were used to calculate significance values: *, $p < 0.05$; **, $p < 0.01$; ***, $p < 0.001$.

3.2 The OCT4-NIPP1/CCNF-PP1-pRB axis promotes cell proliferation and tumorigenic potential

According to our previous studies in mESCs (Schoeftner S. and Scarola M et al., 2013), we decided to investigate the effect of the axis depletion in terms of cell proliferation and the ability to growth in an anchorage-independent condition. First of all, RNAi mediated depletion of the main components of the axis caused a reduction in cell doubling time obtained by growth curve experiments and classical proliferation expression markers *PCNA* and *MKI67* (ki-67) **(Fig. 3.10A and B)**.

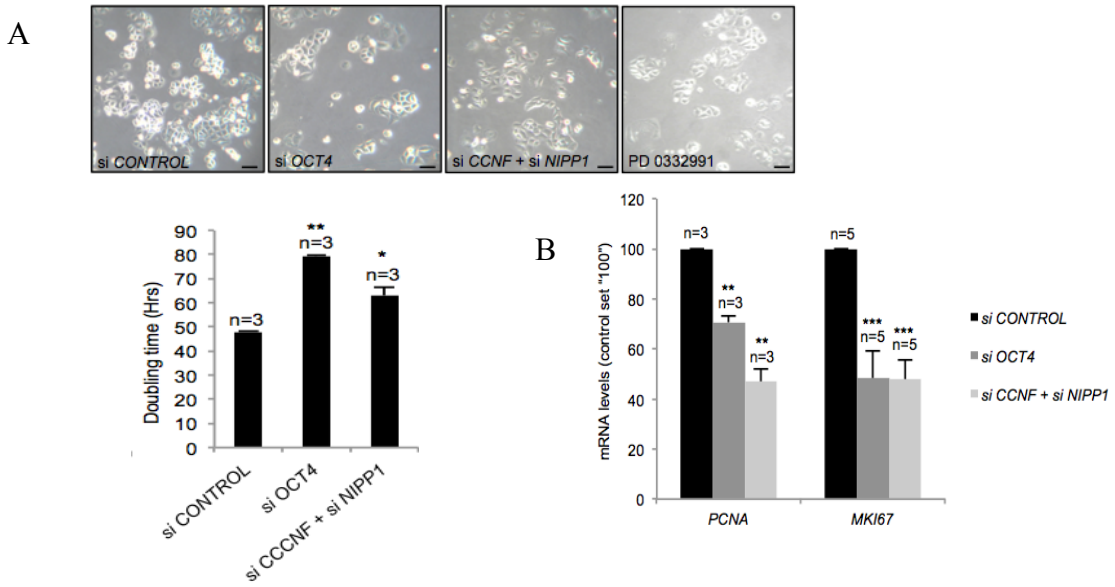

Figure 3.10. The OCT4-NIPP1/CCNF-PP1 axis disruption impairs cell proliferation in OVCAR-3. **(A)** Top, representative images of OVCAR-3 cell line transiently transfected with the indicated siRNAs oligos. Bottom, Proliferation of OVCAR-3 cells transiently transfected with indicated siRNAs. **(B)** Quantitative real-time PCR analysis of *PCNA* and *MKI67* (Ki-67) in OVCAR-3 cells transiently transfected with siRNAs targeting *OCT4* or *CCNF*/*NIPP1*. Control siRNA values were set "100". mRNA levels were normalized against *ACTIN*. n, number of independent experiments carried out; error bars indicate s.d.; a Student's t test was used to calculate significance values: *, $p < 0.05$; **, $p < 0.01$; ***, $p < 0.001$.

Consistent with these data, siRNA mediated-depletion of *OCT4* and *NIPP1*/*CCNF* resulted in a strong decrease of the percentage of cells able to incorporate BrdU **(Fig. 3.11)**, indicating that these cells are cease to further divide.

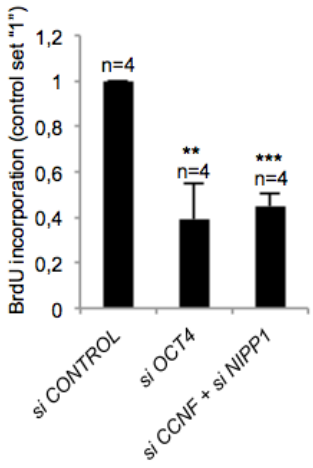

Figure 3.11. Percentage of BrdU-positive cells. Control siRNA value was set "1". n, number of independent experiments carried out; error bars indicate s.d.; a Student's t test was used to calculate significance values: *, $p < 0.05$; **, $p < 0.01$; ***, $p < 0.001$.

Importantly, the treatment with a Cdk4/6 inhibitor (namely PD 0332991 or Palbociclib), already demonstrated to efficiently inhibit pRB phosphorylation **(Fig. 3.12A)** (Fry D. W. et al., 2004), recapitulates the same effects of *OCT4* and *NIPP1*/*CCNF* silencing in terms of doubling time and BrdU incorporation **(Fig. 3.12B and C)**, further enforcing the relevance of the OCT4-pRB connection. Of notice, this treatment did not impact on OCT4 or NIPP1 protein levels, thus supporting the notion that PD 0332991 impairs cell proliferation by reducing pRB phosphorylation levels **(Fig. 3.12A)**.

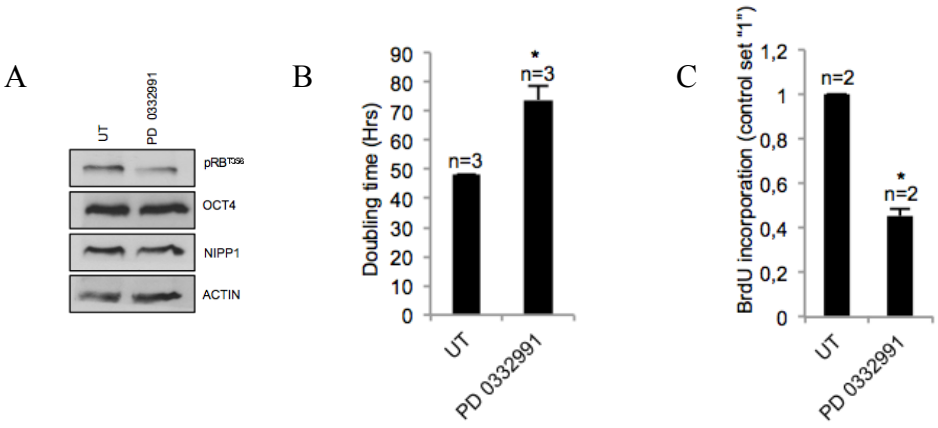

Figure 3.12. **(A)** Western blotting analysis of OVCAR-3 cells treated with PD 0332991 for phospho pRB-T356, OCT4 and NIPP1. ACTIN was used as a loading control. **(B and C)** Doubling time and BrdU incorporation rate of OVCAR-3 cells transiently transfected with indicated siRNAs or after treatment of PD 0332991. n, number of independent experiments carried out; error bars indicate s.d.; a Student's t test was used to calculate significance values: *, $p < 0.05$; **, $p < 0.01$; ***, $p < 0.001$.

In agreement with the OCT4 driven activation of the axis and pRB hyper-phosphorylation, doubling time and BrdU incorporation rate in OVCAR-3 subclones 11, 4 and 9, are found to positively correlate with endogenous OCT4 levels **(Fig. 3.13A, B and C)**. Together, these data indicate that OCT4 and NIPP1/CCNF promote OVCAR-3 cell proliferation by driving the enzymatic inactivation of pRB.

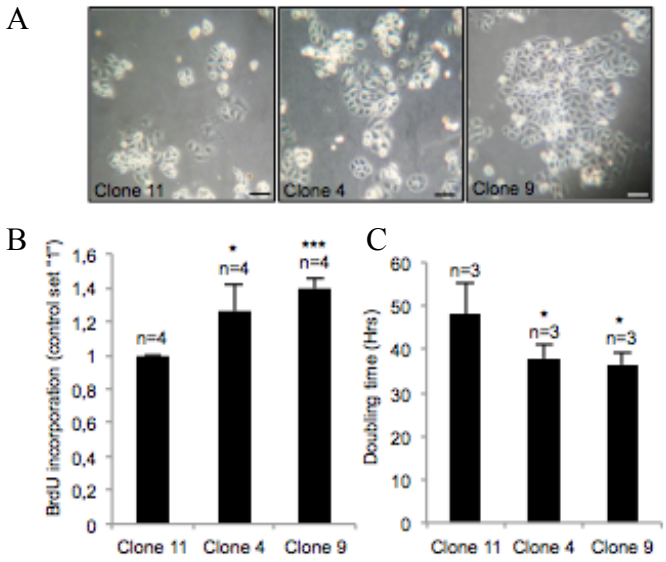

Figure 3.13. Proliferation of OVCAR-3 subclones 11, 4 and 9. **(A)** Representative images of subclones plated at the same concentration three days before. **(B)** Percentage of BrdU-positive cells in culture of OVCAR-3 subclones. Control siRNA value was set "1". **(C)** Doubling time of experimental cells. n, number of independent experiments carried out; error bars indicate s.d.; a Student's t test was used to calculate significance values: *, $p < 0.05$; **, $p < 0.01$; ***, $p < 0.001$.

To understand the impact of the axis on *in vitro* tumorigenic potential of OVCAR-3 cells we performed soft agar colony forming assays to analyse the ability to growth in an anchorage-independent condition. We found that siRNA mediated knock-down of *OCT4* or *NIPP1*/*CCNF* in parental OVCAR-3 pool resulted in strongly reduced colony number and size (**Fig. 3.14A and B**). These effects were recapitulated by PD 0332991 treatment (**Fig. 3.14A and B**)

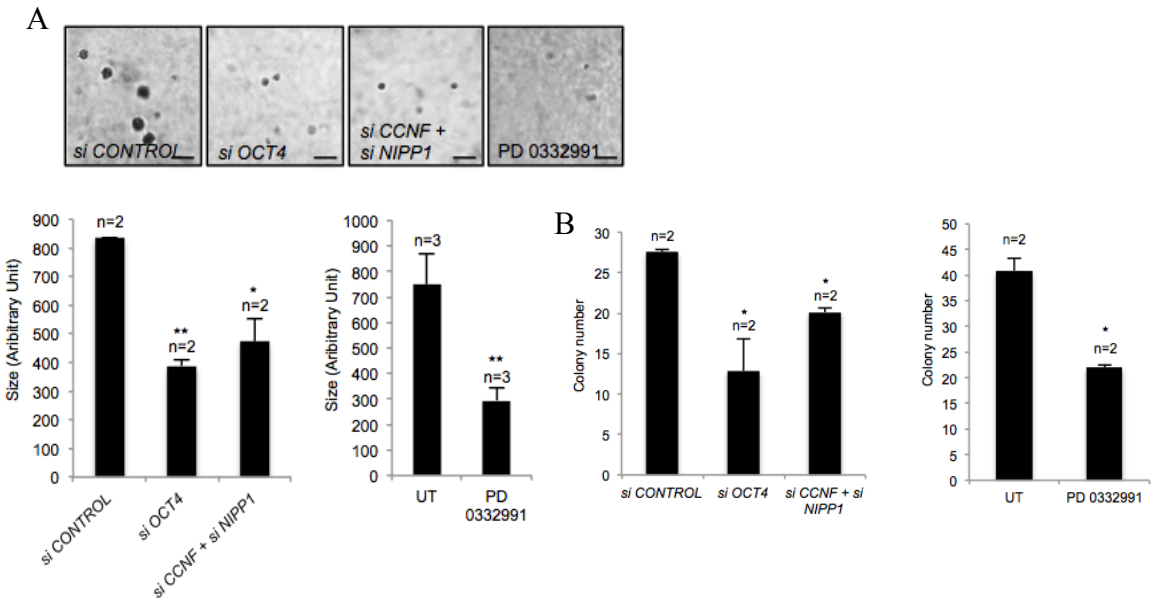

Figure 3.14. **(A)** Bottom panel, soft agar assay of OVCAR-3 cells transiently transfected with the indicated siRNAs oligos or treated with PD 0332991. Colony size is indicated. Top panel, representative images of OVCAR-3 colonies. **(B)** Left panel, quantification of colony number of experimental cells. Right panel, OVCAR-3 cells treated with PD 0332991 quantified for soft agar colony numbers. n, number of independent experiments carried out; error bars indicate s.d.; a Student's t test was used to calculate significance values: *, $p < 0.05$; **, $p < 0.01$; ***, $p < 0.001$.

We next asked whether a dysfunctional axis could affect the ability to growth in an anchorage-independent condition in OVCAR-3 subclones. Importantly, differential axis activation in subclones 11, 4 and 9 reflects a corresponding increase in colony size and numbers **(Fig. 3.15A and B)**.

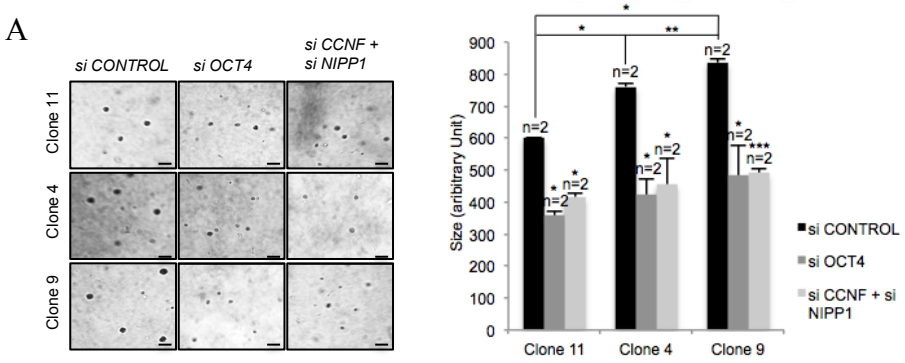

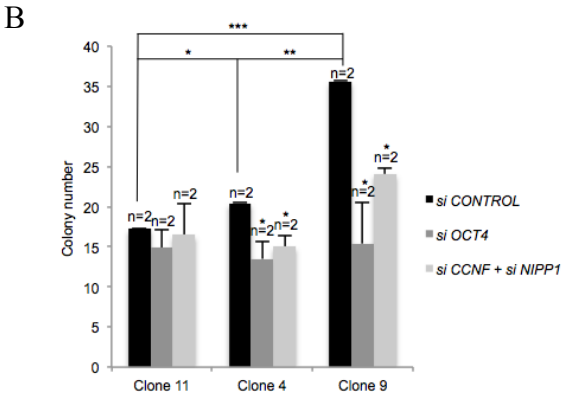

Figure 3.15. **(A)** Right panel, colonies size of OVCAR-3 subclones 11, 4 and 9 transiently transfected with the indicated siRNAs oligos and plated in soft-agar. Left panel, representative images of soft agar colonies in each condition. **(B)** Quantification of colony number of OVCAR-3 subclones 11, 4 and 9 transiently transfected with the indicated siRNAs oligos. n, number of independent experiments carried out; error bars indicate s.d.; a Student's t test was used to calculate significance values: *, $p < 0.05$; **, $p < 0.01$; ***, $p < 0.001$.

Finally, we took advantage of OVCAR-3 subclone 11 that express endogenously low levels of the axis component to transient overexpressed an HA-epitope tagged OCT4 or HA-CCNF/NIPP1: in these conditions we observed a significant increased of tumorigenic potential of transfected subclone 11 cells in soft agar assays **(Fig. 3.16A and B)**.

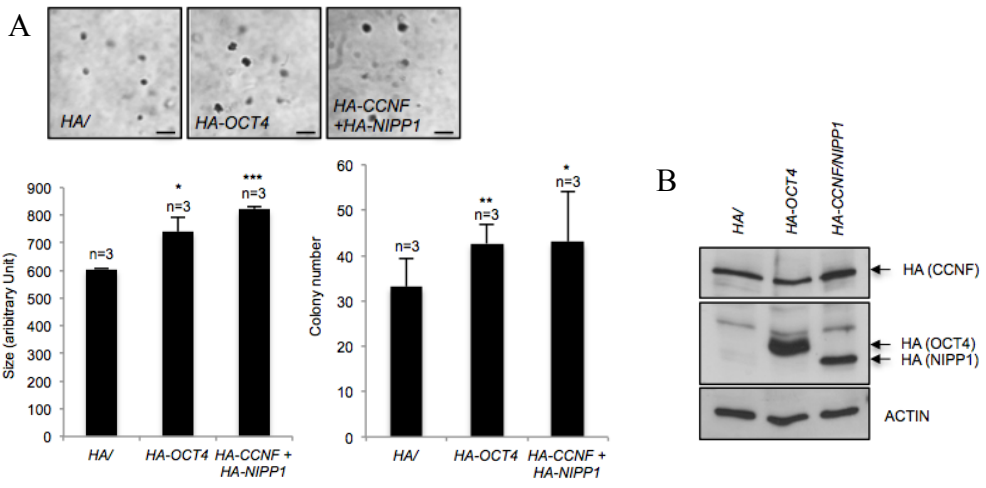

Figure 3.16. **(A)** Soft-agar assay of OVCAR-3 subclone 11 transiently overexpressing *HA-OCT4* or both *HA-CCNF* and *HA-NIPP1*. Top panel, representative images of subclone 11 in each condition. Bottom panel, analysis of soft-agar assay size and numbers of OVCAR-3 subclone 11 transiently overexpressing *HA-OCT4* or both *HA-CCNF* and *HA-NIPP1*. **(B)** Left panel, anti-HA western blotting showing expression of CCNF, OCT4 and NIPP1-tagged protein in experimental cells. ACTIN was used as a loading control. n, number of independent experiments carried out; error bars indicate s.d.; a Student's t test was used to calculate significance values: *, $p < 0.05$; **, $p < 0.01$; ***, $p < 0.001$.

Since the most important feature of ovarian cancer cells is the ability to survive and form multicellular aggregates (spheroids) in the ascitic fluid, leading to a fast dissemination and metastasis in the entire peritoneal cavity, we decided to generate 3-dimensional (3D)-suspension cultures that mimic the ascites microenvironment. To this aim we generated OVCAR-3 cancer cell spheroids (Material and Methods) to address the impact of the OCT4-NIPP1/CCNF-pRB axis in an *in vitro* condition that better resembles multicellular spheroids found in ovarian cancer ascites *in vivo*. We found that ectopic OCT4 expression in OVCAR-3 subclone 11 results in a significantly increased size of cancer-cell spheres **(Fig. 3.17A and B)**.

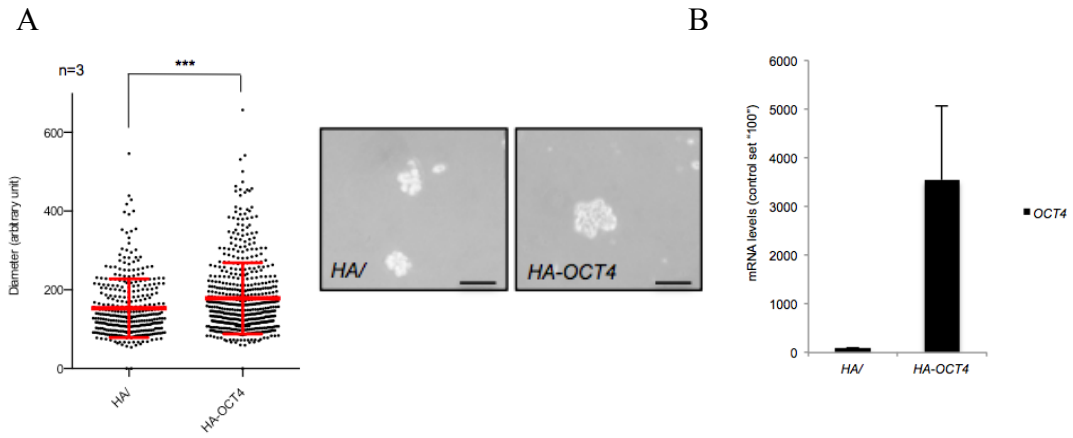

Figure 3.17. **(A)** Cell spheroids derived from OVCAR-3 subclone 11 stably overexpressing HA-epitope tagged OCT4. Left panel, diameter of experimental cells. Right panel, representative images of subclone spheroids growth in suspension. **(B)** Quantification of mRNA levels of *OCT4,* analysed by quantitative real-time PCR of OVCAR-3 subclone 11 stably overexpressing *HA-OCT4*. Control vector values were set "100". mRNA levels were normalized against *ACTIN*. n, number of independent experiments carried out; error bars indicate s.d.; a Student's t test was used to calculate significance values: *, $p < 0.05$; **, $p < 0.01$; ***, $p < 0.001$.

In line with these data, a progressive increase of endogenous OCT4 protein levels in OVCAR-3 subclones 11, 4 and 9, promoted cancer spheroid growth **(Fig. 3.18)**, thus indicating the OCT4-dose dependency of this key feature of ovarian cancer.

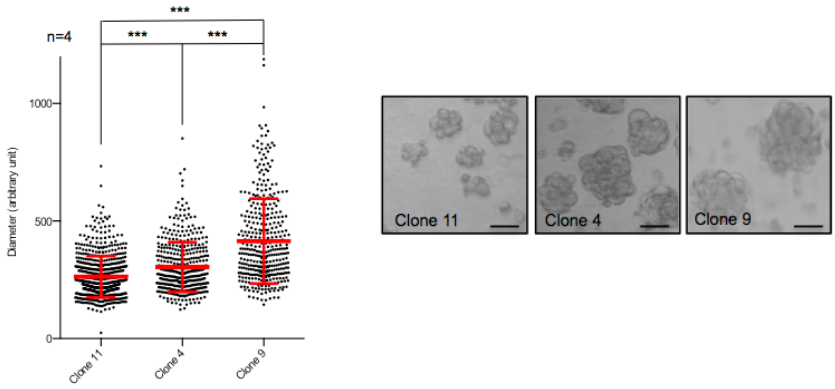

Figure 3.18. **(A)** Spheroids derived from OVCAR-3 subclones 11, 4 and 9. Left panel, diameter of experimental cells. Right panel, representative images of spheroids in each subclone. n, number of independent experiments carried out; a Student's t test was used to calculate significance values: *, $p < 0.05$; **, $p < 0.01$; ***, $p < 0.001$.

Importantly, transient *OCT4* or *CCNF/NIPP1* knock-down, avert or limited significantly the formation of OVCAR-3 spheroids, respectively **(Fig. 3.19A and B)**.

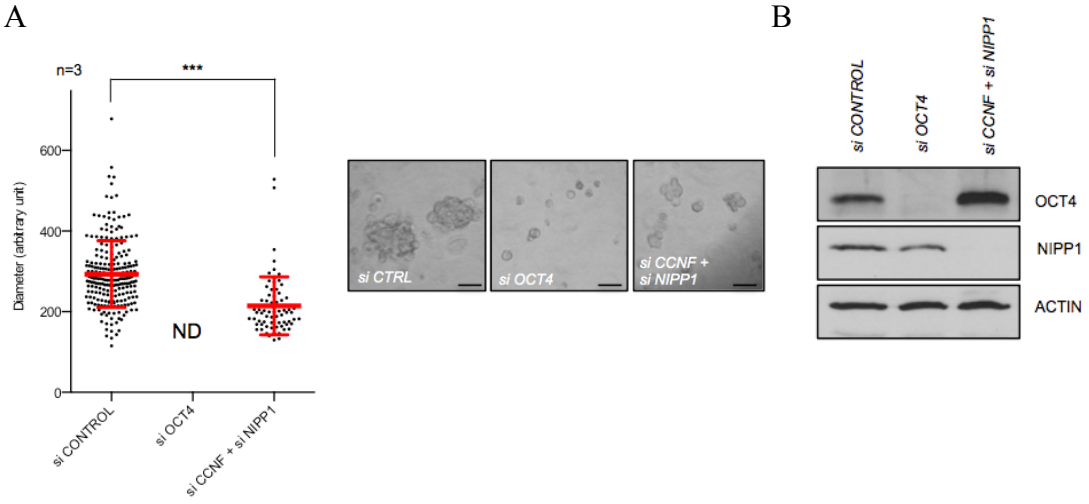

Figure 3.19. **(A)** Spheroids of OVCAR-3 cells transiently transfected with siRNAs targeting *OCT4* or *CCNF*/*NIPP1* (left panel) and representative images of spheroids of experimental cells (right panel). **(B)** Western blotting analysis of OCT4 and NIPP1 in OVCAR-3 cells used for spheroid formation assay after transient knock-down of *OCT4* and *CCNF*/*NIPP1*. ACTIN was used as a loading control. n, number of independent experiments carried out; a Student's t test was used to calculate significance values: *, $p < 0.05$; **, $p < 0.01$; ***, $p < 0.001$.

Together, this indicates a critical role for the OCT4-NIPP1/CCNF axis in promoting cell proliferation and tumorigenic potential of HG-SOC cells *in vitro*.

3.3 The OCT4-NIPP1/CCNF-PP1-pRB axis promotes mitotic progression

Interestingly, OCT4 and NIPP1/CCNF depleted OVCAR-3 cells assume flat and large cell morphologies **(Fig. 3.20A and B)**, resembling senescent cells. We therefore hypothesize that the disruption of the axis could mediate the establishment of cellular senescence programs.

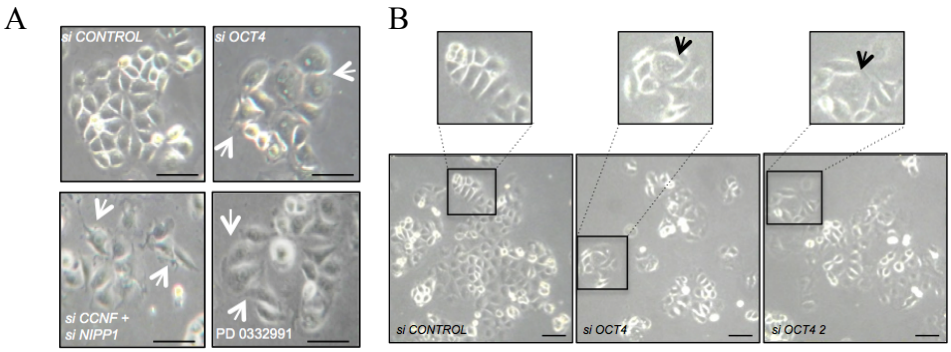

Figure 3.20. **(A)** Morphology of OVCAR-3 cells transfected with the indicated siRNAs oligonucleotides or treated with PD 0332991. White arrows indicate cells with altered morphology. **(B)** Representative images of OVCAR-3 cell morphology after transfection with two different siRNA oligos targeting *OCT4*. Black arrows indicate cells with altered morphology.

As expected, the axis silencing as well as pRB phosphorylation inhibition strongly increased the percentage of beta-galactosidase positive cells **(Fig. 3.21)**, suggesting that these cells are irreversibly arrest.

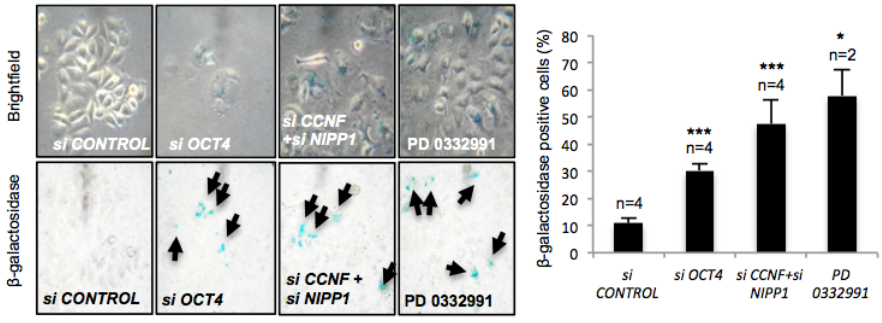

Figure 3.21. Senescence of OVCAR-3 cells transiently transfected with siRNA targeting *OCT4* and *CCNF*/*NIPP1* or treated with PD 0332991 for a duration of 6 days. Left panel, representative images of Senescence-Associated β-galactosidase (SA β-gal) positive cells of experimental OVCAR-3 cells. Right panel, quantification of SA β-gal positive cells. n, number of independent experiments carried out; error bars indicate s.d.; a Student's t test was used to calculate significance values: *, $p < 0.05$; **, $p < 0.01$; ***, $p < 0.001$.

Moreover, we observed that *OCT4* and *NIPP1*/*CCNF* siRNA mediated depletion of OVCAR-3 or treatment with PD 0332991, previously demonstrated to induce senescence in various types of cancer cells (Dean J. L. et al., 2010; Konecny G. E. et al., 2011; Michaud K. et al., 2010), result in reduction of characteristic senescence features such as cyclin B1 and Cdk1, and in $p16^{INK4A}$ up-regulation **(Fig. 3.22A and B)**.

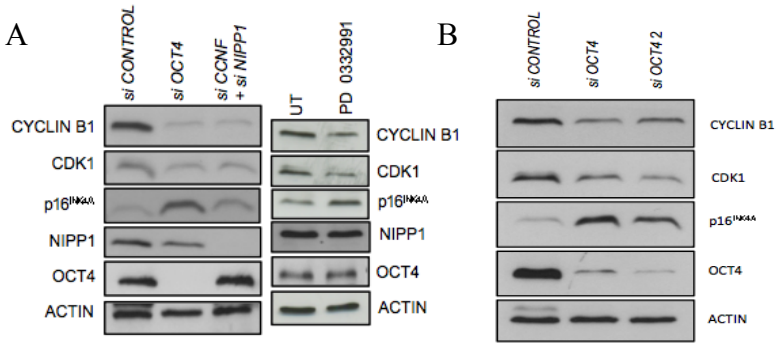

Figure 3.22. **(A)** Western blotting analysis of OVCAR-3 cells transiently transfected with the indicated siRNAs oligos or treated with PD 0332991. ACTIN was used as a loading control. **(B)** Protein levels of cyclin B1 (CCNB1), CDK1, $p16^{INK4A}$ and OCT4 of OVCAR-3 cells in knock-down experiments using siRNAs targeting different *OCT4* mRNA sequences. ACTIN was used as a loading control.

Importantly, senescence and reduced incorporation of BrdU in *OCT4* depleted OVCAR-3 cells were partially rescued by ectopic co-expression of HA-tagged NIPP1 and CCNF (**Fig. 3.23A, B and C**). Altogether these findings suggest that OCT4, activating NIPP1 and CCNF inhibitors to prevent pRB hypo-phosphorylation, support proliferation and promotes tumorigenicity of OVCAR-3 cell line, forcing them to overcome cellular senescence.

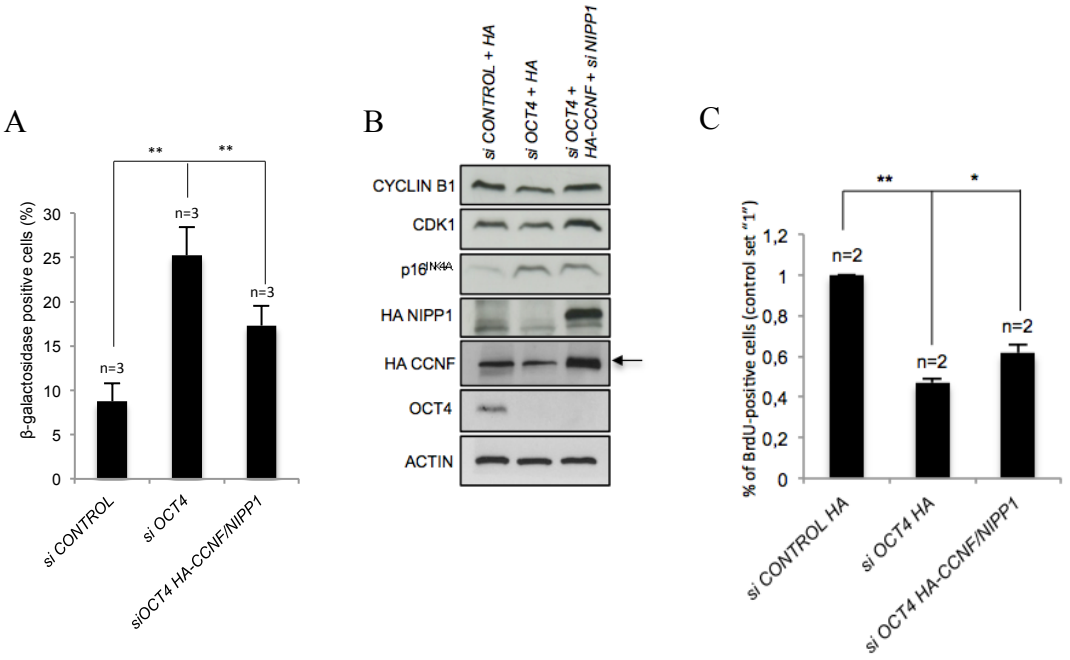

Figure 3.23. **(A)** Quantification of SA β-galactosidase positive OVCAR-3 cells transiently transfected with siRNA targeting *OCT4* alone or in combination with *HA-CCNF* and *HA-NIPP1* expressing vectors. **(B)** Western blotting using the indicated antibodies. ACTIN was used as a loading control. **(C)** Overexpression of CCNF and NIPP1 rescues percentage of BrdU positive cells in *OCT4* depleted OVCAR-3 cells, as determined by BrdU incorporation assay. n, number of independent experiments carried out; error bars indicate s.d.; a Student's t test was used to calculate significance values: *, $p < 0.05$; **, $p < 0.01$; ***, $p < 0.001$.

As expected by the axis levels, progressively increasing OCT4 expression in OVCAR-3 subclones protects from senescence, as demonstrated by cyclin B1, CDK1 and $p16^{INK4A}$ modulation **(Fig. 2.24)**.

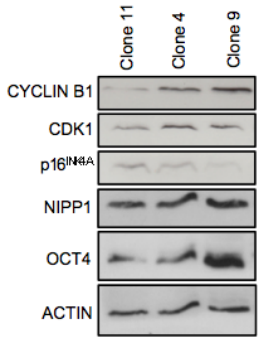

Figure 3.24. Senescence markers as determined by western blotting analysis of subclones 11, 4 and 9. ACTIN was used as a loading control.

Senescent cells are describes as irreversibly arrested in G1/G0 phase of the cell cycle. We decided to confirm our data analyzing cell cycle profile of OVCAR-3 cells upon the

axis depletion. In line with our results we found that acute, siRNA mediated depletion of *OCT4* or *NIPP1/CCNF* for six days results in reduced cell numbers in S, G2/M phases and significantly increased number of cells in G0/G1 phases. Interestingly, this senescent phonotype is accompanied by increasing cells blocked in subG1, suggesting the presence of apoptotic cells. To confirm this data, we analyse PARP and Caspase 3 cleavage (**Fig. 3.25A and B**) by western blotting analysis and we found an augmented levels of these two apoptotic markers. This indicates that total depletion of *OCT4* or *NIPP1/CCNF* finally results in the induction of apoptosis.

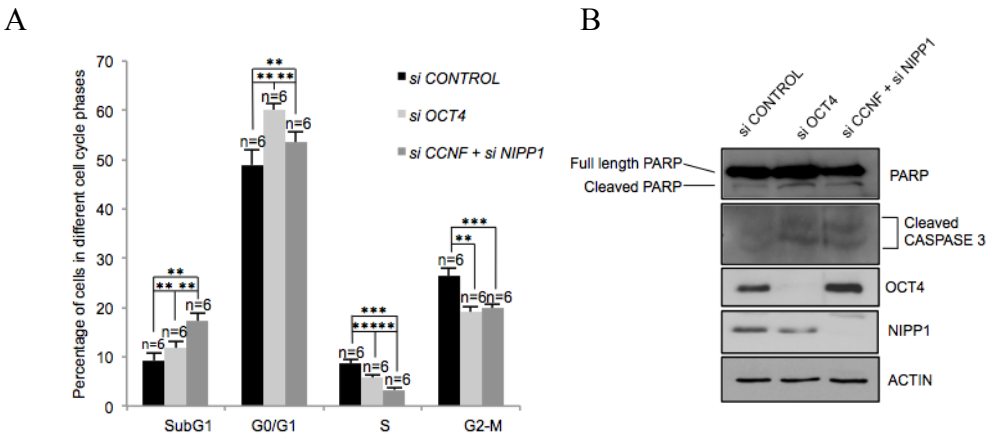

Figure 3.25. **(A)** Percentage of cells in different cell cycle phases of OVCAR-3 transiently transfected with the indicated siRNA oligos for a duration of 6 days. **(B)** Western blotting of cells described in (A). ACTIN was used as a loading control. n, number of independent experiments carried out; error bars indicate s.d.; a Student's t test was used to calculate significance values: *, $p < 0.05$; **, $p < 0.01$; ***, $p < 0.001$.

Next we used OVCAR-3 subclones, to study the impact of fine-tuning differences in OCT4 expression on cell cycle progression. We found that reduced OCT4/NIPP1 expression in OVCAR-3 subclones 11 and 4 significantly reduced cells in S phase **(Fig. 3.26)**. Importantly, we found that low OCT4 expression in subclones 11 and 4 was linked with an accumulation of cells in G2/M phase whereas subG1 numbers did not change significantly **(Fig. 3.26)**. These data suggests that low OCT4 expression in subclone 11 and 4 cells are linked with problems related to mitotic progression. This phenotype could be masked by the induction of apoptosis upon acute depletion of *OCT4* or *NIPP1/CCNF* in transient RNAi experiments (**Fig. 3.25**).

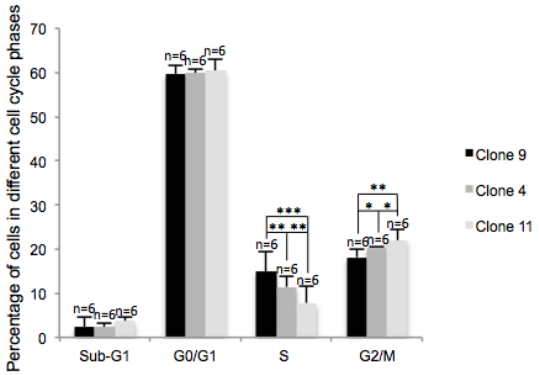

Figure 3.26. Cell cycle profile of OVCAR-3 subclones 11, 4 and 9, as determined by FACS analysis. n, number of independent experiments carried out; error bars indicate s.d.; a Student's t test was used to calculate significance values: *, $p < 0.05$; **, $p < 0.01$; ***, $p < 0.001$.

Given the data obtained, we hypothesized that the self-renewal transcription factor OCT4 does not only promote cell proliferation by inactivating pRB tumorsuppressor gene but also has an important function in stabilizing mitotic progression.

3.4 The OCT4-NIPP1/CCNF-PP1 axis ensures mitotic fidelity by driving the expression of Chromosomal Passenger Complex (CPC)

We next decided to investigate the role of OCT4 and NIPP1/CCNF in the maintenance of mitotic stability in OVCAR-3 cells. To this aim we analyse the contribution of OCT4-CCNF/NIPP1-PP1-pRB axis in micronuclei formation, a classical hallmark of chromosomal instability and mitotic errors. Micronuclei, in fact, mainly originate from chromatid fragments or whole chromosomes that fail to be incorporated in the daughter nuclei at the end of telophase during mitosis because they did not attach correctly with the spindle during the segregation process in anaphase (Fenech M., 2007). These chromosomes or chromosome fragments are morphologically similar to nuclei after conventional nuclear staining – although smaller - since they are enclosed by a nuclear membrane.

We found that siRNA-mediated knockdown of OCT4 or CCNF/NIPP1 strongly increases the percentage of micronuclei in OVCAR-3 subclone 9 **(Fig. 3.27A)**. Importantly, as expected by an increasing activation of the axis, micronuclei formation

is found gradually decrease from subclone 11, 4 to 9 **(Fig. 3.27B)**, anticipating an important function of endogenous OCT4 in improving genome stability.

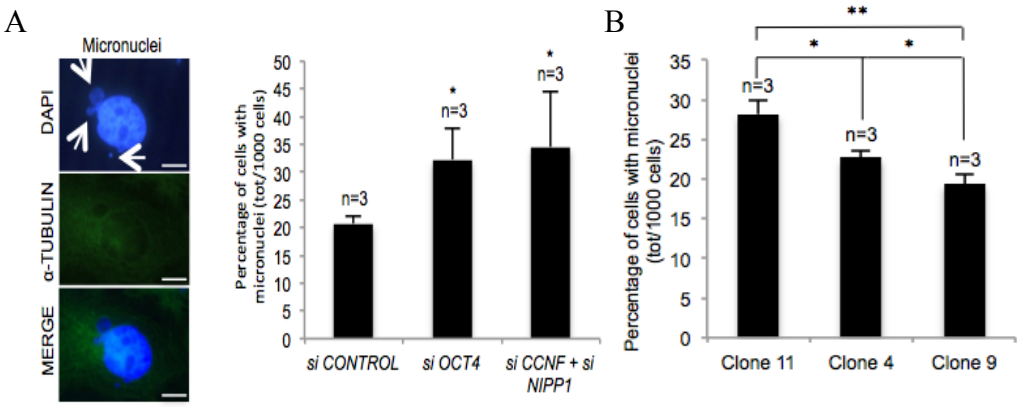

Figure 3.27. **(A)** Micronuclei (white arrows) formation of OVCAR-3 subclone 9 transiently transfected with siRNAs targeting *OCT4* and *CCNF*/*NIPP1*. Left panel, representative image. Right panel, percentage of cells showing micronuclei (1000 cells were analysed). **(B)** Percentage of micronuclei in OVCAR-3 subclones 11, 4 and 9 cells (1000 cells were analysed). n, number of independent experiments carried out; error bars indicate s.d.; a Student's t test was used to calculate significance values: *, $p < 0.05$; **, $p < 0.01$; ***, $p < 0.001$.

To better understand which types of errors occur during mitosis, that generate the observed chromosome segregation defects, we interrupted the OCT4-NIPP1/CCNF-PP1-pRB axis and studied type and frequency of mitotic spindle defects (Ngan V. K. et al., 2001). Importantly, we found that RNAi mediated depletion of *OCT4* or *NIPP1*/*CCNF* resulted in a 10-fold or 5-fold increase in multipolar spindles, respectively (**Fig. 3.28A**). Axis depletion did not cause a significant alteration of the frequency of bipolar spindles with one or more uncongressed chromosomes (type I and II) or monopolar spindles with chromosomes arranged around the mitotic spindle (type III) (firstly described by Jordan M. A. et al., 1991) (**Fig. 3.28A**). OVCAR-3 cells with low OCT4 expression (subclone 11) recapitulated the multipolar spindle phenotype induced by OCT4-NIPP1/CCNF-PP1 axis disruption (**Fig. 3.28B**).

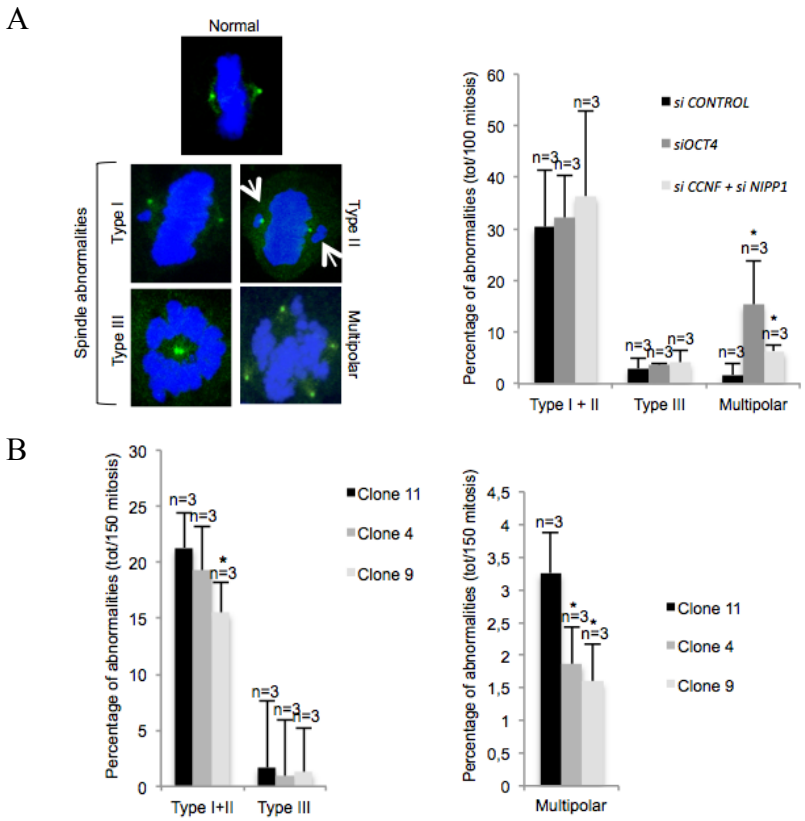

Figure 3.28. **(A)** Left panel, representative images of type I, II, III and multipolar spindle errors (Ngan V. K. et al., 2001). Right panel, percentage of mitotic abnormalities of OVCAR-3 subclone 9 after knock-down of *OCT4* or *CCNF*/*NIPP1* (100 mitosis were analysed). **(B)** Quantification of multipolar spindle defects of subclones 11, 4 and 9 described in (A) (100 mitosis were analysed). n, number of independent experiments carried out; error bars indicate s.d.; a Student's t test was used to calculate significance values: *, $p < 0.05$; **, $p < 0.01$; ***, $p < 0.001$.

Cells surviving multipolar anaphase that are unable to complete mitosis are likely to become giant multinucleated cells (Pihan G. A., 2013), thus, are considered a typical consequence of multipolar spindle formation. Therefore, counting polynucleated cells give us a percentage of cells that have passed through a multipolar state. As expected from multipolar mitosis induction, after *OCT4* or *NIPP1/CCNF* knockdown the frequency of polynucleated cells significantly increased, as well as in subclone 11, which harbour low endogenous OCT4 protein levels **(Fig. 3.29A and B)**.

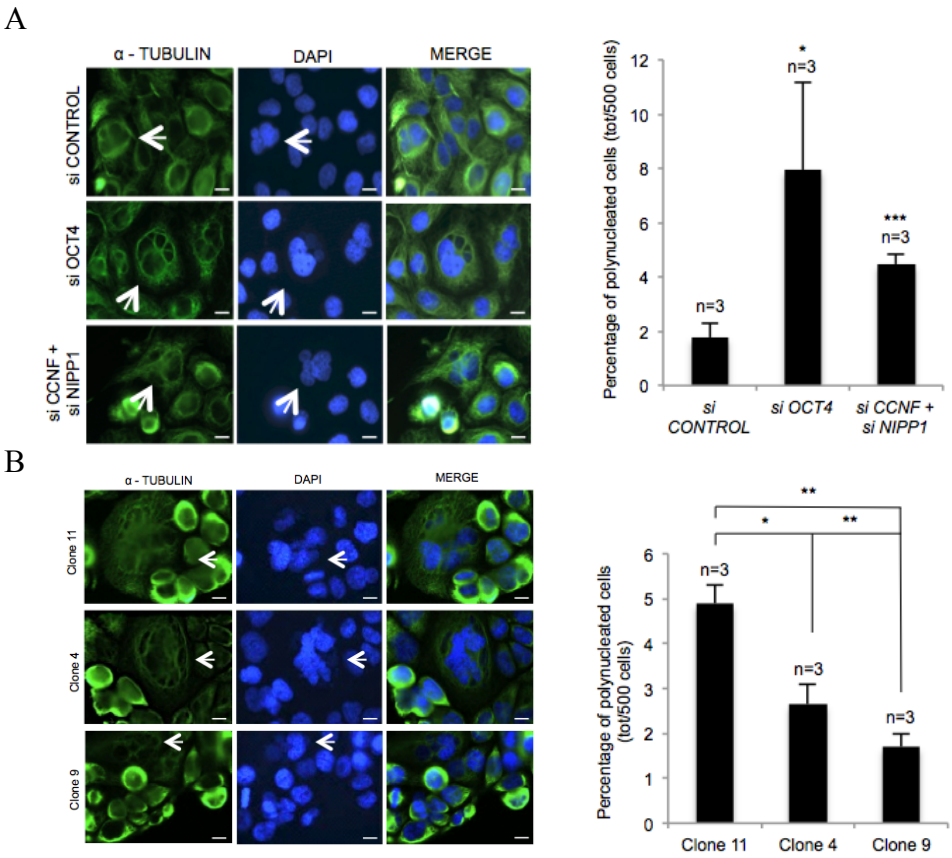

Figure 3.28. **(A)** Polynucleated cells analysis in OVCAR-3 subclone 9 after knock-down of *OCT4* or *CCNF*/*NIPP1*. Left panel, representative images of polynucleated cells found in each condition. Right panel, percentage of polynucleated cells (500 cells were analysed). **(B)** Right, percentage of polynucleated cells of OVCAR-3 subclones 11, 4 and 9 (500 cells were analysed). Left panel, representative immunofluorescence images of polynucleated cells endogenously present in OVCAR-3 subclones. n, number of independent experiments carried out; error bars indicate s.d.; a Student's t test was used to calculate significance values: *, $p < 0.05$; **, $p < 0.01$; ***, $p < 0.001$.

Altogether these data demonstrate that OCT4 and its transcriptional targets NIPP1/CCNF drive cell proliferation by inactivating the tumor suppressing pathway pRB but also have an unknown role in enhancing mitotic stability in HG-SOC.

To discover critical genes or pathways controlled by the axis activity and involved in enhancing mitotic progression, we analysed gene expression profile using Illumina technology of OVCAR-3 cells upon depletion of the axis components. In particular, we identified 1153 genes that were commonly deregulated after *OCT4* or *CCNF*/*NIPP1* depletion (1.4 fold up or down-regulated, $p<0.05$), suggesting that this important group of genes may be concerted by the components of the axis **(Fig. 3.29)**.

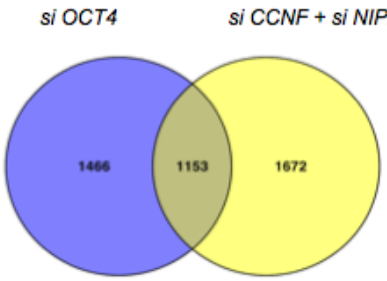

Figure 3.29. Venn Diagram showing overlap between genes differentially expressed in OVCAR-3 cells subjected to RNAi mediated depletion of *OCT4* or *CCNF*/*NIPP1* for a duration of 6 days.

Ingenuity Pathway Analysis (IPA) and GSEA gene ontology on genes that are down-regulated upon *OCT4* and *NIPP1/CCNF* depletion identified defects in molecular pathways linked to mitotic progression. In fact, the genes commonly identified ensure chromosome segregation fidelity and are strongly linked to the mitotic phase of the cell cycle, confirming our hypothesis of an axis role in the maintenance of genomic stability. **(Fig. 3.30)**.

Genes down-regulated after *POU5F1* and *CCNF/NIPP1* silencing			
Ingenuity Pathway Analysis	P-value	**GSEA**	P-value
Segregation of chromosomes	3,0E-08	Neighborhood of PCNA	4,3E-08
Condensation of chromosomes	1,6E-06	REACTOME: Genes involved in DNA Replication	4,5E-08
Arrest in mitosis	2,2E-05	REACTOME: Genes involved in Cell Cycle, Mitotic	1,3E-08
Mitosis	4,1E-07	REACTOME: Genes involved in Regulation of mitotic cell cycle	1,1E-07
Cell cycle progression	1,6E-05	Genes up-regulated in gastric cancer cell lines: doxorubicin [PubChem=31703] resistant vs sensitive.	1,7E-08
Missegregation of chromosomes	1,3E-04		
Quantity of chromosomes	3,4E-04		
Delay in segregation of sister chromatids	1,0E-03		
Delay in initiation of anaphase	2,1E-05		

Figure 3.30. Functional analysis of genes down-regulated after *OCT4* and *CCNF/NIPP1* silencing using the Ingenuity Pathway Analysis tool (IPA) and Gene Set Enrichment Analysis (GSEA). Only genes differentially expressed (logFC<-1.2 and p-value < 0.05) in both *OCT4* and *CCNF/NIPP1* silencing experiments were considered. Right tail Fisher's Exact test was used to calculate significance values: *, $p < 0.05$; **, $p < 0.01$; ***, $p < 0.001$.

Deeper analysis of biological pathways using the Ingenuity Path Explorer tool highlighted the central components of the Chromosomal Passenger Complex (CPC) Aurora B (AURKB), Survivin (BIRC5), Borealin (CDCA8) and Inner Centromere

Protein (INCENP) as downstream targets of the OCT4-NIPP1/CCNF axis **(Fig. 3.31),** suggesting a critical role for such a complex in genome stability controlled by the axis.

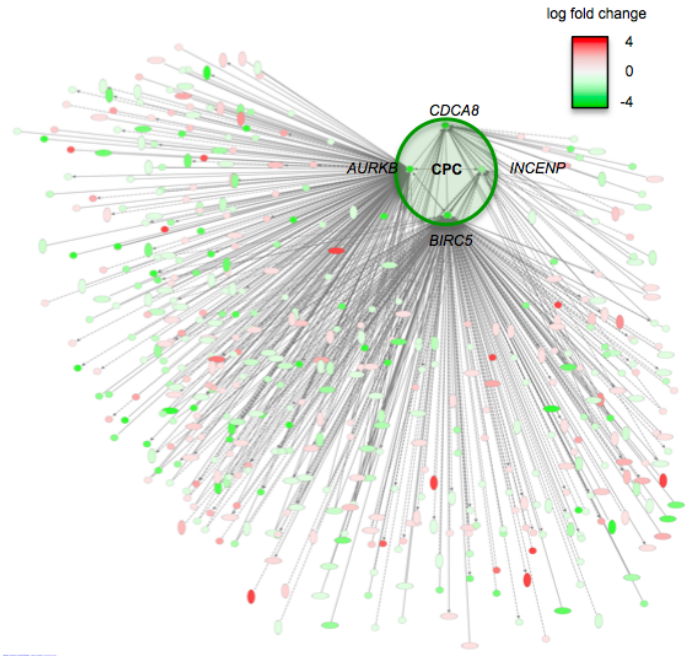

Figure 3.31. Automated literature research using Ingenuity Path Explorer tool using genes significantly regulated by the OCT4-NIPP1/CCNF-PP1 axis.

Down regulation of CPC complex components and additional panel of OCT4-NIPP1/CCNF target genes, discovered by gene expression profile, were validated by quantitative real-time PCR **(Fig. 3.32A and B).**

A

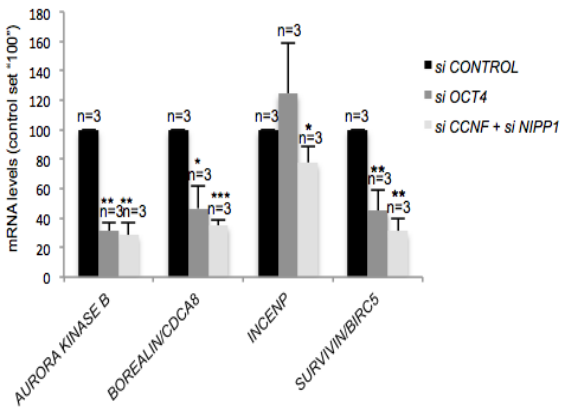

B

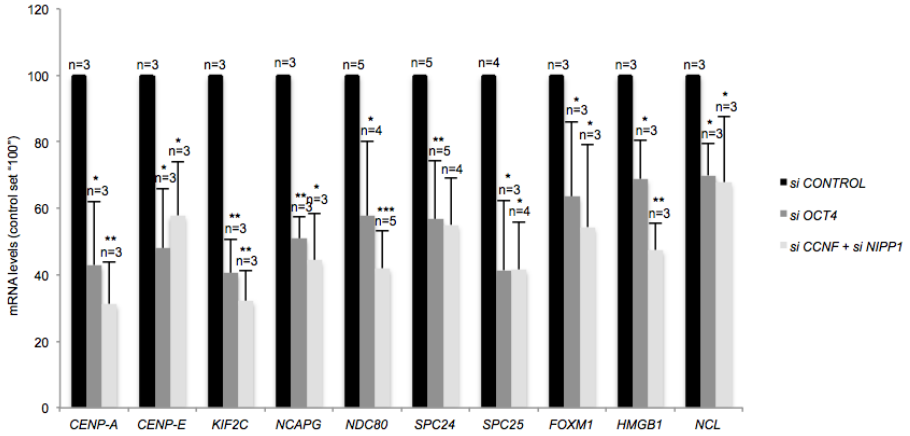

Figure 3.32. Quantitative real-time PCR mRNA analysis of OVCAR-3 after RNAi mediated knock-down of *OCT4* or *CCNF*/*NIPP1*. **(A)** Real-time PCR quantification of CPC components of experimental cells. **(B)** Quantitative real-time PCR validation of gene expression profiling data of *OCT4* and *NIPP1*/*CCNF* co-regulated genes. Control siRNA values were set "100". mRNA levels were normalized against *ACTIN*. n, number of independent experiments carried out; error bars indicate s.d.; a Student's t test was used to calculate significance values: *, $p < 0.05$; **, $p < 0.01$; ***, $p < 0.001$.

Together, our observations and findings suggest that OCT4 and NIPP1/CCNF enhance mitotic stability by driving the expression of CPC components.

3.5 OCT4-CCNF/NIPP1-PP1 axis is essential to ensure CPC function

The Chromosomal Passenger Complex (CPC) is an important mitotic regulatory complex. In early mitosis, this complex promotes chromosome alignment by correcting chromosomes-microtubules errors of the mitotic spindle. At the end of mitosis, the CPC also regulates the correct process of cytokinesis (Carmena M. and Earnshaw W. C., 2003). The CPC is composed of the enzymatic core Aurora B, Survivin, Borealin and the scaffold protein INCENP. Upon entry into mitosis, Aurora B phosphorylates histone H3 at serine 10 (H3-Ser10) and serine 28 (H3-Ser28) (Crosio C. et al., 2002).

To confirm bioinformatics analysis, we depleted *OCT4* or *NIPP1*/*CCNF* and we observed a drastic reduction of Aurora B protein levels and its activity, as detected by the concomitant decrease of phosphorylation at Ser10 and Ser28 of histone H3 (H3-Ser10 and Ser-28) **(Fig. 3.33A and B)**.

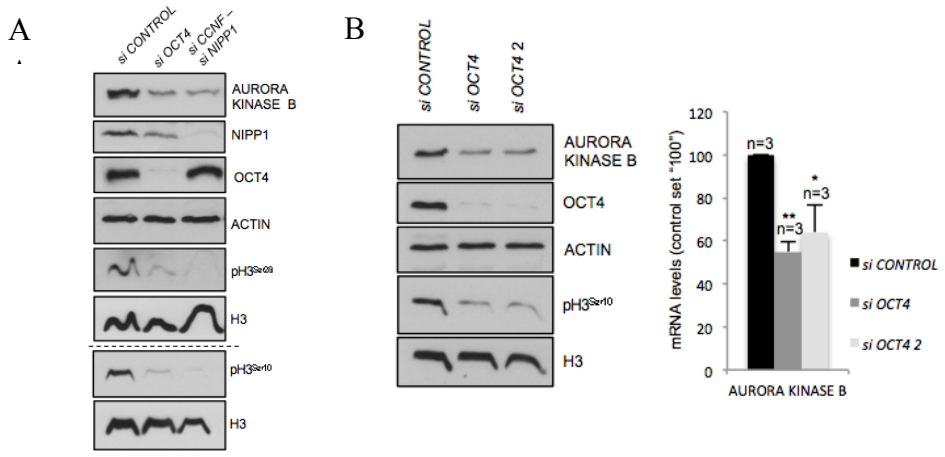

Figure 3.33. The OCT4-NIPP1/CCNF-PP1 axis controls Chromosomal Passenger Complex (CPC) levels and functions. **(A)** Western blotting analysis of Aurora B, phospho H3-Ser28 and Ser10, OCT4 and NIPP1 of OVCAR-3 silenced for *OCT4* and *CCNF/NIPP1*. ACTIN and H3 were used as loading control. **(B)** mRNA and protein analysis of OVCAR-3 cells transfected with two different siRNA oligos targeting *OCT4*. Left panel, western blotting of Aurora B, phospho H3-Ser10 and OCT4 of experimental cells. ACTIN and H3 was used as a loading control. Right panel, real-time PCR for *AURKB* mRNA levels of OVCAR-3 cells transfected with the indicated siRNAs oligos. Control siRNA values were set "100". mRNA levels were normalized against *ACTIN*. n, number of independent experiments carried out; error bars indicate s.d.; a Student's t test was used to calculate significance values: *, $p < 0.05$; **, $p < 0.01$; ***, $p < 0.001$.

During S phase, CPC is first found on pericentromeric heterochromatin. Aurora B phosphorylation on histone H3 at serine 10 (H3-Ser10) and serine 28 (H3-Ser28) causes the dissociation of Aurora B from HP1 along chromosomal arms and finally allows the concentration of the CPC to heterochromatin at inner centromeres (Fischle W. et al., 2005; Hirota T. et al., 2005). At this location CPC conduct its role in correcting improper microtubule-kinetochore attachments, measuring mitotic spindle tension and ensuring the maintenance of the spindle assembly checkpoint (Carmena M. et al., 2012). Thus, CPC components knock-down or Aurora B kinase inhibition results in chromosome congression and segregation defects due to incorrect attachment of microtubules to kinetochores, abnormal mitotic spindles, centrosome duplication and defects in mitotic checkpoint control (van der Horst A. and Lens S. M. A., 2014).

This precise and complex localization mechanism prompted us to perform immunofluorescence experiments to investigate the distribution of Aurora B and H3-Ser10 phosphorylation across OVCAR-3 metaphase chromosomes. In line with western blotting data, RNAi mediated depletion of *OCT4* or *NIPP1/CCNF* caused a reduction of

Aurora B and H3-Ser10 phosphorylation signal intensity along metaphase chromosomes. Moreover, in contrast to control cells that show a centromeric concentration of Aurora B and H3-Ser10 phosphorylation, this histone mark is distributed across large areas of chromosome arms in *OCT4* or *NIPP1/CCNF* knock-down cells **(Fig. 3.34)**. These data indicate that disruption of the OCT4-NIPP1/CCNF axis cause a reduced expression of CPC components leading to an insufficient concentration of Aurora B and H3-Ser10 phosphorylation at centromeres of metaphase chromosomes.

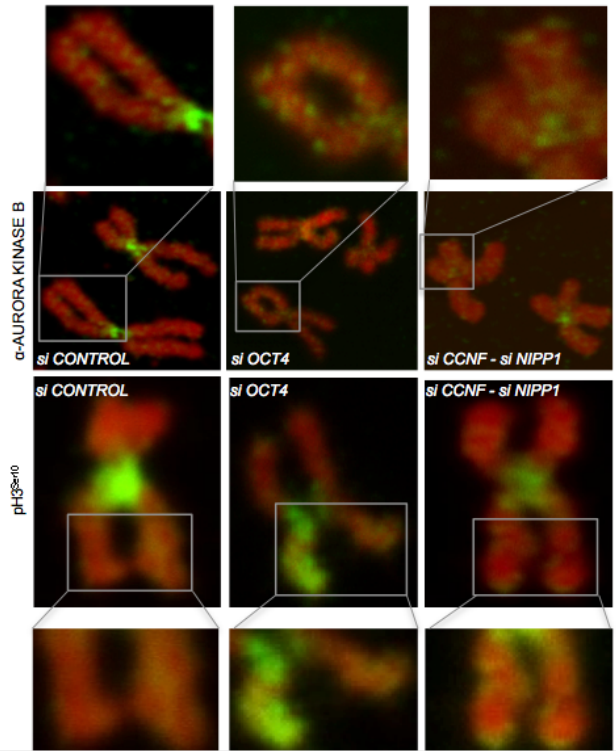

Figure 3.34. Immunofluorescence of metaphase spreads for Aurora B and phospho H3-Ser10 of OVCAR-3 cells transiently transfected with the indicated siRNAs oligos.

OVCAR-3 subclones demonstrate that endogenous OCT4 protein levels show positive correlation with Aurora B and H3-Ser10/28 phosphorylation levels, confirming that CPC expression and activity is OCT4 dosage dependent **(Fig. 3.35)**.

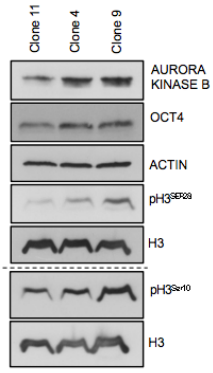

Figure 3.35. Western blotting analysis of OVCAR-3 subclones 11, 4 and 9 using the indicated antibodies. ACTIN and H3 were used as loading control.

Importantly, we were able to observe a rescue of Aurora B and phosphorylated H3-Ser10/Ser28 levels in *OCT4* depleted cells by ectopic expression of NIPP1/CCNF **(Fig. 3.36)**. This indicates that OCT4 regulates CPC expression via its transcriptional target genes NIPP1 and CCNF.

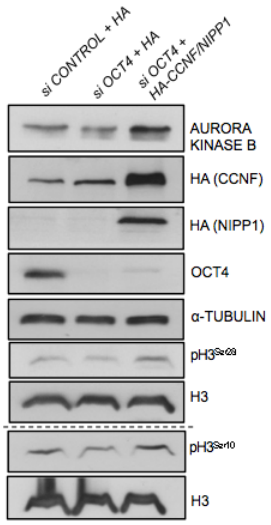

Figure 3.36. Western blotting of OVCAR-3 cells transiently transfected with siRNA targeting *OCT4* or cotransfected with *HA-CCNF* and *HA-NIPP1* vectors using the indicated antibodies. ACTIN and H3 were used as loading control.

The NIPP1/CCNF target, Protein Phosphatase 1 (PP1) is reported to de-phosphorylate and inactivate Aurora B. In addition, PP1 competes with Aurora B in controlling phosphorylation levels of histone H3-Ser10 and H3-Ser28 (Sugiyama K. et al., 2002). In line with this findings, we were able to restore reduced H3-Ser10 and Ser28

phosphorylation in *OCT4* depleted OVCAR-3 cells by treating experimental cells with the PP1 inhibitor Okadaic acid **(Fig. 3.37)**. Together, this provides evidence that OCT4 and its target genes NIPP1/CCNF enhance the expression of CPC components but also its Aurora B activity by suppressing PP1 function, as demonstrated by H3 specific phosphorylation.

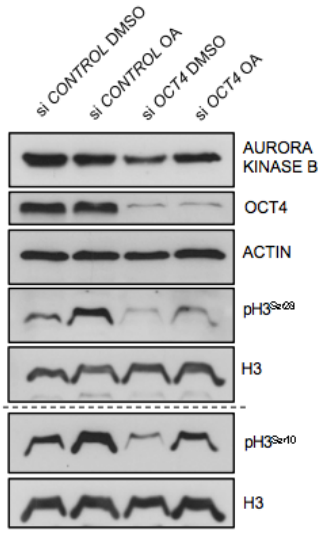

Figure 3.37. Western blotting analysis of OVCAR-3 cells transiently transfected with siRNA targeting *OCT4* alone or treated with 15 nM Okadaic Acid (OA) using the indicated antibodies. ACTIN and H3 were used as loading control.

Recent studies demonstrated that the CPC controls spindle tension at kinetochores and prevents the formation of multipolar mitosis by promoting the clustering of supernumerary centrosomes, called centrosome clustering (Leber B. et al., 2010). Thus, multipolarity lead to the appearance of cells with more then two centrosomes due to the inactivation of centrosome clustering mechanism when alterations in CPC functions occurs. In line with this, we found that depletion of *OCT4* and *NIPP1/CCNF* causes a prominent increase in the frequency of cells containing more than two centrosomes **(Fig. 3.38A)**. In addition, determining centrosome numbers in OVCAR-3 subclones revealed that the centrosome numbers significantly increase in subclones 11 and 4 that are characterized by reduced OCT4 protein expression **(Fig. 3.38B)**.

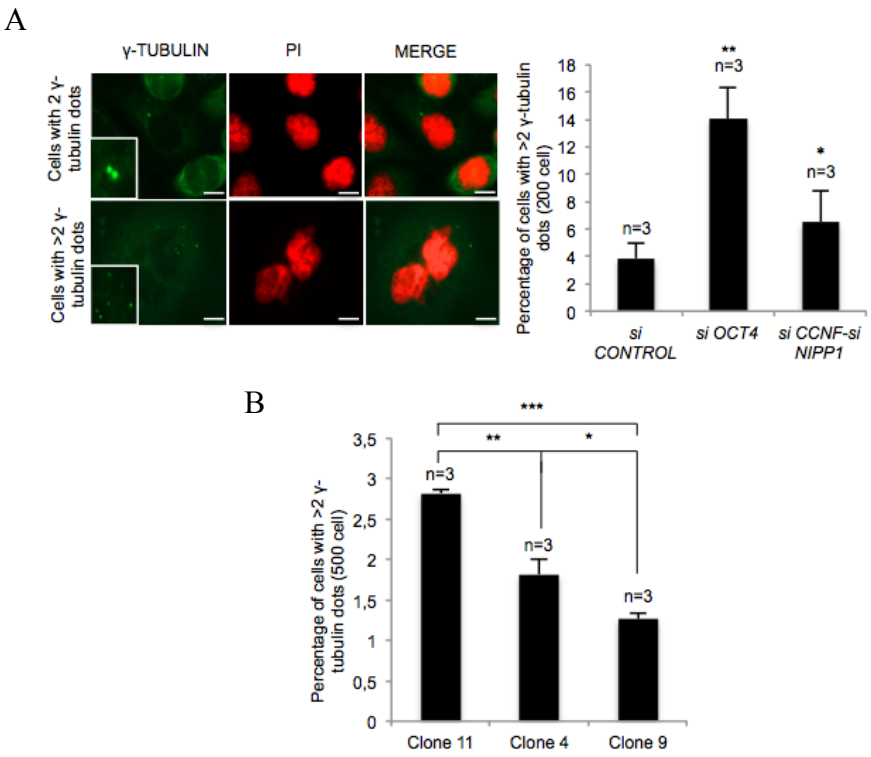

Figure 3.38. **(A)** Quantification of centrosomes number of subclone 9 subjected to RNAi mediated depletion of *OCT4* or *NIPP1*/*CCNF*. Left panel, representative images of immunofluorescence staining showing normal and augmented numbers of centrosomes. Right panel, percentage of cells showing more than 2 centrosomes (200 cells were analysed). **(B)** Number of centrosomes in OVCAR-3 subclones 11, 4 and 9 (500 cells were analysed). n, number of independent experiments carried out; error bars indicate s.d.; a Student's t test was used to calculate significance values: *, $p < 0.05$; **, $p < 0.01$; ***, $p < 0.001$.

To test whether the OCT4-NIPP1/CCNF axis has a general relevance for the maintenance of genomic stability, we ectopically expressed OCT4 in MDA-MB-231 breast cancer cells that express very low OCT4 RNA and protein levels when compared to OVCAR-3 cells **(Fig. 3.39A)**. Importantly, we found that ectopic OCT4 expression increased Aurora B levels as well as its activity as demonstrated by H3-Ser10/28 phosphorylation **(Fig. 3.39B).**

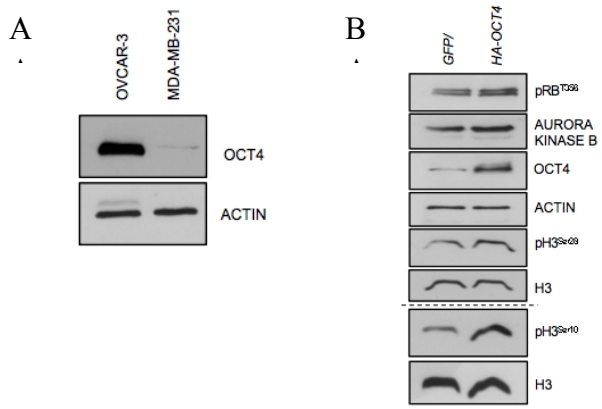

Figure 3.39. **(A)** Western blotting of OCT4 levels of OVCAR-3 and MDA-MB-231 cells. ACTIN was used as a loading control. **(B)** Protein expression analysis using the indicated antibodies in MDA-MB-231 cells stably expressing HA-OCT4 protein as detected by western blotting. ACTIN and H3 were used as loading control.

Most importantly, ectopic expression of OCT4 in MDA-MB-231 cells, lead to an overall increase of genome stability in terms of micronuclei, giant polynucleated cells and centrosomes number **(Fig. 3.40A, B and C)**, as determined by immunofluorescence analysis.

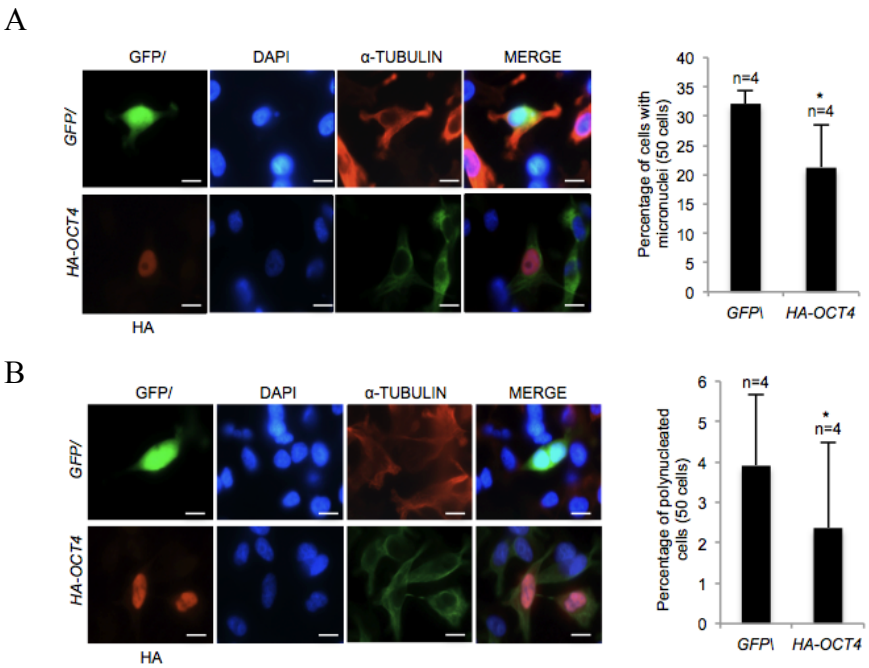

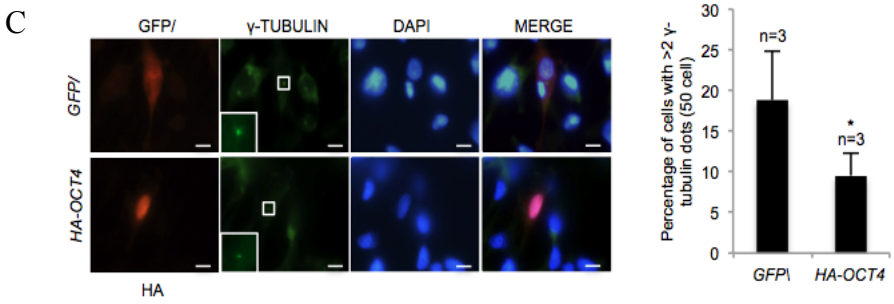

Figure 3.40. **(A)** Left panel, representative images of micronuclei of experimental cells described in Fig. 3.39B. Right panel, percentage of cells with micronuclei (50 cell were analysed). A GFP vector was used as control. **(B)** Left panel, representative images of polynucleated cells described in Fig. 3.39B. Right panel, percentage of polynucleated cells (50 cells were analysed). GFP vector was used as control. **(C)** Left panel, representative images of centrosomes in cells described in Fig. 3.39B. Right panel, percentage of cells with more than 2 centrosomes (50 cells were analysed). n, number of independent experiments carried out; error bars indicate s.d.; a Student's t test was used to calculate significance values: *, $p < 0.05$; **, $p < 0.01$; ***, $p < 0.001$. Scale bars, 10 μm.

Finally, OCT4 overexpression promotes the ability of MDA-MB-231 cells to form spheroids with increased size *in vitro* **(Fig. 3.41A and B)**.

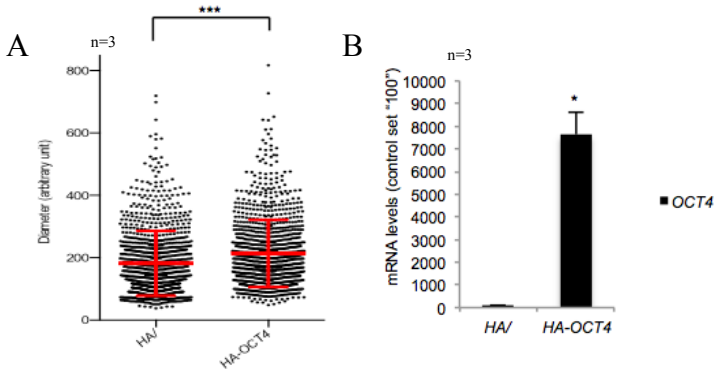

Figure 3.41. **(A)** Cell spheroids diameter of MDA-MB-231 cell line stably expressing HA-OCT4. **(B)** *OCT4* mRNA expression levels of cells described in Fig. 3.39B. Control vector values were set "100". *OCT4* mRNA levels were normalized against *ACTIN*. n, number of independent experiments carried out; error bars indicate s.d.; a Student's t test was used to calculate significance values: *, $p < 0.05$; **, $p < 0.01$; ***, $p < 0.001$.

This shows that the self-renewal transcription factor OCT4 and its downstream targets NIPP1/CCNF regulates genome stability by suppressing the formation of multipolar spindles by driving the clustering of supernumerary centrosomes in diverse types of

cancer cells.

3.6 OCT4-CCNF/NIPP1-PP1-pRB axis correlates with CPC activation and poor prognosis in HG-SOC patients

To evaluate the clinical relevance of the mechanism identified, we next investigated whether the OCT4-NIPP1/PP1 axis impinges on pRB phosphorylation and CPC components expression in HG-SOC patients. Due to the use of non-specific gene probes, the majority of ovarian cancer gene expression data sets do not provide reliable information on OCT4 expression (Liedtke S. et al., 2008). We consequently established a collection of 18 cancer specimen obtained from HG-SOC **(Fig. 3.42)** and examined the expression of *OCT4*, *NIPP1*, *CCNF*, *AURKB*, *BIRC5* (Survivin) and *CDCA8* (Borealin) mRNA by quantitative real-time PCR and immunohistochemistry (IHC).

OCT4 high				OCT4		AURKB		NIPP1				pRB T356	
Istologic number	Date of diagnosis	Diagnosis	Date of death	% positive nuclei	Intensity	% positive nuclei	Intensity	% positive cytoplasm	Intensity	% positive nuclei	Intensity	% positive nuclei	Intensity
B2013.001719	30.01.2013	HG-SOC, G3, St IIIC	DECEASED 29.01.2015	0	0	15	3+	90	2+	0	3+	60	2+
B2007.005557	12.04.2007	HG-SOC, G3,S t IIC	DECEASED 24.06.07	50	2+	30	3+	90	1+	90	2+	80	3+
B2007.002707	21.02.2007	HG-SOC, G3, St IIIA	DECEASED 21.03.2008	5	1+	50	3+	90	2+	80	3+	70	3+
B2011.016594	11.10.2011	METASTASIS FROM HG-SOC, G2, St IA	DECEASED 28.12.2012	50	3+	30	3+	90	1+	90	2+	80	3+
B2009.012538	01.08.2009	HG-SOC, G3, St IIIA	DECEASED 19.11.13	5	2+	20	2+	90	2+	70	3+	10	3+
B2013.014913	05.09.2013	HG-SOC, G3, St IV	DECEASED 14.12.13	undetermined	undetermined	50	3+	90	2+	90	3+	70	3+
B2013.012743	23.07.2013	HG-SOC, G3, IIIC	ALIVE	0	0	20	3+	90	1+	90	3+	70	3+

OCT4 low				OCT4		AURKB		NIPP1				pRB T356	
Istologic number	Date of diagnosis	Diagnosis	Date of death	% positive nuclei	Intensity	% positive nuclei	Intensity	% positive cytoplasm	Intensity	% positive nuclei	Intensity	% positive nuclei	Intensity
B2013.002118	05.02.2013	HG-SOC, G3, St IV	ALIVE	0	0	5	2+	90	1+	90	2+	80	3+
B2013.010634	19.06.2013	HG-SOC, G3, IIIC	ALIVE RELAPSE	0	0	10	2+	50	1+	0	0	10	1+
B2013.009716	05.06.2013	HG-SOC, G3, IIC	ALIVE	0	0	20	3+	90	3+	0	0	70	3+
B2012.020856	13.12.2012	HG-SOC, G3, St IA	ALIVE	0	0	10	3+	90	1+	70	2+	50	3+
B2007.011273	27.07.2007	HG-SOC, G3, St IIIA	ALIVE	0	0	5	2+	90	1+	30	2+	50	3+
B2012.006636	17.04.2012	HG-SOC, G3, St IIIB	DECEASED 31.03.14	5	1+	2	2+	90	2+	20	1+	15	2+
B2006.000702	18.01.2006	HG-SOC, G3, St IIIC	ALIVE	0	0	15	3+	90	3+	0	0	20	2+
B2007.013711	19.09.2007	HG-SOC, G3, St IIIC	DECEASED 03.03.2011	0	0	15	3+	90	2+	0	0	10	2+
B2007.007804	23.05.2007	HG-SOC, G3, St IIIB	ALIVE	0	0	20	3+	90	1+	70	1+	15	2+
B2009.007141	29.04.2009	HG-SOC, G3,St IIA	ALIVE	0	0	0	0	90	3+	0	0	10	2+s
B2008.019310	11.12.2008	HG-SOC, G3, St IV	DECEASED 13.09.09	0	0	20	3+	90	3+	40	1+	15	2+

Figure 3.42. Histopathological classification, outcome and immunohistochemistry quantification (percentage of positive nuclei or cytoplasm and intensity) of 18 HG-SOC patients classified according to their *OCT4* levels in "*OCT4* high" and "*OCT4* low" as described in Materials and Methods.

In order to subdivide patients in "OCT4 high" and "OCT4 low" subgroups, we used the z-score allocation of *OCT4* mRNA expression levels **(Fig. 3.43** and Materials and Methods**)**.

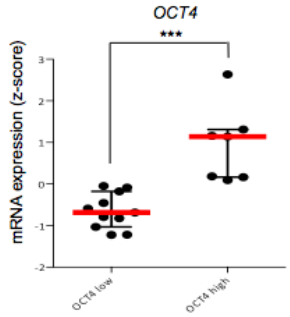

Figure 3.43. Quantification of *OCT4* mRNA expression levels in HG-SOC patients allocated according to z-score analysis into "high" or "low" mRNA *OCT4* expressing patients. A Linear regression model was used to calculate significance values: *, $p < 0.05$; **, $p < 0.01$; ***, $p < 0.001$.

Importantly, bioinformatics subdivision was confirmed in immunohistochemistry analysis since the majority of cancer samples classified as "*OCT4* mRNA high" contain OCT4 positive cells in histological section **(Fig. 3.44 and 3.43)**. On the other hand, in specimen classified as "*OCT4* mRNA low", OCT4 protein expressing cells are completely absent in almost all cancer samples **(3.44 and 3.43)**.

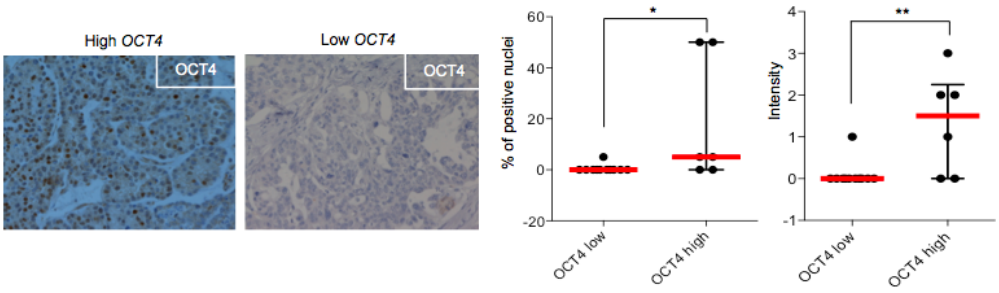

Figure 3.44. Left panel, OCT4 immunohistochemistry analysis of two representative samples (B2011.16594 and B2007.13711). Right panel, quantification of percentage of OCT4 positive cells in cancer specimen.

Western blotting also confirmed increased OCT4 protein levels in specimen categorized as "*OCT4* mRNA high" by RT-PCR and the absence in samples classified as "*OCT4* mRNA low" **(Fig. 3.45)**.

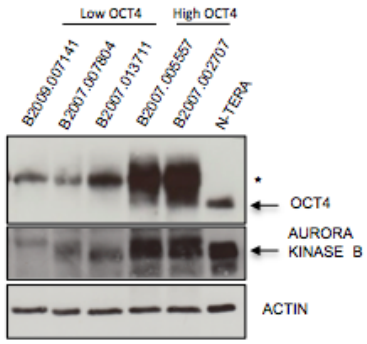

Figure 3.45. Western blotting analysis of OCT4 and Aurora B of the indicated HG-SOC patients. ACTIN was used as a loading control; *, non-specific band.

In line with data from cell line experiments we found that high *OCT4* mRNA expression is associated with high *AURKB*, *BIRC5* (Survivin) and *CDCA8* (Borealin) mRNA levels in HG-SOC specimen **(Fig. 3.46)**. Protein analysis also confirms AURKB increased expression in patients classified as "*OCT4* mRNA high" compared to patients classified as "*OCT4* mRNA low" **(Fig. 3.45)**.

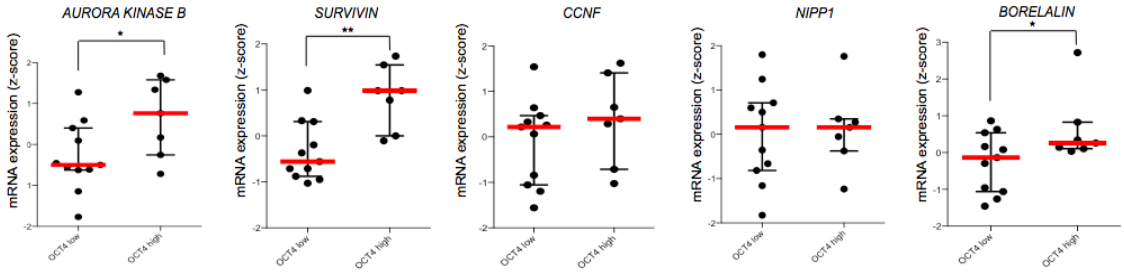

Figure 3.46. Real-time PCR analysis of *CCNF*, *NIPP1* and CPC components in HG-SOC patients in "*OCT4* mRNA high" and "*OCT4* low mRNA" expressing specimen (see Fig. 3.43**)**. A Linear regression model was used to calculate significance values: *, $p < 0.05$; **, $p < 0.01$; ***, $p < 0.001$.

To validate our *in vitro* data using OVCAR-3 cells we investigated the expression of OCT4, NIPP1, AURKB and pRB phosphorylated at position T356 by immunohistochemistry (**Fig. 3.47A**). Although we did not notice significant differences

in *NIPP1* mRNA levels in patients classified according to OCT4 levels, we found that "*OCT4* high" specimen displayed a strong increased number of NIPP1, phospho pRB-T356 and AURKB positive cells as well as increased staining intensity (**Fig. 3.47B, C and Fig. 3.42**).

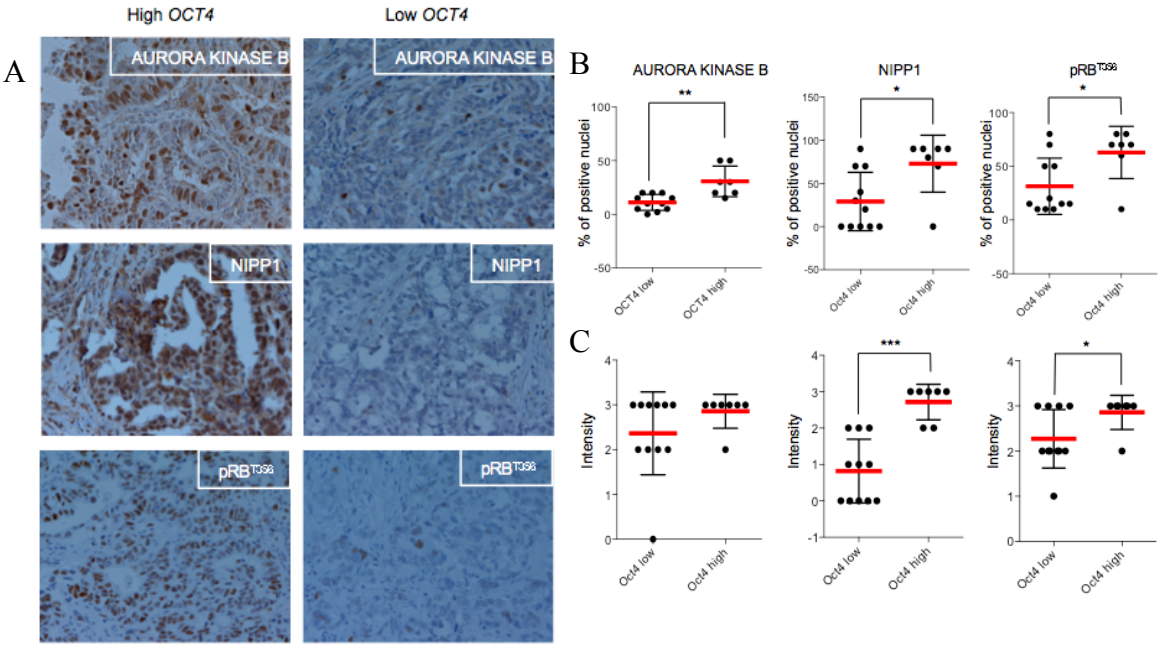

Figure 3.47. **(A)** Immunohistochemistry of HG-SOC patients specimen (analysed in A, B) for Aurora B, NIPP1 and phospho pRB-T356 protein. Samples were classified according to *OCT4* expression levels. **(B and C)** IHC on cancer specimen. Quantification of percentage of staining positive cells **(B)** and staining intensity **(C)**. Samples were classified according to *OCT4* expression levels.

Using mRNA expression data to build Kaplan-Meier survival curves we found that the "*OCT4* high" group of our cohort displays a dramatically reduced overall survival compared to "*OCT4* low" HG-SOC patients **(Fig. 3.48A and 3.42)**. Importantly, poor overall survival is worsen when high *OCT4* expression was combined with increased mRNA expression of OCT4 downstream targets *AURKB* or *CDCA8* **(Fig. 3.48B)**.

These data highlight that increased expression of the CPC components, activated by OCT4 and NIPP1/CCNF, results in an aggressive subtype of HG-SOC associated with poor survival.

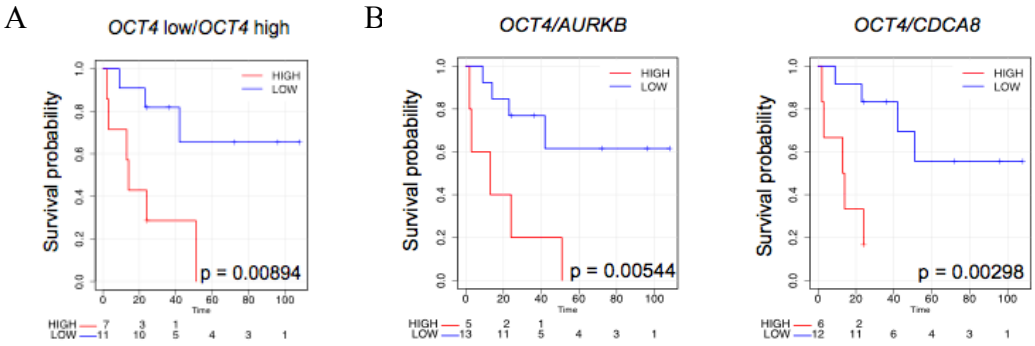

Figure 3.48. **(A)** Kaplan-Meier survival curve of HG-SOC patients according to "high" or "low" *OCT4* levels. **(B)** Kaplan-Meier survival curves of HG-SOC patients considering *OCT4* or combined *OCT4*/CPC component expression. A Log-Rank test was used to calculate significance values: *, $p < 0.05$; **, $p < 0.01$; ***, $p < 0.001$.

Finally, we decided to extend the Kaplan-Meier survival analysis on more than 850 HG-SOC samples from an ovarian cancer dataset. We confirmed poor overall survival of patients with high expression of all axis *CCNF*, *NIPP1*, *RB1* and CPC components but also when only considering the most significant genes, validated in IHC, *NIPP1*, *RB1* and *AURKB* **(Fig. 3.49A and B)**.

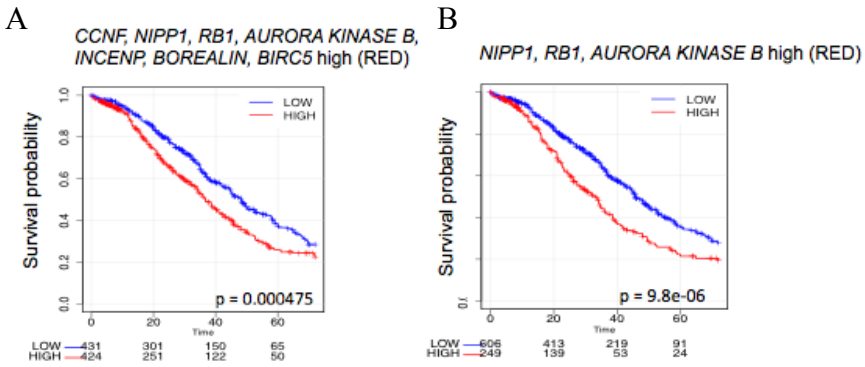

Figure 3.49. **(A)** Kaplan-Meier survival curves of overall survival (OS) of 850 high-grade serous ovarian cancer patients who were classified according to their *CCNF*, *NIPP1*, *RB1*, *AURKB*, *INCENP*, *CDCA8* and *BIRC5* expression. **(B)** Kaplan-Meier survival curve of OS of 850 high-grade serous ovarian cancer patients according to their *NIPP1*, *RB1*, *AURKB* expression. A Log-Rank test was used to calculate significance values: *, $p < 0.05$; **, $p < 0.01$; ***, $p < 0.001$.

Together our data indicate that expression of OCT4 and NIPP1/CCNF in HG-SOC

cells, leading to a functional CPC activity, dramatically increases cancer aggressiveness causing poor overall patient survival.

3.7 Final model

In this study we show that the self-renewal transcription factor OCT4 mediates accelerated proliferation and invasiveness, bypassing senescence and apoptosis. We demonstrated the activation of two pathways in HG-SOC: OCT4 drives the expression of NIPP1/CCNF that inhibit the activity of PP1 resulting in pRB hyper-phosphorylation (inactivation) and accelerated cell cycle. Inactivation of pRB pathway is found to be related to genome instability (Amato A. et al., 2009; Iovino F. et al., 2006).

In parallel, OCT4 and its downstream target genes NIPP1/CCNF mediate increased expression of CPC components, resulting in elevated Aurora B activity and impinging on chromosome segregation and centrosome clustering mechanism. This finally enhances mitotic spindle function and genome stability and therefore suppresses genomic instability caused by inactivation of tumor suppressing pathway such as the pRB pathway **(Fig. 3.50)**. In conclusion, we found that OCT4, through the axis identified, promotes cancer aggressiveness and reduced overall patient survival.

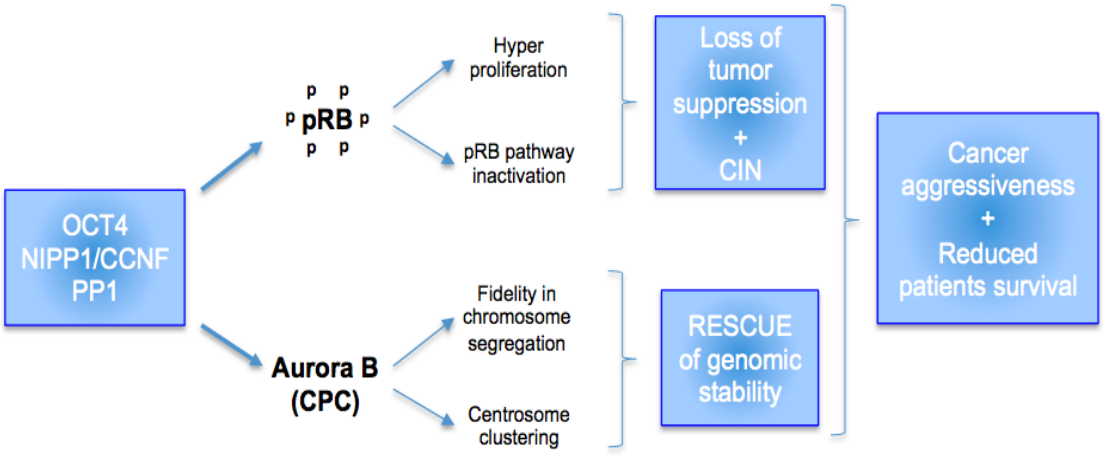

Figure 3.50. Model describing the impact of the OCT4-CCNF/NIPP1-PP1 axis on the RB pathway and mitotic stability in HG-SOC. OCT4 drives the expression of NIPP1 and CCNF causing the inhibition of PP1 and pRB hyper-phosphorylation, therefore leading to hyper-proliferation and, at the same time, CIN (chromosome instability). However, OCT4-NIPP1/CCNF promotes also the expression of the CPC components Aurora B, Borealin and Survivin to enhance mitotic stability and therefore counteract and compensate pRB driven genomic instability.

Our *in vitro* and *in vivo* data suggest that the disruption of the OCT4-NIPP1/CCNF-PP1/AURKB axis represents a promising strategy to target an aggressive subpopulation of HG-SOC cells characterized by elevated levels of OCT4 and its downstream targets NIPP1, CCNF and CPC components.

4. CONCLUSIONS AND DISCUSSION

The self-renewal transcription factor OCT4 plays a crucial role in ovarian tumorigenesis, both in tumor initiation and progression (Zhang J. et al., 2010; Samardzija C. et al., 2015). It has also been found correlated with tumor grade, disease progression, metastasis and shorter patients survival rate in different neoplasms (Zhao P.-P. et al., 2012; Zhang X. et al., 2010; Huang P. et al., 2012; Rijlaarsdam M. A. et al., 2011; Lin H. et al., 2014; Kong D. et al., 2014; Li Z. et al., 2014; Jóźwicki W. et al., 2014; He W. et al., 2012; Chen Z. et al., 2012; Karoubi G. et al., 2009; Liu T. et al., 2014; Li N. et al., 2015; Yin J. Y. et al., 2015). In addition, OCT4 promotes the tumorigenicity of cancer initiating cells, suggesting its role in the acquisition of cancer stem cell-like features (Levings P.-P- et al., 2009; Hu L. et al., 2010; Chen Y.-C. et al., 2008).

We found that ovarian cancer expresses the highest levels of OCT4 protein compared to a panel of different cancer cell line, suggesting that this cancer possess stemness features. In this context, we demonstrate that OCT4 drives the expression of NIPP1 and CCNF, both reported enzymatic inhibitor of Protein Phosphatase 1 (PP1) that targets and de-phosphorylates pRB. Consequently, OCT4 ensures pRB hyper-phosphorylation by mediating the enzymatic inhibition of PP1 in OVCAR-3 HG-SOC cells. The *in vivo* relevance of the axis was demonstrated analysing pRB phosphorylation levels from TCGA ovarian carcinoma. It was shown that elevated expression of the axis components is linked with high pRB phosphorylation levels at the PP1 target sites pRB-S807/T356 and reduced patient overall survival. This suggests a clinical relevance of the OCT4-NIPP1/CCNF-PP1-pRB axis and proposes that OCT4 has a significant contribution to the enzymatic inactivation of the pRB tumorsuppressor pathway, a phenomenon observed in 70% of HG-SOC tumors. On the contrary, only 2% of HG-SOC carries mutations in genes encoding Retinoblastoma family proteins (Bell D. et al., 2011).

In order to confirm the clinical relevance of the axis, we noticed that siRNA-mediated depletion of the axis, *OCT4* or both *CCNF* and *NIPP1*, leads to decrease cell proliferation, reduce *in vitro* cell invasion and the induction of both senescence and

apoptosis to a similar extent, suggesting a role for the activated axis in tumor aggressiveness. In addition, siRNA mediated depletion of the axis causes the appearance of severe mitotic defects, including the formation of micronuclei, multipolar spindles and supernumerary centrosomes.

There are increasing body of evidence showing that pRB not only regulates the transition from G1 to S phase of the cell cycle (Weinberg R. A., 1995) but also the chromosomal instability and aneuploidy in mitosis (Amato A. et al., 2009; Coschi C. H. et al., 2009; Hernando E. et al., 2004; Iovino F. et al., 2006; Isaac C. E. et al., 2006; Manning A. L. et al., 2010; Mayhew C. N. et al., 2007; Srinivasan S. V. et al., 2007). In fact, pRB plays a role in the regulation of mitotic protein expression, replication progression and chromatin structure (Manning A. L. et al., 2010; Coschi C. H. et al., 2010; van Harn T. et al., 2010; Schvartzman J. M. et al., 2011; Kabeche L. and Compton D. A., 2012; Bester A. C. et al., 2011). Accordingly, we expect that the OCT4-CCNF/NIPP1-PP1 activation, leading to pRB inactivation, would cause an increase of genomic instability. In contrast to this, our data show that the axis promotes the enzymatic inactivation of pRB but at the same time dramatically increases mitotic stability. This suggests that the axis activates, as an additional function, a mitotic stability pathway that suppresses genomic instability caused by the inactivation of the tumorsuppressor pRB pathway. Consequently, OCT4-expressing cancer cells can take proliferative advantage of the enzymatic inactivation of pRB in terms of hyper-proliferation, without risking mitotic defects and excessive chromosome instability. In line with this findings, a gene expression profile of OVCAR-3 cells depleted for the axis components shows that the most important commonly down-regulated genes, involved in the M phase of the cell cycle, belong to the Chromosomal Passenger Complex (CPC). Since this complex is one of the major regulators of cell division in all eukaryotes and orchestrates proper chromosome segregation by targeting to specific locations at different stages of mitosis (Carmena M. et al., 2012) as well as the "centrosome clustering mechanism" (Leber B. et al., 2010), we speculate a modulation of the CPC components mediated by the axis. In line with our hypothesis the OCT4-NIPP1/CCNF axis regulates the CPC components, Survivin, Borealin and the kinase Aurora B. In particular, the axis modulates levels, activity and localization of Aurora B, impinging on its ability to correct kinetochore-microtubule attachments errors, to activate the centrosome clustering mechanism and to complete cytokinesis. When the axis is

activated, all these events enhance the mitotic fidelity of OVCAR-3 cells, leading to increase genomic stability. Accordingly, reduced CPC function is associated with the appearance of supernumerary centrosomes, multipolar spindles and polyploidy in *OCT4* or *NIPP1/CCNF* depleted OVCAR-3 cells.

The model that emerges from our data comprises two parallel pathways: OCT4 drives the expression of NIPP1 and CCNF causing the inhibition of PP1 and pRB hyper-phosphorylation, thus leading to increase proliferation. At the same time, OCT4-NIPP1/CCNF promotes the expression of the CPC components Aurora B, Borealin and Survivin to enhance mitotic stability. The latter pathway compensates increased mitotic instability caused by enforced enzymatic inactivation of the pRB pathway in axis-active cells. Most probably the axis modulates Aurora B functions and localization through the activity of PP1. PP1 was reported to inactivate Aurora B by de-phosphorylation and also competes with Aurora B to control phosphorylation levels of histone H3-Ser10 (Sugiyama K. et al., 2002). Consequently, inhibition of PP1 by the OCT4-NIPP1/CCNF axis further enhances the regulatory strength of Aurora B during mitotic progression. Together, this highlights a central role of OCT4 in driving cell proliferation by inactivating the pRB pathway and enhancing mitotic stability by strengthen the functions of CPC components.

Finally, to direct demonstrate a role of the axis in a clinical context, we analysed HG-SOC tissue samples. We found that increased OCT4 expression was linked with increased expression of NIPP1, Aurora B, Borealin, Survivin and pRB-T356 phosphorylation levels, demonstrating the activity of the axis also in ovarian cancer patients. Importantly, the overall survival of HG-SOC patients expressing high levels of OCT4 was significantly decreased compared with those in which OCT4 was low. Poor survival of HG-SOC patients was even more exacerbated when high OCT4 expression was paired with high Aurora B or Borealin expression, thus highlighting the relevance of the OCT4-NIPP1/CCNF-PP1-pRB axis in a specific subtype of aggressive HG-SOC. Interestingly, the novel tumor promoting OCT4-NIPP1/CCNF-PP1-pRB axis classify the ovarian cancer disease in terms of overall survival independently of the histopathological classification, that nowadays continue not to be strictly related to prognosis. Remarkably, the presence of about 5% OCT4 positive cells found in IHC was sufficient to predict poor patient survival. We thus propose that OCT4 expression in HG-SOC cells is limited to a small population of cells that supports a pool of

aggressive cancer cells with stable genetic identity. Successive loss of OCT4 and the axis activity in daughter cells lead to the generation of a more differentiated cancer cells with increase mitotic defects and chromosome instability that could contribute to tumor progression and cancer cell diversity. We speculate that an activated axis could be restricted to a cancer stem cell-like cells. In line with this hypothesis, OCT4 expressing ovarian cancer cells were demonstrated to carry cancer initiating potential, high invasive ability and increased chemoresistance (Levings P. P. et al., 2009; Hu L. et al., 2010; Chen Y.-C. et al., 2008; Vathipadiekal V. et al., 2012; Zhang J. et al., 2010; Bapat S. A. et al., 2005; Rizzo S. et al., 2011; Gao M. Q. et al., 2010; Latifi A. et al., 2012). It is also interesting to note that human embryonic stem cells, which display high endogenous OCT4 level, harbour extra centrosomes (Holubcová Z. et al., 2011) that, in this view, could be clusterized through the activity of the axis via Aurora B/CPC functions, safeguarding genomic integrity. This suggests that the axis identified could activate a general mechanism to ensure genome stability.

These findings and hypothesis open the interesting possibility that disrupting the OCT4-NIPP1/CCNF-PP1-pRB axis in cancer cells in which this is active, could reduce the most stemness cells in a tumor bulk. According to the "cancer stem cell hypothesis" those cells are responsible for chemoresistance and relapse because of the inability of the classical chemotherapy to target specifically these cells. In ovarian cancer context these cells could be those that survive chemotherapy in the ascetic fluid of the patients and generate spheroids/cell aggregates leading to peritoneal dissemination and relapse in a very short period of time.

Our evidences reveal a critical OCT4-driven transcriptional program, increasing the expression of CCNF and NIPP1, that could promote ovarian cancer progression and metastasis. From these data emerge the therapeutic potential of targeting OCT4 and/or other pathways components.

Overexpression of Aurora kinases has been identified in many human cancers (Sorrentino R. et al., 2005; Vischioni B. et al., 2006; Ikezoe T. et al., 2007; Katayama H. et al., 1999), suggesting that the overexpression of Aurora kinases is strongly associated with tumorigenesis. Importantly, Aurora A, B and pan-Aurora kinase inhibitors are being developed as potential anticancer drugs and many of these agents are in phase I and II clinical trials (Falchook G. S. et al., 2015). Of notice, these drugs would only affect cells undergoing mitosis and may not have strong side effects that

antimitotic agents have. However, Aurora B inhibitors may reduce chromosome stability, suggesting the need for safety controls of these agents. Aurora kinases are found to be expressed in gynecologic malignant tumors (Li P. et al, 2008; Kurai M. et al., 2005; Chen Y. J. et al., 2009). Chemotherapy with taxanes or platinum-containing anticancer drugs currently plays key roles in the treatment of gynecologic malignant tumors. Combination of these regimens with Aurora kinase inhibitors is likely to produce synergistic effects that may increase cellular sensitivity to antimitotic drugs, enhancing drastically genomic instability that leads to cell death. In light of our findings, the ability to classify patients according to their axis expression could be also used to specifically prescribe Aurora B inhibitors, in combination with classical chemotherapy, only in those patients in which there is information of the axis activation. This would avoid worthless treatments in patients that do not display this particular expression signature.

In addition, we could also speculate to screen small compounds able to interfere with the axis proprieties. Of notice, recent discoveries pinpoint also novel small molecule inhibitors of centrosome clustering mechanism (Kawamura E. et al, 2013). Thanks to the ability of these compounds to inhibit this important mechanism, cancer cells with an activated axis are no longer able to clusterize their extra centrosomes, leading to the generation of inviable daughter cells. The final goal will be the combination of diverse compounds to limit cancer progression, dissemination and metastasis in patients allocated to a poor prognosis disease.

5. MATERIALS AND METHODS

Cell culture

All cell lines used in this study were obtained from the American Type Culture Collection (ATCC) and have not been cultured in the laboratory for longer than 6 months. OVCAR-3 cells were cultured in RPMI-1640 medium (BioWhittaker, Lonza) supplemented with 20% (v/v) Fetal Bovine Serum (FBS), insulin (10 μg/ml; I9278, Sigma) and 1% (v/v) penicillin/streptomycin (Lonza). MDA-MB-231 cell line was maintained in DMEM medium (Dulbecco's Modified Eagle's Medium, BioWhittaker, Lonza) supplemented with 10% (v/v) FBS and 1% (v/v) penicillin/streptomycin (Lonza). OVCAR-3 subclones were obtained by plating the cells at a low concentration and individual colonies were picked and allowed to grow in a 24-well plate. Cell lines were maintained as monolayers at 37 °C in a humidified 5% CO_2 atmosphere.

Tissue sample collection

Human High-Grade Serous Ovarian Cancer (HG-SOC) samples were collected by the Institute of Pathology of the University of Udine after obtaining an informed consent, in accordance with the Declaration of Helsinki, and with approval by the Independent Ethics Committee of the University-Hospital of Udine. We solely focused on cases involving primary interventions with a diagnosis of HG-SOC and excluded patients who underwent chemotherapy before surgery. The histopathologic grading of these cases was evaluated using the Malpica system (low and high grade) (Malpica A. et al., 2004). All cases were classified into stages according to the International Federation of Gynecology and Obstetrics (FIGO) staging system (stages I, II, III, and IV) (Benedet J. L. et al., 2000) and the TNM classification of malignant tumors for ovarian cancer (Edge S. B. et al., 2010). Data collection included date of diagnosis and death, and histopathological classification. Frozen ovarian cancer tissue samples (n=18) were homogenized (ULTRA-TURRAX T25, Janke & Kunkel) and processed for total RNA

extraction using TRIzol reagent (Invitrogen) and protein extraction according to standard procedures.

Transient transfection of plasmids

Transient transfections of plasmids were performed using *Trans*IT®-LT1 transfection reagent (#MIR-2300, Mirus). *OCT4*, *NIPP1* and *CCNF* genes were PCR amplified from OVCAR-3 cells cDNA oligonucleotide, cloned into pcDNA3-HA plasmid downstream of HA-epitope tag; costructs were sequence verified. Oligonucleotides:

OCT4 F: GGGAATTCGAATTCATGGCGGGACACCTGGCTTCGG;

OCT4 R: GGGAATTCTCTAGATCAGTTTGAATGCATGGGAGAG;

NIPP1 F: GGGAATTCGAATTCATGGCGGCAGCCGCGAACTCCGGC;

NIPP1 R: GGGAATTCCTCGAGTCAAATCAGCAAGGAAGGTGTGGGC;

CCNF F: GGGAATTCGAATTCATGGGGAGCGGCGGCGTGGTCCA;

CCNF R: GGGAATCCTCGAGTTACAGCCTCACAAGGCCCAGGTTC.

Transient transfection of siRNA oligos

Transient transfections of siRNAs were performed using Lipofectamine RNAiMAX reagent (Invitrogen). OVCAR-3 cell lines were transiently transfected with siRNAs targeting *OCT4* (CATCAAAGCTCTGCAGAAA, Thermo Scientific Dharmacon), *OCT4* 2 (AGGAGAAGCTGGAGCAAAA, Thermo Scientific Dharmacon), *PP1CB* (CACCAGACCTGCAATCTAT, Thermo Scientific Dharmacon) or a mix of *NIPP1* (GGACTTGACTCCTGTTGTG, Thermo Scientific Dharmacon) and *CCNF* (TCACAAAGCATCCATATTG, Thermo Scientific Dharmacon) according to the manufacturer's suggestions. Control siRNA was used as a negative control (Non-Targeting siRNA#1, TAGCGACTAAACACATCAA, Thermo Scientific Dharmacon). Total RNA and protein was prepared 72 hours after transfection unless othewise specified.

Analysis of mRNA expression

Total RNA was extracted and purified using TRIzol reagent (Invitrogen). 700 ng of

total RNA was subjected to reverse transcription using QuantiTect Reverse Transcription Kit (Promega) according to the manufacturer's suggestions. Quantitative real-time PCR was performed using the SYBR Green Master Mix (Applied Biosystem) and analysed with a StepOnePlus real-time PCR machine (Applied Biosystem) after three days of transfection, unless specified. mRNA levels were normalized against *ACTIN*. The oligos used for quantitative real-time PCR are reported below:

ACTIN F: CCAACCGCGAGAAGATGA ***ACTIN*** R: CCAGAGGCGTACAGGGATAG
OCT4A F: GGAGCCCTGCACCGTCA ***OCT4A*** R: ATGGTCGTTTGGCTGAAT
NIPP1 F: GTTTCCCGGCGTGCTTAGGG ***NIPP1*** R: AACCGGGAGGGGGCTTACCT
CCNF F: ATGAGGCCCGCGCAGAAGTG ***CCNF*** R: CTTCCGCTCACCGACCACGG
AURKB F: AAGGAGCTGCAGAAGAGCTG ***AURKB*** R: ACGGAAGCGGGGAACTTTAG
CENP-E F: CCTGTGCCAAAGGAATCACC ***CENP-E*** R: GGACCTGGCTGAGAATCCAC
CENP-A F: AGAAGCCAGCCTTTCGCTC ***CENP-A*** R: TGCTTCTGCTGCCTCTTGTAG
BIRC5 F: TGACGACCCCATAGAGGAACA ***BIRC5*** R: CGCACTTTCTCCGCAGTTTC
KIF2C F: TTCCGTGAGAGCAAGCTGAC ***KIF2C*** R: ACAGGAGCTTATGCCTGGTG
CDCA8 F: ACGTGCCTGGCGACTTCTT ***CDCA8*** R: GTTTCCTCCAAGGGCGAAG
INCENP F: CCAAGTGCAGCTTCGTCGAG ***INCENP*** R: GCTTGTCCTCCTCCACCTTC
MKI67 F: AAGAAGCAGAGGGTTGCTCC ***MKI67*** R: GTCCATCTCTGGGGAGGTCT
PCNA F*:* GTGTTGGAGGCACTCAAGGA ***PCNA*** R: TAGGTGTCGAAGCCCTCAGA
HMGB1 F: AAGTGAGAGCCGGACGGGCA ***HMGB1*** R: GGGCCTTGTCCGCTTTTGCCA
FOXM1 F: TGTGTCTGAGCGGCCACCCT ***FOXM1*** R: TGCTCGGGCAATTGTGGAGACC
NCL F: TGCGCCACTTGTCCGCTTCAC ***NCL*** R: GGTTGCAGCAGCCTTCTTGCC
SPC24 F: TGCTGGAAACGCAAGACGGT ***SPC24*** R: TCCTTGAGCTCTTCCAGCTCTC
SPC25 F: TAGAGTCCGGCTGTTGGCTA ***SPC25*** R: GTGCCAGTTCGTCCTCTACC
NDC80 F: CTTCCTGTGCCCCTCATACG ***NDC80*** R: GCTGTCGGCACCACTCATAA
NCAPG F: CGCTCTCTTCTCCCAAAGCG ***NCAPG*** R: ATCATCCATCGTGCGGTAGG

Western blotting analysis and antibodies

Western blotting analysis was performed according to standard procedures. OVCAR-3 and MDA-MB-231 lysates were prepared with ice-cold lysis buffer containing 10 mM Tris-HCl, pH 7.4, 100 mM NaCl, 1 mM PMSF, 20 mM β–glycerophosphate (Sigma-Aldrich), 1 mM Na_3VO_4, 1 mM Na_2F, 5 mM EDTA, protease inhibitor cocktail (Sigma) and 1% Triton X-100 (Sigma-Aldrich). For OCT4 detection in OVCAR-3 cell nuclear extracts were prepared as described (Ono M. et al., 2010) with minor modifications (cytoplasmic lysis buffer: 10 mM HEPES pH 7.9, 1.5 mM $MgCl_2$, 10 mM KCl, 0.5 mM DTT, 0.1 % Nonidet P-40, 1 mM PMSF, 20 mM β–glycerophosphate (Sigma-Aldrich), 1 mM Na_3VO_4, 1 mM Na_2F and protease inhibitor cocktail (Sigma); nuclear lysis buffer: 20 mM HEPES pH 7.9, 25% glycerol, 1.5 mM $MgCl_2$, 420 mM NaCl, 0.2 mM EDTA, 0.5 mM DTT, 1 mM PMSF, 20 mM β–glycerophosphate, 1 mM Na_3VO_4, 1 mM Na_2F and protease inhibitor cocktail). Primary antibodies: rabbit polyclonal anti-OCT4 (#2750, Cell Signaling), rabbit monoclonal anti-phospho RB (pT356) (ab76298, clone EPR2153AY, Abcam), mouse monoclonal anti-NIPP1 (sc-136425, Santa Cruz Biotechnology), rabbit polyclonal anti-Aurora B (ab2254, Abcam), rabbit anti-phospho H3 (Ser 28) (#07-145, Upstate), rabbit anti-phospho H3 (Ser10) (Cat# 06-570, Millipore), rabbit anti-H3 (ab1791, Abcam), mouse monoclonal Cyclin B1 (V152, #4135, Cell Signaling), mouse monoclonal anti-CDC2/p34 (CDK1) (sc-54, Santa Cruz Biotechnology), purified mouse anti-$p16^{INK4a}$ (clone G175-405, 551153, BD Pharmingen), rabbit monoclonal anti-Protein Phosphatase 1β (PP1, ab53315, EP1804Y, Abcam), mouse monoclonal anti-PARP (clone C-2-10, Cat# AM30, Calbiochem), rabbit monoclonal anti-cleaved Caspase-3 (Asp175 – 5A1, #9664, Cell Signaling) and rabbit polyclonal anti-ACTIN (A2066, Sigma). Secondary antibodies coupled to horseradish peroxidase were obtained from Sigma (anti-rabbit IgG peroxidase conjugate A-6154; anti-mouse IgG peroxidase conjugate A-4416).

Senescence-Associated β-galactosidase (SA β-gal) assay

OVCAR-3 cells were plated in 6-well dish at a concentration of 6×10^4 cell/ml and transiently transfected with the indicated siRNAs. After 72 hours cells were harvested and 6×10^4 cell/ml were transiently re-transfected with siRNAs. After 72 hours cells were rinsed twice with PBS/$MgCl_2$ and fixed in 0.5% glutaraldehyde (G6257, Sigma-

Aldrich) in PBS/$MgCl_2$ for 20 min at room temperature. Subsequently, cells were covered with staining solution (0,1 M $K_4Fe(CN)_6$, 0,1 M $K_3Fe(CN)_6$ in PBS 2 mM $MgCl_2$, pH 6); X-gal (5Br-4Cl-3-indolyl-β-D-galactopiranoside) was added to a final concentration of 1 mg/ml at 37 °C and incubated in the dark for 16 hours. When blue color was visible the cells were washed and covered with 50% glycerol/H_2O. Cells positive for *in situ* detection of SA β-galactosidase activity were counted with an optical microscope (Leica DMIL).

Soft-agar assay

10×10^4 OVCAR-3 cells were resuspended in 0.5% (w/v) top agar and plate onto 1% (w/v) basal agar. Complete medium was added on top of agarose every 3 days; when indicated, PD 0332991 was added to 0.25 μM final concentration. After 20 days, colonies were analysed for size and number using ImageJ software.

Cell proliferation analysis

OVCAR-3 cell lines were plated at a concentration of 6×10^4 per well in a 12-well dish. Cell number was counted with an optical microscope (Leica DMIL). The population doubling time was calculated from total cell numbers at day 0 and 4 and was determined using the following formula: $t\ [LN(2)/LN(C_f/C_i)]$, where t is the overall time, C_f is the final cell concentration and C_i is the starting concentration of cells.

BrdU incorporation assay

For BrdU (5-bromo-2'-deoxyuridine) incorporation assay, 6×10^4 cells/ml were plated and transiently transfected with the indicated siRNAs oligos. After 72 hours, cells were trypsinized and 6×10^4 cells/ml were plated on coverslips and transiently re-transfected with siRNAs molecules. After 72 hours, cells were pulsed with 50 μM BrdU for 1 h and fixed with paraformaldehyde. To detect incorporated BrdU, coverslips were treated with 50 mM NaOH for 30 s and washed with PBS. BrdU was revealed by anti-BrdU monoclonal antibody (GH Healthcare) followed by incubation with goat anti-mouse IgG-TRIC (Sigma). Nuclei were counterstained with DAPI (4',6-Diamidino-2-Phenylindole).

Flow cytometry

For fluorescence-activated cell sorting (FACS) analysis, cells were fixed in ethanol. After rehydration, cells were suspended in 1X PBS, 0.1% Nonidet P-40 and treated with 200 μg/ml RNase A for 10 minutes. Nuclei were stained with propidium iodide to a final concentration of 50 μg/ml. Cells were analysed on a flow cytometer (FACSCalibur, Becton Dickinson). FACS data were analysed using FlowJo software.

Spheroids formation

Spheroids were generated using a liquid overlay techniques as previously described (Desjardins M. et al., 2014). 24-well tissue culture plates were coated with 500 μl of 0.5 % agarose in complete media and allowed to solidify for 10 minutes at room temperature. OVCAR-3 cells and MDA-MB-231 cells were trypsinized and suspended in appropriate media containing 2% fetal bovine serum. Cells were plated on top of the agarose-coated wells at a volume of 1 ml/well (50000 cells/ml) and incubated at 37 °C. After 4 days spheroids were analysed using ImageJ software. For RNAi experiments, cells were transfected 2 days before plating on agar.

PD 0332991 and Okadaic Acid treatments

PD 0332991 isethionate (Sigma-Aldrich) was added to a final concentration of 0,25 μM in the medium for 3 days after cells passaging as indicated, unless specified. After the incubation period cells were trypsinized and assayed as described.

Okadaic Acid (Cat# 495604, Calbiochem) was added to a final concentration of 15 nM in the medium for 36 h and cells were assayed as described.

Immunofluorescence and confocal analysis

OVCAR-3 experimental cells were plated on coverslips in a 24-well dish and transiently transfected with the indicated siRNAs oligonucleotide. For immunofluorescence staining, cells were fixed with 4% paraformaldehyde for 10 minutes, washed with PBS, and incubated in PBS with 0.1% Triton X-100 for 5 minutes. For centrosomes analysis, methanol/acetone fixation (1:1) was used for 7

minutes at -20 °C. After washing, PBS with 5% BSA was used to block aspecific sites for 30 minutes before the addition of primary antibody against α-tubulin (DM1A, Cat# CP06, Calbiochem) and γ-tubulin (ab11316, Abcam) for 2 hours at room temperature. For MDA-MB-231 experiments, GFP was stained using α-TRITC secondary antibody because methanol/acetone fixation quenches its endogenous green fluorescence. Cells were washed twice in PBS and incubated with goat anti-mouse Alexa Fluor^{R} 488 secondary antibodies (Invitrogen) for 1 hour at room temperature. z-stack sections of each mitosis were acquired using Zeiss LSM 510 Meta confocal microscope and analysed with ImageJ software. Nuclei were counterstained with DAPI (4',6-Diamidino-2-Phenylindole) or propidium iodide (Sigma-Aldrich). For centrosomes and micronuclei analysis cells were analysed on Leica DM 4000B fluorescence microscope. Mitotic errors were analysed according to Ngan V. K. et al. classification (Ngan V. K. et al., 2001): normal mitosis consisted of bipolar metaphase spindles with completely congressed chromosomes; types I and II were bipolar spindles with one or more uncongressed chromosomes; type III were monopolar spindles with chromosomes arranged around the spindle; multipolar were mitosis with more than two spindles.

Immunofluorescence of metaphase spreads

Cells arrested in metaphase with 1 μg/ml colcemid (Karyo MAX^{R} COLCEMID^{R} Solution, gibco) for 4 h were collected by trypsinization and resuspended in 0.2% (w/v) and 0.2% (w/v) trisodium citrate hypotonic buffer at room temperature for 15 minutes. Cells are then spun onto glass slides using a centrifuge (Cytospin, Cytopro^{TM}, Wescor) at 2000 rpm for 4 minute, fixed in 4% paraformaldehyde for 10 minutes at room temperature, permeabilized in KCM buffer (120 mM KCl, 20 mM NaCl, 10 mM Tris (pH 7.5) and 0.1% Triton X-100) and processed for indirect immunofluorescence. The following primary and secondary antibodies were used: rabbit polyclonal anti-Aurora B (ab2254, Abcam), rabbit anti-phospho H3 (Ser 10) (Cat# 06-570, Millipore) and secondary antibody goat anti-rabbit Alexa Fluor^{R} 488 (Invitrogen). z-stack sections of each mitosis were acquired using Zeiss LSM 510 Meta Confocal microscope and analysed with ImageJ software. Nuclei were counterstained with propidium iodide (Sigma-Aldrich).

Immunohistochemistry

For antigen retrieval and de-paraffinization, slides were heated for 20 minutes at 98°C in Target Retrieval Solution (low pH, K8005; DAKO, Glostrup, Denmark) with PT-link (DAKO). The slides were then incubated at room temperature in hydrogen peroxide for 10 minutes to block endogenous peroxidase activity. The sections were rinsed in phosphate-buffered saline and then incubated in a wet chamber at room temperature for 1 hour with the following primary antibodies: rabbit polyclonal anti-OCT4 (ab19857, abcam), rabbit monoclonal anti-phospho RB (pT356) (ab76298, clone EPR2153AY, Abcam), mouse monoclonal anti-NIPP1 (sc-136425, Santa Cruz Biotechnology), rabbit polyclonal anti-Aurora B (ab2254, Abcam). A DAKO REAL EnVision Rabbit/Mouse (K5007) was used as a secondary antibody. Horseradish peroxidase activity was detected using DAKO REAL 3,3'-diaminobenzidine + chromogen (K5007) as substrate for 3 minutes in accordance with the manufacturer's instructions. Sections were counterstained with hematoxylin with a cover slip. Sections incubated with nonimmune rabbit serum instead of the primary antibody were used as negative controls. Semiquantitative analysis of the immunohistochemical staining was performed and the staining was semiquantitatively evaluated (percentage of positive-stained cells and intensity score evaluated as 3 = strong, 2 = moderate, and 1 = weak).

Microarray Hybridization and low level analysis

Gene expression profiling was performed using Illumina HumanHT-12-v4-BeadChips according to the manufacturer's suggestions. OVCAR-3 cells were subjected to RNAi mediated depletion of OCT4 and CCNF/NIPP1 and collected for total RNA extraction after 6 days of transfection (re-transfected after three days). The probe intensities were calculated and normalized using GenomeStudio Data Analysis Software's Gene Expression Module (GSGX) Version 1.9 (Illumina). Further data processing was performed in the R computing environment (http://www.r-project.org/) version 3.1, with BioConductor packages (http://www.bioconductor.org/). Statistical analysis for differentially expressed genes was performed with *limma* (Ritchie M. E. et al., 2015). p-values were adjusted for multiple testing using Benjamini and Hochberg's method to control the false discovery rate.

Functional analysis

Functional analysis was performed using Gene Set Enrichment Analysis (Subramanian A. et al., 2005) and the Ingenuity Pathway Analysis tool (IPA, www.ingenuity.com). Transcripts were associated with biological functions/transcriptional regulators in the Ingenuity Knowledge Base and right-tailed Fisher's exact test was used to calculate a p-value determining the probability that each biological function assigned to that data set is due to chance alone. CPC biological network was obtained using the Path Explorer Function included in IPA tool, taking into account only the experimentally confirmed findings in literature.

Survival analysis

Kaplan–Meier survival analysis was performed considering overall survival (OS) of ovarian cancer patients. Data was obtained from a cohort of 18 patients collected by the Institute of Pathology of the University of Udine. Samples were classified according to the expression of the genes and gene signatures of interest. Statistical analysis survival analysis was performed with *survival* packages in the R computing environment (http://www.r-project.org/) version 3.1. To verify the correlation of the gene signatures and ovarian cancer clinical data, survival analysis was also performed using a ovarian cancer meta-dataset composed by more than 850 samples (Györffy B. et al., 2010). The samples were split into two groups according to various quantile expressions of the proposed signatures. The two groups were then compared by a survival analysis. The Kaplan-Meier curves of relapse free survival time (OS), the hazard ratio with 95% confidence intervals and log-rank P value were calculated.

Protein phosphorylation analysis

The protein phosphorylation data were obtained from the TCGA ovarian carcinoma dataset (Provisional dataset accessed at September 2015) via cBioPortal (http://www.cbioportal.org/public-portal/index.do). In particular, using OCT4-axis genes (*NIPP1, CCNF*) as the genes of interest in the input form, we selected the proteins displaying differential phosphorylation according to the RPPA data.

Statistical analysis

Statistical analysis and graphical representation have been performed using R statistical environment. Significance of the difference between the means of the experimental conditions and control has been calculated performing a Student's t-test. P-values are shown. In bar plots, error bars represent standard deviation. Each finding was confirmed by three independent biological replicates, unless specified.

6. REFERENCES

1. Abiko K., Mandai M., Hamanishi J., Matsumura N., Baba T., Horiuchi A. et al. Oct4 expression in immature teratoma of the ovary: relevance to histologic grade and degree of differentiation. *Am. J. Surg. Pathol*. (2010), 34: 1842-1848;
2. Abubaker K., Latifi A., Luwor R., Nazaretian S., Zhu H., Quinn M. A., Thompson E. W., Findlay J. K. and Ahmed N. Short-term single treatment of chemotherapy results in the enrichment of ovarian cancer stem cell-like cells leading to an increase tumor burden. *Mol. Cancer* (2013), 12: 24;
3. Adams R. R., Maiato H., Earnshaw W. C. and Carmena M. Essential roles of *Drosophila* inner centromere protein (INCENP) and Aurora-B in histone H3 phosphorylation, metaphase chromosome alignment, kinetochore disjunction, and chromosome segregation. *J. Cell Biol.* (2001a), 153: 865–880;
4. Adams R. R., Wheatley S. P., Gouldsworthy A. M., Kandels-Lewis S. E., Carmena M., Smythe C., Gerloff D.L. and Earnshaw W. C. INCENP binds the Aurora-related kinase AIRK2 and is required to target it to chromosomes, the central spindle and cleavage furrow. *Curr. Biol*. (2000), 10: 1075–1078;
5. Adams, R. R., Eckley D. M., Vagnarelli P., Wheatley S. P., Gerloff D. L., Mackay A. M., Svingen P. A., Kaufmann S. H. and Earnshaw W. C. Human INCENP colocalizes with the Aurora-B/AIRK2 kinase on chromosomes and is overexpressed in tumour cells. *Chromosoma* (2001b), 110: 65-74;
6. Aghajanian C., Blank S. V., Goff B. A., Judson P. L., Teneriello M. G., Husain A., Sovak M. A., Yi J. and Nycum L. R. OCEANS: a randomized, double-blind, placebo-controlled phase III trial of chemotherapy with or without bevacizumab in patients with platinum-sensitive recurrent epithelial ovarian, primary peritoneal, or fallopian tube cancer. *J. Clin. Oncol.* (2012), 30: 2039-2045;
7. Aguilar-Gallardo C., Rutledge E. C., Martinez-Arroyo A. M., Hidalgo J. J., Domingo S. and Simon C. Overcoming challenges of ovarian cancer stem cells: novel therapeutic approaches. *Stem Cell Rev.* (2012), 8 (3): 994-1010;
8. Ahmed A. A., Etemadmoghadam D., Temple J., Lynch A. G., Riad M., Sharma R., Stewart C., Fereday S., Caldas C., de Fazio A., Bowtell D. and Brenton J. D. Driver mutations in TP53 are ubiquitous in high grade serous carcinoma of the ovary. *J. Pathol.* (2010), 221: 49-56;
9. Ahmed N., Abubaker K., Findlay J., Quinn M. Cancerous ovarian stem cells: obscure targets for therapy but relevant to chemoresistance. *J. Cell Biochem.* (2013), 114 (1): 21-34;
10. Ainsztein A. M., Kandels-Lewis S. E., Mackay A. M. and Earnshaw W. C. INCENP centromere and spindle targeting: identification of essential conserved motifs and involvement of heterochromatin protein HP1. *J. Cell Biol.* (1998), 143: 1763–1774;
11. Altieri D.C. Survivin, versatile modulation of cell division and apoptosis in cancer. *Oncogene* (2003), 22: 8581-8589;
12. Amato A., Lentini L., Schillaci T., Iovino F. and Di Leonardo A. RNAi mediated acute depletion of retinoblastoma protein (pRb) promotes aneuploidy in human primary cells via micronuclei formation. *BMC Cell Biol*. (2009), 10: 79;
13. Anderhub S. J., Krämer A. and Maier B. Centrosome amplification in tumorigenesis. *Cancer Letters* (2012), 322: 8-17;
14. Andrews P. D., Ovechkina Y., Morrice N., Wagenbach M., Duncan K., Wordeman L. and Swedlow J. R. Aurora B regulates MCAK at the mitotic centromere. *Developmental cell* (2004), 6: 253–268;
15. Armstrong D. K., Bundy B., Wenzel L., Huang H. Q., Baergen R., Lele S., Copeland L. J., Walker J. L., Burger R. A. and the Gynecological Oncology Group. Intraperitoneal cisplatin and paclitaxel in ovarian cancer. *N. Eng. J. Med.* (2006), 354: 34-43;
16. Azimzadeh J. and Bornens M. Structure and duplication of the centrosome. *J. Cell Sci.* (2007), 120: 2139-2142;
17. Bai C., Sen P., Hofmann K., Ma L., Goebl M., Harper J. W. and Elledge S. J. SKP1 connects cell cycle regulators to the ubiquitin proteolysis machinery through a novel motif, the F-box.

Cell (1996), 86 (2): 263-274;
18. Banerjee S. and Kaye S. B. New strategies in the treatment of ovarian cancer: current clinical perspectives and future potential. *Clinical Cancer Research* (2013), 19 (5): 961-968;
19. Bapat S. A., Mali A. M., Koppikar C. B. and Kurrey N. K. Stem and progenitor-like cells contribute to the aggressive behaviour of human epithelial ovarian cancer. *Cancer Res.* (2005), 65: 3025-3029;
20. Bast R. C. Jr., Hennessy B. and Mills G. B. The biology of ovarian cancer: new opportunities for translation. *Nat. Rev. Cancer* (2009), 9: 415-428;
21. Basto R., Brunk K., Vinadogrova T., Peel N., Franz A., Khodjakov A. and Raff J. W. Centrosome amplification can initiate tumorigenesis in flies. *Cell* (2008), 133, 1032-1042;
22. Bell D., Berchuck A., Birrer M. and The Cancer Genome Atlas Research Network. Integrated genomic analyses of ovarian carcinoma. *Nature* (2011), 474: 609-615;
23. Beltran A. S., Rivenbark A. G., Richardson B.T., Yuan Z., Quian H., Hunt J. P. et al. Generation of tumor-initiating cells by exogenous delivery of OCT4 transcription factor. *Breast Cancer Res.* (2011), 13: R94;
24. Benedet J. L., Bender H., Jones H., Ngan H. Y. and Pecorelli S. FIGO staging classifications and clinical practice guidelines in the management of gynecologic cancers. FIGO Committee on Gynecologic Oncology. *Int J Gynaecol Obstet*. (2000), 70: 209–62;
25. Bester A. C., Roniger M., Oren Y. S., Im M. M., Sarni D., Chaoat M., Bensimon A., Zamir G., Shewach D. S. and Kerem B. Nucleotide deficiency promotes genomic instability in early stages of cancer development. *Cell* (2011), 145: 435–446;
26. Bettencourt-Dias M. and Glover D. M. Centrosome biogenesis and function: centrosomics brings new understanding. *Nat. Rev. Mol. Cell Biol.* (2007), 8: 451-463;
27. Beullens M. and Bollen M. The protein phosphatase-1 regulator NIPP1 is also a splicing factor involved in a late step of spliceosome assembly. *J. Biol. Chem.* (2002), 277 (22): 19855-19860;
28. Beullens M., Van Eynde A., Stalmans W. and Bollen M. The isolation of novel inhibitory polypeptides of protein phosphatase 1 from bovine thymus nuclei. *J. Biol. Chem.* (1992), 267 (23): 16538-44;
29. Bischoff, J. R., Anderson L., Zhu Y., Mossie K., Ng L., Souza B., Schryver B., Flanagan P., Clairvoyant F., Ginther C., Chan C. S., Novotny M., Slamon D. J. and Plowman G. D. A homologue of Drosophila aurora kinase is oncogenic and amplified in human colorectal cancers. *EMBO J.* (1998), 17 (11): 3052-3065;
30. Bishop J. D. and Schumacher J. M. Phosphorylation of the carboxyl terminus of inner centromere protein (INCENP) by the Aurora B Kinase stimulates Aurora B kinase activity. *J. Biol. Chem.* (2002), 277, 27577–27580;
31. Bodner M., Castrillo J. L., Theill L. E., Deerinck T., Ellisman M. and Karin M. The pituary-specific transcription factor GHF-1 is a homeobox-containing protein. *Cell* (1988), 55: 505-518;
32. Bollen M. Combinatorial control of protein phosphatase-1. *Trends Biochem. Sci.* (2001), 26, 426-431;
33. Bolton, M. A., Lan W., Powers S. E., McCleland M. L., Kuang J. and Stukenberg P. T. Aurora B kinase exists in a complex with survivin and INCENP and its kinase activity is stimulated by survivin binding and phosphorylation. *Mol. Biol. Cell* (2002), 13: 3064–3077;
34. Bornens M. Centrosome composition and microtubule anchoring mechanisms. *Curr. Opin. Cell Biol.* (2002), 14: 25-34;
35. Bornens M. The centrosome in cells and organisms. *Science* (2012), 335: 422-6;
36. Boudrez A., Beullens M., Groenen P., Van Eynde A., Vulsteke V., Jagiello I., Murray M., Krainer A. R., Stalmans W. and Bollen M. NIPP1-mediated interaction of protein phosphatase-1 with CDC5L, a regulator of pre-mRNA splicing and mitotic entry. *J. Biol. Chem*. (2000), 275 (33): 25411-25417;
37. Boveri T. Zur frage der entstehung der malignen tumoren (translated "The Origin of Malignant Tumors" in 1929). *Williams and Wilkins* (1914), Baltimore, MD;
38. Buchkovich K., Duffy L. A. and Harlow E. The retinoblastoma protein is phosphorylated during specific phases of the cell cycle. *Cell* (1989), 58 (6): 1097-105;
39. Burger R. A., Brady M. F., Bookman M. A., Fleming G. F., Monk B. J. M., Huang H., Mannel R. S., Homesley H. D., Fowler J., Greer B. E., Boente M., Birrer M. J., Liang S. X. and the Gynecological Oncology Group. Incorporation of bevacizumab in the primary treatment of ovarian cancer. *N. Engl. J. Med.* (2011), 356: 2474-2483;
40. Burkhart D. L. and Sage J., Cellular mechanisms of tumor suppression by the retinoblastoma gene. *Nature reviews* (2008), 8: 671-682;

41. Burleson K. M., Boente M. P., Pambuccian S. E. and Skubitz A. P. Disaggregation and invasion of ovarian carcinoma ascites spheroids. *J. Transl. Med.* (2006), 4: 6;
42. Buys S. S., Partridge E., Black A., Johnson C. C. et al. Effects of screening on ovarian cancer mortality. *JAMA* (2011), 305: 2295-2303;
43. Callahan M. J., Crum C. P., Medeiros F., Kindelberger D. W., Elvin J. A., Garber J. E., Feltmate C. M., Berkowits R. S. and Muto M. G. Primary fallopian tube malignancies in BRCA-positive women undergoing surgery for ovarian cancer risk reduction. *J. Clin. Oncol.* (2007), 25: 3985-3990;
44. Campbell P. A., Perez-Iratxeta C., Andrade-Navarro M. A. and Rudnicki M. A. Oct4 targets regulatory nodes to modulate stem cell function. *Plos one* (2007), 6: 1-11;
45. Campisi J. and d'Adda di Fagagna F. Cellular senescence: when bad things happen to good cells. *Nat. Rev. Mol. Cell. Biol.* (2007), 8 (9): 729-740;
46. Carcangiu M. L., Radice P., Manoukian S., Spatti G., Gobbo M., Pensotti V., Crucianelli R. and Pasini B. Atypical epithelial proliferation in fallopian tubes in prophylactic salpingo-oophorectomy specimens from BRCA1 and BRCA2 germline mutation carriers. *Int. J. Gynecol. Pathol.* (2004), 23: 35-40;
47. Cardozo T. and Pagano M. The SCF ubiquitin ligase: insights into a molecular machine. *Nat. Rev. Mol. Cell. Biol.* (2004), 5 (9): 739-51;
48. Carmena M. and Earnshaw W. C. The cellular geography of aurora kinases. *Nat. Rev. Mol. Cell. Biol.* (2003), 4: 842-854;
49. Carmena M., Wheelock M., Funabiki H. and Earnshaw W. C. The chromosomal passenger complex (CPC): from easy rider to the godfather of mitosis. *Nat. Rev. Mol. Cell. Biol.* (2012), 13 (12): 789-803;
50. Carvalho A., Carmena M., Sambade C., Earnshaw W. C. and Wheatley S. P. Survivin is required for stable checkpoint activation in taxol-treated HeLa cells. *J. Cell Sci. (2003),* 116: 2987–2998;
51. Castiel A., Visochek L., Mittelman L., Dantzer F., Izraeli S. and Cohen-Armon M. A phenanthrene derived PARP inhibitor is an extra-centrosomes de-clustering agent exclusively eradicating human cancer cells. *BMC Cancer* (2011), 11: 412;
52. Chan C. S. and Botstein D. Isolation and characterization of chromosome-gain and increase-in-ploidy mutants in yeast. *Genetics* (1993), 135: 677–691;
53. Chang, J. L., Chen T. H., Wang C. F., Chiang Y. H., Huang Y. L., Wong F. H., Chou C. K., Chen C. M. Borealin/Dasra B is a cell cycle-regulated chromosomal passenger protein and its nuclear accumulation is linked to poor prognosis for human gastric cancer. *Exp. Cell Res.* (2006), 312: 962-973;
54. Chantalat, L., Skoufias D. A., Kleman J. P., Jung B., Dideberg O. and Margolis R. L. Crystal structure of human survivin reveals a bow tie-shaped dimer with two unusual alfa-helical extensions. *Mol. Cell* (2000), 6: 183–189;
55. Chen P. L., Scully P., Shew J. Y., Wang J. Y. and Lee W. H. Phosphorylation of the retinoblastoma gene product is modulated during the cell cycle and cellular differentiation. *Cell* (1989), 58 (6): 1193-1198;
56. Chen V. W., Ruiz B., Killeen J. L., Cotè T. R., Wu X. C. and Correa C. N. Pathology and classification of ovarian tumors. *Cancer* (2003), 97: 2631-2642;
57. Chen Y.-C., Hsu H.-S., Chen Y.-W., Tsai T.-H., How C.-K., Wang C.-Y. et al. Oct-4 expression maintained cancer stem-like properties in lung cancer-derived CD133-positive cells. *PLoS One* (2008), 3: e2637-e2637;
58. Chen Y.-J-, Chen C.-M., Twu N.-F., Yen M.-F., Lai C.-R., Wu H.-H., Wang P-H., Yuan C.-C. Overexpression of Aurora B is associated with poor prognosis in epithelial ovarian cancer patients. *Virchows Arch.* (2009), 455: 431-440;
59. Chen Z, Wang T, Cai L, Su C, Zhong B, Lei Y, et al. Clinicopathological significance of non-small cell lung cancer with high prevalence of Oct-4 tumor cells. *J. Exp. Clin. Cancer Res*. (2012), 31: 10;
60. Chen, J., Jin S., Tahir S. K., Zhang H., Liu X., Sarthy A. V., McGonigal T. P., Liu Z., Rosenberg S. H. and Ng S.C. Survivin enhances Aurora-B kinase activity and localizes Aurora-B in human cells. *J. Biol. Chem.* (2003), 278: 486–490;
61. Cheng L., Thomas A., Roth L. M., Zheng W., Michael H. and Karim F. W. OCT4: a novel biomarker for dysgerminoma of the ovary. *Am. J. Surg. Pathol.* (2004), 28: 1341-1346;
62. Chiroli E., Rancati G., Catusi I., Lucchini G. and Piatti S. Cdc14 inhibition by the spindle assembly checkpoint prevents unscheduled centrosome separation in budding yeast. Mol. Biol.

Cell (2009), 20: 2626-2637;
63. Cimini D., Wan X., Hirel C. B. and Salmon E. D. Aurora kinase promotes turnover of kinetochore microtubules to reduce chromosome segregation errors. *Curr. Biol.* (2006), 16: 1711–1718;
64. Clarke-Pearson D. L. Screening for ovarian cancer. *N. Engl. J. Med*. (2009), 361: 170-177;
65. Classon M. and Harlow E. The retinoblastoma tumour suppressor in development and cancer. *Nat. Rev. Cancer* (2002), 2: 910-917;
66. Cohen, P. T. W. Novel protein serine/threonine phosphatases: Variety is the spice of life. *Trends Biochem. Sci.* (1997), 22, 245- 251;
67. Connell-Crowley L., Harper J. W. and Goodrich D. W. Cyclin D1/Cdk4 regulates retinoblastoma protein-mediated cell cycle arrest by site-specific phosphorylation. *Mol. Biol. Cell.* (1997), 8 (2): 287-301;
68. Cooke C. A., Heck M. M. and Earnshaw W. C. The inner centromere protein (INCENP) antigens: movement from inner centromere to midbody during mitosis. *J. Cell Biol.* (1987), 105: 2053–2067;
69. Cooke C. A., Heck M. M. and Earnshaw W. C. The inner centromere protein (INCENP) antigens: movement from inner centromere to midbody during mitosis. *J. Cell Biol.* (1987), 105: 2053–2067;
70. Coschi C. H., Martens A. L., Ritchie K., Francis S. M., Chakrabarti S., Berube N. G. et al. Mitotic chromosome condensation mediated by the retinoblastoma protein is tumor-suppressive. *Genes Dev.* (2010), 24: 1351-63;
71. Crosio C., Fimia G. M., Loury R., Kimura M., Okano Y., Zhou H., Sen S., Allis C. D. and Sassone-Corsi P. Mitotic Phosphorylation of Histone H3: Spatio-Temporal Regulation by Mammalian Aurora Kinases. *Molecular and cellular biology* (2002), 22 (3): 874–885;
72. Curley M. D., Garrett L. A., Schorge J. O., Foster R. and Rueda B. R. Evidence for cancer stem cells contributing to the pathogenesis of ovarian cancer. Front. Biosci. (2011), 16: 368-392;
73. D'Angiolella V., Donato V., Vijayakumar S., Saraf A., Florens L., Washburn M. P., Dynlacht B. and Pagano M. SCF(Cyclin F) controls centrosome homeostasis and mitotic fidelity through CP110 degradation. *Nature* (2010), 466 (7302): 138-142;
74. D'Assoro A. B., Lingle W. L. and Salisbury J. L. Centrosome amplification and the development of cancer. *Oncogene* (2002), 21: 6146–6153;
75. Date D., Dreier M. R., Borton M. T., Bekier M. E. and Taylor W. R. Effects of phosphatase and proteasome inhibitors on Borealin phosphorylation and degradation. *J. Biochem.* (2012), 151: 361–369;
76. de Jong J. and Looijenga L. H. Stem cell marker OCT3/4 in tumor biology and germ cell tumor diagnostics: History and future. *Crit. Rev. Oncog.* (2006), 12: 171–203;
77. Dean J. L., Thangavel C., McClendon A. K., Reed C. A. and Knudsen E. S. Therapeutic CDK4/6 inhibition in breast cancer: key mechanisms of response and failure. *Oncogene* (2010), 29: 4018–4032;
78. DeCaprio J. A., Ludlow J. W., Figge J., Shew J. Y., Huang C. M., Lee W. H., Marsilio E., Paucha E. and Livingston D. M. SV40 large tumor antigen forms a specific complex with the product of the retinoblastoma susceptibility gene. *Cell* (1988), 54: 275-283;
79. DeCaprio J. A., Ludlow J. W., Lynch D., Furukawa Y., Griffin J., Piwnica-Worms H., Huang C.-M. and Livingston D. M. The product of the retinoblastoma susceptibility gene has properties of a cell cycle regulatory element. *Cell* (1989), 58 (6): 1085-95;
80. Desjardins M., Xie J., Gurler H., Muralidhar G. G., Sacks J. D., Burdette J. E. et al. Versican regulates metastasis of epithelial ovarian carcinoma cells and spheroids. *J. Ovarian Res*. (2014), 7: 70;
81. Diaz-Rodriguez E., Sotillo R., Schvartzman J.-M. and Benezra R. Hec1 overexpression hyperactivates the mitotic checkpoint and induces tumor formation in vivo. *Proc. Natl. Acad. Sci. USA* (2008), 105: 16719-16724;
82. Dick F. A. Structure-function analysis of the retinoblastoma tumor suppressor protein - is the whole a sum of its parts? *Cell Div.* (2007), 2: 26;
83. Ditchfield C., Johnson V. L., Tighe A., Ellston R., Haworth C., Johnson T., Mortlock A., Keen N. and Taylor S. S. Aurora B couples chromosome alignment with anaphase by targeting BubR1, Mad2, and Cenp-E to kinetochores. *The Journal of cell biology* (2003), 161: 267–280;
84. Doorbar J. Molecular biology of human papillomavirus infection and cervical cancer. *Clin. Sci.* (2006), 110: 525–541;
85. Doxsey S. J., Stein P., Evans L., Calarco P. D. and Kirschner M. Pericentrin, a highly conserved

centrosome protein involved in microtubule organization, *Cell* (1994), 76: 639-650;
86. Du Bois A., Reuss A., Pujade-Lauraine E., Harter P., Ray-Coquard I. and Pfisterer J. Role of surgical outcome as prognostic factor in advance epithelial ovarian cancer: a combined exploratory analysis of 3 prospectively randomized phase 3 multicenter trials: by the Arbeitsgeneinschaft Gynaekologische Onkologie Studiengruppe Ovarialkarzinom (AGO-OVAR) and the Group d'Investigateurs Nationaux Pour les Etudes des Cancers de l'Ovaire (GINECO). *Cancer* (2009), 115: 1234-1244;
87. Dyson N., Guida P., Munger K. and Harlow E. Homologous sequences in adenovirus E1A and human papillomavirus E7 proteins mediate interaction with the same set of cellular proteins. *J. Virol.* (1992), 66: 6893-6902;
88. Earnshaw W. C. and Bernat R. L. Chromosomal passengers: toward an integrated view of mitosis. *Chromosoma* (1991), 100: 139–146;
89. Easwaran H., Tsai H.-C. and Baylin S. B. Cancer Epigenetics: Tumor Heterogeneity, Plasticity of Stem-like States, and Drug Resistance. *Mol. Cell Rev.* (2014), 54: 716-727;
90. Edge S. B., Byrd D. R., Compton C. C., Fritz A. G. and Greene F. L. T. American Joint Committee on Cancer (AJCC). Cancer staging manual. 7th ed. *Springer New York* (2010), 1–648;
91. Ewen M. E., Xing Y., Lawrence J. B. and Livingston D. M. Molecular cloning, chromosomal mapping, and expression of the cDNA for p107, a retinoblastoma gene product-related proteins. *Cell* (1991), 66: 1155-1164;
92. Falchook G. S., Bastida C. C. and Kurzrock R. Aurora Kinase Inhibitors in Oncology Clinical Trials: Current State of the Progress. *Seminars in Oncology* (2015), 42 (6): 832-848;
93. Fenech M. Cytokinesis-block micronucleus cytome assay. *Nature Protocols* (2007), 2: 1084 – 1104;
94. Ferlay J., Steliarova-Foucher E., Lortet-Tieulent J., Rosso S., Coebergh J. W. W., Comber H., Forman D., Bray F. Cancer incidence and mortality paterns in Europe: Estimates for 40 countries in 2012. *European Journal of Cancer* (2013), 49: 1374-1403;
95. Ferretti C., Totta P., Fiore M., Mattiuzzo M., Schillaci T., Ricordy R., Di Leonardo A. and Degrassi F. Expression of the kinetochore protein Hec1 during the cell cycle in normal and cancer cells and its regulation by the pRb pathway. *Cell Cycle* (2010), 9: 4147-4182;
96. Fischle W., Tseng B. S., Dormann H. L., Ueberheide B. M., Garcia B. A., Shabanowitz J., et al. Regulation of HP1-chromatin binding by histone H3 methylation and phosphorylation. *Nature* (2005), 438: 1116–1122;
97. Foley E. A. and Kapoor T. M. Microtubule attachment and spindle assembly checkpoint signalling at the kinetochore. *Nat. Rev. Mol. Cell Biol.* (2013), 14, 25-37;
98. Friend S. H., Bernards R., Rogelj S., Weinberg R. A., Rapaport J. M., Albert D. M. and Dryja T. P. A human DNA segment with properties of the gene that predisposes to retinoblastoma and osteosarcoma. *Nature* (1986), 323, 643–646;
99. Fry D. W., Harvey P. J., Keller P. R., Elliott W. L., Meade M., Trachet E. et al. Specific inhibition of cyclin-dependent kinase 4/6 by PD 0332991 and associated antitumor activity in human tumor xenografts. *Mol Cancer Ther*. (2004), 3: 1427–1438;
100. Fu J. and Glover D. M. Structured illumination of the interface between centriole and peri-centriolar material. *Open Biol.* (2012), 2 (8): 120104;
101. Fukasawa K. Oncogenes and tumour suppressors take on centrosomes. *Nat. Rev. Cancer* (2007), 7, 911-924;
102. Fung T. K., Siu W. Y, Yam C. H., Lau A. and Poon R. Y. Cyclin F is degraded during G2-M by mechanisms fundamentally different from other cyclins. *J. Biol. Chem.* (2002), 277 (38): 35140-35149;
103. Fung Y. K., Murphree A. L., T'Ang A., Qian J., Hinrichs S. H. and Benedict W. F. Structural evidence for the authenticity of the human retinoblastoma gene. *Science* (1987), 236, 1657–1661;
104. Galderisi U., Cipollaro M. and Giordano A. The retinoblastoma gene is involved in multiple aspects of stem cell biology. *Oncogene* (2006), 25(38): 5250-5256;
105. Ganem N. J., Godinho S. A. and Pellman D. A mechanism linking extra centrosomes to chromosomal instability. *Nature* (2009), 460, 278-282;
106. Gao L., Yang Y., Xu H., Liu R., Li D., Hong H., Qin M. and Wang Y. MiR-335 functions as a tumor suppressor in pancreatic cancer by targeting OCT4. *Tumour Biol.* (2014), 35 (8): 8309-18;
107. Gao M.-Q., Choi Y.-P., Kang S., Youn J. H. and Cho N.-H. CD24+ cells from hierarchically organized ovarian cancer are enriched in cancer stem cells. *Oncogene* (2010), 29: 2672–2680;

108. Gao Y., Wang X., Han J., Xiao Z., Chen B., Su G. and Dai J. The novel OCT4 spliced variant OCT4B1 can generate three protein isoforms by alternative splicing into OCT4B. *J. Genet. Genomics* (2010), 37: 461–465;
109. Gao Y., Wei J., Han J., Wang X., Su G., Zhao Y., Chen B., Xiao Z., Cao J. and Dai J. The novel function of OCT4B isoform-265 in genotoxic stress. *Stem cells* (2012), 30 (4): 665-672;
110. Garcia-Cao M., Gonzalo S., Dean D. and Blasco M. A. A role for the Rb family of proteins in controlling telomere length. *Nature Genet.* (2002), 32: 415-419;
111. Gascoigne K. E. and Taylor S. S., Cancer cells display profound intra- and interline variation following prolonged exposure to antimitotic drugs. *Cancer cell* (2008), 14: 111–122;
112. Gassmann R. *et al.* Borealin: a novel chromosomal passenger required for stability of the bipolar mitotic spindle. *J. Cell Biol. (2004),* 166: 179–191;
113. Gergely F. and Basto R. Multiple centrosomes: together they stand, divided they fall. *Genes & Development* (2008), 22: 2291–2296;
114. Gidekel S., Pizov G., Bergman Y. and Pikarsky E. Oct-3/4 is a dose-dependent oncogenic fate determinant. Cancer cell (2003), 4: 361-370;
115. Glinsky G. V. "Stemness" Genomics Law Governs Clinical Behavior of Human Cancer: Implications for Decision Making in Disease Management. *J. clinic. Oncol.* (2008), 26: 2846-2853;
116. Goff B. A., Mandel L. S., Melancon C. H. and Muntz H. G. Frequency of symptoms of ovarian cancer in woman presenting to primary case clinics. *JAMA* (2004), 291: 2705-2712;
117. González- Martín A. J., Calvo E., Bover I., Rubio M. J., Arcusa A., Casado A., Ojeda B., Balañá C., Martínez E., Herrero A., Pardo B., Adrover E., Rifá J., Godes M. J., Moyano A. and Cercantes A. Randomized phase II trial of carboplatin versus paclitaxel and carboplatin in platinum-sensitive recurrent advanced ovarian carcinoma: a GEICO (Grupo Espanol de Investigacion en Cancer de Ovaio) study. *Ann. Oncol.* (2005), 16: 749-755;
118. Gonzalo S., García-Cao M., Fraga M. F., Schotta G., Peters A. H., Cotter S. E., Eguía R., Dean D. C., Esteller M., Jenuwein T. and Blasco M. A. Role of the RB1 family in stabilizing histone methylation at constitutive heterochromatin. *Nature Cell Biol.* (2005), 7: 420–428;
119. Goodrich D. W., Wang N. P., Qian Y. W., Lee E. Y. and Lee W. H. The retinoblastoma gene product regulates progression through the G1 phase of the cell cycle. *Cell* (1991), 67(2): 293-302;
120. Gregório L. K., Esteves S. L. C. and Fardilha M. Protein phosphatase 1 catalytic isoforms: specificity toward interacting proteins. *Translational Research* (2014), 164 (5): 366-391;
121. Guerrero A. A., Martinez A. C. and van Wely K. H. Merotelic attachments and non-homologous end joining are the basis of chromosomal instability. *Cell Div.* (2010), 5: 13;
122. Györffy B., Lanczky A., Eklund A. C., Denkert C., Budczies J., Li Q. et al. An online survival analysis tool to rapidly assess the effect of 22,277 genes on breast cancer prognosis using microarray data of 1,809 patients. *Breast Cancer Res Treat.* (2010), 123: 725–731;
123. Hanahan D. and Weinberg R. A. Hallmarks of cancer: the next generation. *Cell* (2011), 144 (5): 646-674;
124. Hannon G. J., Demetrick D. and Beach D. Isolation of the Rb-related p130 through its interaction with CDK2 and cyclins. *Genes Dev.* (1993), 7: 2378-2391;
125. Hansemann D. Ueber asymmetrische zelltheilung in epithelkrebsen und deren biologische bedeutung [On the asymmetrical cell division in epithelial cancers and its biological significance]. *Arch. Pathol. Anat. Physiol. Klin. Med.* (Virchow's Arch) (1890), 119: 299–326;
126. Hansemann D. Ueber Pathologische Mitosen [On pathological mitoses]. *Arch. Pathol. Anat. Physiol. Klin. Med.* (Virchow's Arch) (1891), 356-370;
127. Harbour J. W. and Dean D. C. The Rb/E2F pathway: expanding roles and emerging paradigms *Genes Dev.* (2000), 14: 2393-2409;
128. Hauf S., Cole R. W., LaTerra S., Zimmer C., Schnapp G., Walter R., Heckel A., van Meel J., Rieder C. L. and Peters J. M. The small molecule Hesperadin reveals a role for Aurora B in correcting kinetochore-microtubule attachment and in maintaining the spindle assembly checkpoint. *The Journal of cell biology* (2003), 161: 281–294;
129. Hayama S., Daigo Y., Kato T., Ishikawa N., Yamabuki T., Miyamoto M., Ito T., Tsuchiya E., Kondo S. and Nakamura Y. Activation of CDCA1-KNTC2, members of centromere protein complex, involved in pulmonary carcinogenesis. *Cancer Res.* (2006), 66: 10339-10348;
130. Hayama S., Daigo Y., Yamabuki T., Hirata D., Kato T., Miyamoto M., Ito T., Tsuchiya E., Kondo S. and Nakamura Y. Phosphorylation and activation of cell division cycle associated 8 by aurora kinase B plays a significant role in human lung carcinogenesis. *Cancer Res.* (2007), 67:

4113–4122;
131. He W., Li K., Wang F., Qin Y.-R. and Fan Q.-X. Expression of OCT4 in human esophageal squamous cell carcinoma is significantly associated with poorer prognosis. *World J. Gastroenterol.* (2012), 18: 712–9;
132. Helin K., Lees J. A., Vidal M., Dyson N., Harlow E. and Fattaey A. A cDNA encoding a pRB-binding protein with properties of the transcription factor E2F. *Cell* (1992), 70 (2): 337-50;
133. Henley S. A. and Dick F. A. The retinoblastoma family of proteins and their regulatory functions in the mammalian cell division cycle. *Cell Division* (2012), 7 (10): 1-14;
134. Hernando E., Nahlé Z., Juan G., Diaz-Rodriguez E., Alaminos M., Hemann M, et al. Rb inactivation promotes genomic instability by uncoupling cell cycle progression from mitotic control. *Nature* (2004), 430: 797–802;
135. Herr W., Sturm R. A., Clerc R. G., Corcoran L. M., Baltimore D., Sharp P. A., Ingraham H. A., Rosenfeld M. G., Finney M., Ruvkun G. and Horvitz H. R. The POU domain: a large conserved region in the mammalian pit-1, oct-1, oct-2 and Caenorhabditis elegans unc-86 gene products. *Genes Dev.* (1988), 2 (12A): 1513-1516;
136. Herrera R. E., Sah V. P., Williams B. O., Makela T. P., Weinberg R. A. and Jacks T. Altered cell cycle kinetics, gene expression, and G1 restriction point regulation in Rb-deficient fibroblasts. *Mol. Cell Biol.* (1996), 16: 2402-2407;
137. Hiebert S. W., Chellappan S. P., Horowitz J. M., and Nevins J. R. The interaction of pRb with E2F inhibits the transcriptional activity of E2F. *Genes & Dev.* (1992), 6: 177-185;
138. Hirota T., Lipp J. J., Toh B. H., Peters J. M. Histone H3 serine 10 phosphorylation by Aurora B causes HP1 dissociation from heterochromatin. *Nature* (2005), 438: 1176–1180;
139. Holland A. J. and Cleveland D. W. Boveri revisited: chromosomal instability, aneuploidy and tumorigenesis. *Nat. Rev. Mol. Cell. Biol.* (2009), 10: 478–487;
140. Honda R., Korner R. and Nigg E. A. Exploring the functional interactions between Aurora B, INCENP, and survivin in mitosis. *Mol. Biol. Cell (2003),* 14: 3325–3341;
141. Holubcová Z., Matula P., Sedláčková M., Vinarský V., Doležalová D., Bárta T., Dvořák P., and Hampl A. Human embryonic stem cells suffer from centrosomal amplification. *Stem Cells* (2011), 29 (1): 46-56;
142. Hsu L.-C., Kapali M., DeLoia J. A. and Gallion H. H. Centrosome abnormalities in ovarian cancer. *Int. J. Cancer.* (2005), 113: 746–751;
143. Hu L., McArthur C. and Jaffe R. B. Ovarian cancer stem-like side-population cells are tumorigenic and chemoresistant. *Br. J. Cancer* (2010), 102: 1276-1283;
144. Hu Q. J., Dyson N. and Harlow E. The regions of the retinoblastoma protein needed for binding to adenovirus E1A and SV40 large T antigen are common sites for mutations. *EMBO J.* (1990), 9: 1147-1155;
145. Hu T., Liu S., Breiter D. R., Wang F., Tang Y. and Sun S. Octamer 4 Small Interfering RNA Results in Cancer Stem Cell–Like Cell Apoptosis. *Cancer Res* (2008), 68: 6533;
146. Huang P, Chen J, Wang L, Na Y, Kaku H, Ueki H, et al. Implications of transcriptional factor, OCT-4, in human bladder malignancy and tumor recurrence. *Med. Oncol*. (2012); 29: 829–34;
147. Huschtscha L. I. and Reddel R. R. p16INK4a and the control of cellular proliferative life span. *Carcinogenesis* (1999), 20 (6): 921–926;
148. Ikezoe T., Yang J., Nishioka C., Tasaka T., Taniguchi A., Kuwayama Y., Komatsu N., Bandobashi K., Togitani K., Koeffler H. P. and Taguchi H. A novel treatment strategy targeting Aurora kinases in acute myelogenous leukemia. *Mol. Cancer Ther*. (2007), 6: 1851–1857;
149. Indjeian V.B., Stern B.M. and Murray A.W. The centromeric protein Sgo1 is required to sense lack of tension on mitotic chromosomes. *Science* (2005), 307: 130-133;
150. Ingraham H. A., Chen R. P., Mangalam H. J., Elsholtz H. P., Flynn S. E., Lin C. R., Simmons D. M., Swanson L. and Rosenfeld M. G. A tissue-specific transcription factor containing a homeodomain specifies a pituitary phenotype. *Cell* (1988), 55: 519-529;
151. Iovino F., Lentini L., Amato A., Di Leonardo A. RB acute loss induces centrosome amplification and aneuploidy in murine primary fibroblasts. *Mol. Cancer* (2006), 5: 38;
152. Isaac C. E., Francis S. M., Martens A. L., Julian L. M., Seifried L. A., Erdmann N. et al. The retinoblastoma protein regulates pericentric heterochromatin. *Mol. Cell Biol.* (2006), 26: 3659–71;
153. Jayson G. C., Kohn E. C., Kitchener H. C. and Ledermann J. A. Ovarian cancer. *The Lancet* (2014), 384 (9951), 1376-1388;
154. Jelluma N., Brenkman A. B., van den Broek N. J., Cruijsen C. W., van Osch M. H., Lens S. M.,

Medema R. H. and Kops G. J. Mps1 phosphorylates Borealin to control Aurora B activity and chromosome alignment. *Cell* (2008), 132: 233–246;
155. Jin Q., van Eynde A., Beullens M., Roy N., Thiel G., Stalmans W. and Bollen M. The protein phosphatase-1 (PP1) regulator, nuclear inhibitor of PP1 (NIPP1), interacts with the polycomb group protein, embryonic ectoderm development (EED), and functions as a transcriptional repressor. *J. Biol. Chem.* (2003), 278 (33): 30677-30685;
156. Jones M. P. and Drapkin R. Modeling high-grade serous carcinoma: how insights into pathogenesis and genetics are driving better experimental platforms. *Front. Oncol.* (2013), 3: 217;
157. Jordan M. A., Thrower D. and Wilson L. Mechanism of Inhibition of Cell Proliferation by Vinca Alkaloids. *Cancer Res.* (1991), 51: 2212-2222;
158. Jóźwicki W., Brozyna A. A. and Siekiera J. Expression of OCT4A: the first step to the next stage of urothelial bladder cancer progression. *Int. J. Mol. Sci.* (2014), 15 (9): 16069-16082;
159. Kabeche L. and Compton D. A. Checkpoint-independent stabilization of kinetochore–microtubule attachments by Mad2 in human cells. *Curr. Biol.* (2012), 22: 638–644;
160. Kaelin W. G. Jr., Krek W., Sellers W. R., DeCaprio J. A., Ajchenbaum F., Fuchs C. S., Chittenden T., Li Y., Farnham P. J., Blanar M. A. et al. Expression cloning of a cDNA encoding a retinoblastoma-binding protein with E2F-like properties. *Cell* (1992), 70 (2): 351-64;
161. Karna P, Rida PC, Pannu V, Gupta KK, Dalton WB, Joshi H et al. A novel microtubule-modulating noscapinoid triggers apoptosis by inducing spindle multipolarity via centrosome amplification and declustering. *Cell Death Differ.* (2011), 18: 632–644;
162. Karoubi G, Gugger M, Schmid R, Dutly A. OCT4 expression in human non-small cell lung cancer: implications for therapeutic intervention. *Interact. Cardiovasc. Thorac. Surg.* (2009), 8: 393–7;
163. Katayama H., Ota T., Jisaki F., Ueda Y., Tanaka T., Odashima S., Suzuki F., Terada Y. and Tatsuka M. Mitotic kinase expression and colorectal cancer progression. *J. Natl. Cancer Inst*. (1999), 91: 1160–1162;
164. Katsumata N., Yasuda M., Takahashi F., Isonishi S., Jobo T., Aoki D., Tsuda H., Sugiyama T., Kodama S., Kimura E., Ochiai K., Noda K and the Japanese Gynecologic Oncology Group. Dose-dense paclitaxel once a week in combination with carboplatin every 3 weeks for advanced ovarian cancer: a phase 3, open-label, randomised controlled trial. *Lancet* (2009), 374 (9698): 1331-1338;
165. Kaur H., Bekier M. E. and Taylor W. R. Regulation of Borealin by phosphorylation at serine 219. *J. Cell. Biochem.* (2010), 111: 1291–1298;
166. Kawamura E., Fielding A. B., Kannan N., Balgi A., Eaves C. J., Roberge M. and Dedhar S. Identification of novel small molecule inhibitors of centrosome clustering in cancer cells. *Oncotarget* (2013), 4 (10): 1763-76;
167. Kawashima S. A., Yamagishi Y., Honda T., Ishiguro K. and Watanabe Y. Phosphorylation of H2A by Bub1 prevents chromosomal instability through localizing shugoshin. *Science* (2010), 327: 172–177;
168. Kelly A. E., Ghenoiu C., Xue J. Z., Zierhut C., Kimura H. and Funabiki H. Survivin reads phosphorylated histone H3 threonine 3 to activate the mitotic kinase Aurora B. *Science* (2010), 330: 235–239;
169. Kemler I., Screiber E., Müller M. M., Matthias P. and Schaffner W. Octamer transcription factor bind to two different sequence motif of the immunoglobulin heavy chain promoter. *EMBO J.* (1989), 8: 2001-2008;
170. Kim J. and Orkin S. H. Embryonic stem cell-specific signatures in cancer: insights into genomic regulatory networks and implications for medicine. *Genome medicine* (2011), 3: 1-8;
171. Kim J. B., Sebastiano V., Wu G., Araúzo-Bravo M. J., Sasse P-. Gentile L., Ko K., Ruau D., Ehrich M., van den Boom D., Meyer J., Hübner K., Bernemann C., Ortmeuer C., Zenke M., Fleischmann B. K., Zaehers H. and Schöler H. R. Oct4-induced pluripotency in adult neural stem cells. *Cell* (2009), 136: 411-419;
172. Kim R. j. and Nam J. S. OCT4 expression enhances features of cancer stem cells in mouse model of breast cancer. *Lab. Anim. Res.* (2011), 27: 147-152;
173. Kindelberger D. W., Lee Y., Miron A., Hirsch M. S., Feltmate C., Medeiros F., Callahan M., Garner E. O., Gordon R. W., Birch C., Berkowitz R. S., Muto M. G. and Crum C. Intraepithelial carcinoma of the fimbria and pelvic serous carcinoma: evidence for a causal relationship. *Am. J. Surg. Pathol.* (2007), 31: 161-169;
174. Kitagawa M. and Lee S. H. The chromosomal passenger complex (CPC) as a key orchestrator of

orderly mitotic exit and cytokinesis. *Front. Cell Dev. Biol.* (2015), 3: 14;
175. Klijn C., Durinck S., Stawiski E. W., Haverty P. M., Jiang Z., Liu H. et al. A comprehensive transcriptional portrait of human cancer cell lines. *Nat. Biotechnol.* (2014), 33: 306–312;
176. Knudsen E. S. and Knudsen K. E. Tailoring to RB: tumour suppressor status and therapeutic response. *Nat Rev Cancer.* (2008), 8 (9): 714–724;
177. Knudson A. G. Jr. Mutation and Cancer: Statistical Study of Retinoblastoma. *Proc. Natl. Acad. Sci. U. S. A.* (1971), 68 (4): 820-823;
178. Konecny G. E., Winterhoff B., Kolarova T., Qi J., Manivong K., Dering J. et al. Expression of p16 and retinoblastoma determines response to CDK4/6 inhibition in ovarian cancer. *Clin. Cancer Res*. (2011), 17: 1591–1602;
179. Kong D., Su G., Zha L., Xiang J., Xu W., Tang Y. and Wang Z. Coexpression of HMGA2 and Oct4 predicts an unfavourable prognosis in human gastric cancer. *Med. Oncol.* (2014), 31 (8): 130;
180. Krämer A., Maier B. and Bartek J. Centrosome clustering and chromosomal (in)stability: a matter of life and death. *Mol. Oncol.* (2011), 5 (4): 324-335;
181. Krishnan R. R., Jamry I. and Chaplin D. D. Feature mapping of the HLA class I region: localization of POU5F1 and TCF19 genes. *Genomics* (1995), 30 (1): 53-58;
182. Kurai M., Shiozawa T., Shih H. C, Miyamoto T., Feng Y. Z., Kashima H., Suzuki A. and Konishi I. Expression of Aurora kinases A and B in normal, hyperplastic, and malignant human endometrium: Aurora B as a predictor for poor prognosis in endometrial carcinoma. *Hum. Pathol.* (2005), 36: 1281-1288;
183. Kuriyama R. and Borisy G. G. Centriole cycle in Chinese hamster ovary cells as determined by whole-mount electron microscopy. *J. Cell Biol.* (1981), 91: 814– 821;
184. Kurman R. J. and Shih I.-M. The origin and pathogenesis of epithelial ovarian cancer: a proposed unifying theory. *Am. J. Surg. Pathol* (2010), 34: 433-443;
185. Kwon M., Godinho S. A., Chandhok N. S., Ganem N. J., Azioune A., Thery M. and Pellman, D. Mechanisms to suppress multipolar divisions in cancer cells with extra centrosomes. *Genes Dev.* (2008), 22, 2189-2203;
186. L'esperance S., Bachvarova M., Tetu B., Mes-Masson A. M. and Bachvarov D. Global gene expression analysis of early response to chemotherapy treatment in ovarian cancer spheroids. *BMC Genomics* (2008), 9 (1): 99;
187. Lampson M. A. and Cheeseman I. M. Sensing centromere tension: Aurora B and the regulation of kinetochore function. *Trends Cell Biol.* (2011), 21 (3): 133–140;
188. Lampson M. A., Renduchitala K., Khodjakov A. and Kapoor T. M. Correcting improper chromosome-spindle attachments during cell division. *Nature cell biology* (2004), 6: 232–237;
189. Latifi A., Abubaker K., Castrechini N., Ward A. C., Liongue C., Dobill F., Kumar J., Thompson E. W., Quinn M. A., Findlay J. K. and Ahmed N. Cisplatin treatment of primary and metastatic epithelial ovarian carcinomas generates residual cells with mesenchymal stem cell-like profile. J. *Cell Biochem.* (2011), 112: 2850–2864;
190. Latifi A., Luwor R. B., Bilandzic M., Nazaretian S., Stenvers K., Pyman J., Zhu H., Thompson E. W., Quinn M. A., Findlay J. K. and Ahmed N. Isolation and characterization of tumor cells from the ascites of ovarian cancer patients: molecular phenotype of chemoresistant ovarian tumors. *PLoS One* (2012), 7 (10): e46858;
191. Lawo S., Hasegan M., Gupta G. D. and Pelletier L. Subdiffraction imaging of centrosomes reveals higher-order organizational features of pericentriolar material. *Nat. Cell Biol.* (2012), 14 (11): 1148-1158;
192. Leber, B., Maier B., Fuchs F., Chi J., Riffel P., Anderhub S., Wagner L., Ho A. D., Salisbury J. L., Boutros M. and Krämer A. Proteins required for centrosome clustering in cancer cells. *Sci. Transl. Med.* (2010), 2: 32-38;
193. Ledermann J., Harter P., Gourley C., Friedlander M., Vergote I., Rustin G., Scott C., Meier W., Shapira-Frommer R., Safra T., Matei D., Macpherson E., Watkins C., Carmichael J. and Matulonis U. Olaparib maintenance therapy in platinum-sensitive relapsed ovarian cancer. *N. Engl. J. Med.* (2012), 366: 1382-1392;
194. Ledermann J. A., Raja F. A., Fotopoulou C., Gonzalez-Martin A., Colombo N. and Sessa C., on behalf of the ESMO Guidelines Working Group. Newly diagnosed and relapsed epithelial ovarian carcinoma: ESMO clinical practice guidelines for diagnosis, treatment and follow-up. *Annals of oncology* (2013), 24: vi24-vi32;

195. Lee W. H., Lee W. H., Bookstein R., Hong F., Young L. J., Shew J. Y. and Lee E. Y. Human retinoblastoma susceptibility gene: cloning, identification, and sequence. *Science* (1987), 235, 1394–1399;
196. Levings P. P., McGarry S. V., Currie T. P., Nickerson D. M., McClellan S., Ghivizzani S. C. et al. Expression of an exogenous human Oct-4 promoter identifies tumor-initiating cells in osteosarcoma. *Cancer Res*. (2009), 69: 5648–5655;
197. Li N., Deng W., Ma J., Wei B., Guo K., Shen W. and Luo S. Prognostic evaluation of Nanog, Oct4, Sox2, PCNA, Ki67 and E-cadherin expression in gastric cancer. *Med. Oncol.* (2015), 32 (1): 433;
198. Li P., Zhou Q., Ren L. and Xiao L. Clinical implication of the expression of Aurora B in normal endometrium and endometrial carcinoma. *J. Huazhong Univ. Sci. Technolog. Med. Sci.* (2008), 28 (3): 337-339;
199. Li Z., Li X., Li C., Su Y., Fang W., Zhong C., Ji W., Zhang Q. and Su C. Transcription factor OCT4 promotes cell cycle progression by regulating CCND1 expression in esophageal carcinoma. *Cancer Lett.* (2014), 354 (1): 77-86;
200. Liedtke S., Enczmann J., Waclawczyk S., Wernet P. and Kögler G. Oct4 and its pseudogenes confuse stem cell research. *Cell Stem Cell* (2007), 1: 364–366;
201. Liedtke S., Stephan M. and Kogler G. Oct4 expression revisited: Potential pitfalls for data misinterpretation in stem cell research. *Biol. Chem.* (2008), 389: 845–850;
202. Lin H., Sun L. H., Han W., He T. Y., Xu X. J., Cheng K., Geng C., Su L. D., Wen H., Wang X. Y. and Chen Q. L. Knockdown of OCT4 suppresses the growth and invasion of pancreatic cancer cells through inhibition of the AKT pathway. *Mol. Med. Rep.* (2014), 10 (3): 1335-1342;
203. Linn D. E., Yang X., Sun F., Xie Y., Chen H., Jiang R. et al. A role for OCT4 in tumor initiation of drug-resistant prostate cancer cells. *Genes & Cancer* (2011), 1: 908-916;
204. Liu D., Vader G., Vromans M. J. M., Lampson M. A. and Lens S. M. A. Sensing chromosome bi-orientation by spatial separation of aurora B kinase from kinetochore substrates. *Science* (2009), 323: 1350-1353;
205. Liu D., Vleugel M., Backer C. B., Hori T., Fukagawa T., Cheeseman I. M. and Lampson M. A. Regulated targeting of protein phosphatase 1 to the outer kinetochore by KNL1 opposes Aurora B kinase. *J. Cell Biol.* (2010), 188 (6): 809-820;
206. Liu T., Sun B., Zhao X., Li Y., Gu Q., Dong X. and Liu F. OCT4 expression and vasculogenic mimicry formation positively correlate with poor prognosis in human breast cancer. *Int. J. Mol. Sci.* (2014), 15 (11): 19634-19649;
207. Mahen R. and Venkitaraman A. R. Pattern formation in centrosome assembly. *Curr. Opin. Cell Biol.* (2012), 24: 14–23;
208. Malpica A., Deavers M. T., Lu K., Bodurka D. C., Atkinson E. N., Gershenson D. M. et al. Grading ovarian serous carcinoma using a two-tier system. *Am. J. Surg. Pathol*. (2004), 28: 496–504;
209. Manning A. L. and Dyson N. J. pRB, a tumor suppressor with a stabilizing presence. *Trends Cell. Biol.* (2011), 21 (8): 433-441;
210. Manning A. L. and Dyson N. J. RB: mitotic implications of a tumour suppressor. *Nat. Rev. Cancer* (2012), 12 (3): 220-226;
211. Manning A. L., Longworth M. S. and Dyson N. J. Loss of pRB causes centromere dysfunction and chromosomal instability. *Genes Dev.* (2010), 24: 1364–76;
212. Marthiens V., Piel M. and Basto R. Never tear us apart—the importance of centrosome clustering. *J. Cell Sci.* (2012), 125, 3281-3292;
213. Mayhew C. N., Carter S. L., Fox S. R., Sexton C. R., Reed C. A., Srinivasan S. V., Liu X., Wikenheiser-Brokamp K., Boivin G. P., Lee J. S. et al. RB loss abrogates cell cycle control and genome integrity to promote liver tumorigenesis. *Gastroenterology* (2007), 133: 976–984;
214. McGuire W. P., Hoskins W. J., Brady M. F., Kucera P. R., Partridge E. E., Look K. Y., Clarke-Pearson D. L. and Davidson M. Cyclophosphamide and cisplatin compared with paclitaxel and cisplatin in patients with stage III and stage IV ovarian cancer. *N. England J. Med.* (1996), 334: 1-6;
215. Medema J. P. Cancer stem cells: the challenges ahead. *Nat. Cell Biol.* (2013), 15 (4): 338-344;
216. Mennella V., Keszthelyi B., McDonald K. L., Chhun B., Kan F., Rogers G. C., Huang B. and Agard D. A. Subdiffraction-resolution fluorescence microscopy reveals a domain of the centrosome critical for pericentriolar material organization. *Nat. Cell Biol.* (2012), 14 (11): 1159-1168;
217. Meuwissen R., Linn S. C., Linnoila R. I., Zevenhoven J., Mooi W. J. and Berns A. Induction of

small cell lung cancer by somatic inactivation of both Trp53 and Rb1 in a conditional mouse model. *Cancer Cell* (2003), 4: 181–189;
218. Michaud K., Solomon D. A., Oermann E., Kim J.-S., Zhong W.-Z., Prados M. D. et al. Pharmacologic inhibition of cyclin-dependent kinases 4 and 6 arrests the growth of glioblastoma multiforme intracranial xenografts. *Cancer Res.* (2010), 70: 3228–3238;
219. Mitchison T. J. and Kirschner M. W. Properties of the kinetochore in vitro. II. Microtubule capture and ATP-dependent translocation. *J. Cell Biol.* (1985), 101: 766–777;
220. Mitra A. K., Davis D. A., Tomar S., Roy L., Gurler H., Xie J. et al. In vivo tumor growth of high-grade serous ovarian cancer cell lines. *Gynecol. Oncol.* (2015), 138: 372–377;
221. Miwa M. and Masutani M. PolyADP-ribosylation and cancer. *Cancer Sci.* (2007), 98: 1528–1535;
222. Morris E. J. and Dyson N. J. Retinoblastoma protein partners. *Adv. Cancer Res.* (2001), 82: 1-54;
223. Munakata T., Liang Y., Kim S., McGivern D. R., Huibregtse J., Nomoto A. and Lemon S. M. Hepatitis C virus induces E6AP-dependent degradation of the retinoblastoma protein. *PLoS Pathog.* (2007), 3: 1335–1347;
224. Munro S., Carr S. and La Thangue N. B. Diversity within the pRb pathway: is there a code of conduct? *Oncogene* (2012), 31: 4343-4352;
225. Negrini S., Gorgoulis V. G. and Halazonetis T. D. Genomic instability - an evolving hallmark of cancer. *Nat. Rev. Mol. Cell Biol.* (2010), 11 (3): 220-228;
226. Ngan V. K., Bellman K., Hill B. T., Wilson L. and Jordan M. A. Mechanism of mitotic block and inhibition of cell proliferation by the semisynthetic Vinca alkaloids vinorelbine and its newer derivative vinflunine. *Mol. Pharmacol.* (2001), 60: 225–232;
227. Nguyen H. G., Makitalo M., Yang D., Chinnappan D., St Hilaire C. and Ravid K. Deregulated Aurora-B induced tetraploidy promotes tumorigenesis. *FASEB J.* (2009), 23: 2741-2748;
228. Nguyen M.-H., Koinuma J., Ueda K., Ito T., Tsuchiya E., Nakamura Y. and Daigo Y. Phosphorylation and activation of cell division cycle associated 5 by mitogen-activated protein kinase play a crucial role in human lung carcinogenesis. *Cancer Res.* (2010), 70: 5337-5347;
229. Nichols J., Zevnik B., Anastassiadis K., Niwa H., Klewe-Nebenius D., Chambers I., Schöler H. and Smith A. Formation of pluripotent stem cells in the mammalian embryo depends on the POU transcription factor Oct4. *Cell* (1998), 95: 379-391;
230. Nicklas R. B. and Koch C. A. Chromosome micromanipulation. 3. Spindle fiber tension and the reorientation of mal-oriented chromosomes. *The Journal of cell biology* (1969), 43: 40–50;
231. Nicklas R. B. and Ward S. C. Elements of error correction in mitosis: microtubule capture, release, and tension. *The Journal of cell biology* (1994), 126: 1241–1253;
232. Nigg E. A. Centrosome aberrations: cause or consequence of cancer progression? *Nature Rev. Cancer* (2002), 2 (11): 815-825;
233. Nigg E. A. Origins and consequences of centrosome aberrations in human cancers. *Int. J. Cancer* (2006) 119: 2717–2723;
234. Nozawa R.-S., Nagao K., Masuda H.-T., Iwasaki O., Hirota T., Nozaki N., et al. Human POGZ modulates dissociation of HP1α from mitotic chromosome arms through Aurora B activation. *Nat. Cell Biol.* (2010), 12: 719–727;
235. Ogden A., Rida P. C. G. and Aneja R. Let's huddle to prevent a muddle: centrosome declustering as an attractive anticancer strategy. *Cell Death and Differentiation* (2012), 19: 1255–1267;
236. Okita K. and Yamanaka S. Induction of pluripotency by defined factors. *Experimental Cell Research* (2010), 316: 2565–2570;
237. Ono M., Kajitani T., Uchida H., Arase T., Oda H., Nishikawa-Uchida S. et al. OCT4 expression in human uterine myometrial stem/progenitor cells. *Hum Reprod*. (2010), 25: 2059–2067;
238. Orford K. W. and Scadden D. T. Deconstructing stem cell self-renewal: genetic insights into cell-cycle regulation. *Nat. Rev. Genet.* (2008), 9 (2): 115-128;
239. Panda D., Rathinasamy K., Santra M. K. and Wilson L. Kinetic suppression of microtubule dynamic instability by griseofulvin: implications for its possible use in the treatment of cancer. *Proc. Natl. Acad. Sci. USA* (2005), 102: 9878–9883;
240. Papmichos S. I., Kotoula V., Tarlatzis B. C., Agoratos T., Papzisis K. and Lambropoulos A. F. OCT4B1 isoform: the novel OCT4 alternative spiced variant as a putative marker of stemness. *Mol. Hum. Reprod.* (2009), 15 (5): 269-270;
241. Parmar M. K., Ledermann J. A., Colombo N. and the ICON and AGO Collaborators. Paclitaxel plus platinum-based chemotherapy versus conventional platinum-based chemotherapy in women

with relapsed ovarian cancer: the ICON4/AGO-OVAR-2.2 trials. *Lancet* (2003), 361: 2099-2106;
242. Perez-Ordonez B., Beauchemin M. and Jordan R. C. Molecular biology of squamous cell carcinoma of the head and neck. *J. Clin. Pathol.* (2006), 59: 445–453;
243. Perren T. J., Swart A. M., Pfisterer J., Ledermann J. A., Pujade-Lauraine E., Kristensen G., Carey M. S., Beale P., Cervantes A., Kurzeder C., du Bois A., Sehouli J., Kimmig R., Stähle A., Collinson F., Essapen S., Gourley C., Lortholary A., Selle F., Mirza M. R., Leminen A., Plante M., Stark D., Qian W., Parmer M. K. B., Oza A. M. and the ICON7 Investigators. A phase 3 trial of bevacizumab in ovarian cancer. *N. Eng. J. Med.* (2011), 365: 2484-2496;
244. Pfisterer J., Plante M., Vergote I., du Bois A., Hirte H., Lacave A. J., Wagner U., Stähle A., Stuart G., Kimmig R., Olbricht S., Le T., Emerich J., Kuhn W., Bentley J., Jackisch C., Lück H.-J., Rochon J., Zimmermann A. H., Eisenhauer E. and the AGO-OVAR, and the NCIC CTG, and the EORTC GCG. Gemcitabine plus carboplatin compared with carboplatin in patients with platinum-sensitive recurrent ovarian cancer: an intergroup trial of the AGO-OVAR, the NCIC CTG, and the EORTC GCG. *J. Clin. Oncol.* (2006), 24: 4699-4707;
245. Pihan G. A. Centrosome dysfunction contributes to chromosome instability, chromoanagenesis, and genome reprograming in cancer. *Front. Oncol.* (2013), 3: 277;
246. Prat J. New insights into ovarian cancer pathology. *Annals of oncology* (2012), 23: x111-x117;
247. Pujade-Lauraine E., Hilpert F., Weber B., Reuss A., Poveda A., Kristensen G., Sorio R., Vergote I., Witteveen P., Bamias A., Pereira D., Wimberger P., Oaknin A., Mirza M. R., Follana P., Bollag D., Ray-Coquard I. on behalf of the ENGOT-GCIG investigators. AURELIA: A randomized phase III trial evaluating bevacizumab (BEV) plus chemotherapy (CT) for platinum (OT)-resistant recurrent ovarian cancer (OC). *2012 Annual Meeting of the American Society of Clinical Oncology*; Chicago, IL (2012), June 1-5 LBA5002;
248. Pujade-Lauraine E., Wagner U., Aavall-Lundqvist E., Gebski V., Heywood M., Vasey P. A., Volgger B., Vergote I., Pignata S., Ferrero A., Sehouli J., Lortholary A., Kristensen G., Jackisch C., Joly F., Brown C., Le Fur N. and de Bois A. Pegylated liposomal Doxorubicin and Carboplatin compared with Paclitaxel and Carboplatin for patients with platinum-sensitive ovarian cancer in late relapse. *J. Clin. Oncol.* (2010), 28: 3323-3329;
249. Qian J., Beullens M., Lesage B. and Bollen M. Aurora B defines its own chromosomal targeting by opposing the recruitment of the phosphatase scaffold Repo-Man. *Curr. Biol.* (2013), 23: 1136–1143;
250. Qin X. Q., Chittanden T., Livingston D. M. and Kaelin W. G. Jr. Identification of a growth suppression domain within the retinoblastoma gene product. *Genes Dev.* (1992), 6: 953-964;
251. Quintyne N. J., Reing J. E., Hoffelder D. R., Gollin S. M. and Saunders W. S. Spindle multipolarity is prevented by centrosomal clustering. *Science* (2005), 307, 127-129;
252. Rebacz B., Larsen T. O., Clausen M. H., Ronnest M. H., Loffler H., Ho A. D. et al. Identification of griseofulvin as an inhibitor of centrosomal clustering in a phenotype-based screen. *Cancer Res.* (2007), 67: 6342–6350;
253. Rijlaarsdam M. A., van Herk H. A. D. M., Gillis A. J. M., Stoop H., Jenster G., Martens J. et al. Specific detection of OCT3/4 isoform A/B/B1 expression in solid (germ cell) tumours and cell lines: confirmation of OCT3/4 specificity for germ cell tumours. *Br. J. Cancer* (2011), 105: 854–63;
254. Ritchie M. E., Phipson B., Wu D., Hu Y., Law C. W., Shi W. et al. limma powers differential expression analyses for RNA-sequencing and microarray studies. *Nucleic Acids Res*. (2015), 43 (7): e47;
255. Rizzo S., Hersey J. M., Mellor P., Dai W., Santos-Silva A., Liber D. et al. Ovarian cancer stem cell-like side populations are enriched following chemotherapy and overexpress EZH2. *Mol. Cancer Ther*. (2011), 10: 325–335;
256. Roy N., Van Eynde A., Beke L., Nuytten M. and Bollen M. The transcriptional repression by NIPP1 is mediated by Polycomb group proteins. *Biochim. Biophys. Acta.* (2007), 1769 (9- 10): 541-545;
257. Ruchaud S., Carmena M. and Earnshaw W. C. Chromosomal passengers: conducting cell division. *Nature Rev. Mol. Cell. Biol.* (2007), 8: 798–812 (2007);
258. Samardzija C., Luwor R. B., Volchek M., Quinn M. A., Findlay J. K. and Ahmed N. A critical role of Oct4A in mediating metastasis and disease-free survival in a mouse model of ovarian cancer. *Molecular Cancer* (2015), 14: 152;
259. Samardzija C., Quinn M., Findlay J. K. and Ahmed N. Attributes of Oct4 in stem cell biology: perspectives on cancer stem cells of the ovary. *J. Ovarian Res.* (2012), 5 (1): 37;

260. Savatier P., Huang S., Szekely L., Wiman K. G. and Samarut J. Contrasting patterns of retinoblastoma protein expression in mouse embryonic stem cells and embryonic fibroblasts. *Oncogene* (1994), 9 (3): 809-818;
261. Schoeftner S., Scarola M., Comisso E., Schneider C. and Benetti R. An Oct4-pRb axis, controlled by MiR-335, integrates stem cell self-renewal and cell cycle control. *Stem Cells* (2013), 31 (4): 717-728;
262. Schvartzman J. M., Duijf P. H., Sotillo R., Coker C. and Benezra R. Mad2 is a critical mediator of the chromosome instability observed upon Rb and p53 pathway inhibition. *Cancer Cell* (2011), 19: 701–714;
263. Sessa F., Mapelli M., Ciferri C., Tarricone C., Areces L. B., Schneider T. R., Stukenberg P. T. and Musacchio A. Mechanism of Aurora B activation by INCENP and inhibition by hesperadin. *Mol. Cell* (2005), 18: 379–391;
264. Shan B., Zhu X., Chen P. L., Durfee T., Yang Y., Sharp D. and Lee W. H. Molecular cloning of cellular genes encoding retinoblastoma- associated proteins: identification of a gene with properties of the transcription factor E2F. *Mol. Cell. Biol.* (1992), 12 (12): 5620-31;
265. Shaw P. A., Rouzbahman M., Pizer E. S., Pintilie M. and Begley H. Candidate serous cancer precursors in fallopian tube epithelium of BRCA1/2 mutation carriers. *Mod. Pathol.* (2009), 22: 1133-1138;
266. Shield K., Ackland M. L., Ahmed N. and Rice G. E. Multicellular spheroids in ovarian cancer metastases: biology and pathology. *Gynecological Oncology* (2009), 113: 143-148;
267. Shih I. M. and Kurman R. J. Ovarian tumorigenesis: a proposed model based on morphological and molecular genetic analysis. *Am. J. Pathol* (2004), 164: 1511-1518;
268. Silkworth W. T., Nardi I. K., Scholl L. M. and Cimini D. Multipolar spindle pole coalescence is a major source of kinetochore mis-attachment and chromosome mis-segregation in cancer cells. *PLoS One* (2009), 4: e6564;
269. Sissons J., Alsam S., Jayasekera S., Kim K. S., Stins M. and Khan N. A. Acanthamoeba induces cell-cycle arrest in host cells. *J. Med. Microbiol.* (2004), 53: 711-717;
270. Sorrentino R., Libertini S., Pallante P. L., Troncone G., Palombini L., Bavetsias V., Spalletti-Cernia D., Laccetti P., Linardopoulos S., Chieffi P., Fusco A. and Portella G. Aurora B overexpression associates with the thyroid carcinoma undifferentiated phenotype and is required for thyroid carcinoma cell proliferation. *J. Clin. Endocrinol. Metab.* (2005), 90 (2): 928–935;
271. Srinivasan S. V., Mayhew C. N., Schwemberger S., Zagorski W., Knudsen E. S. RB loss promotes aberrant ploidy by deregulating levels and activity of DNA replication factors. *J. Biol. Chem.* (2007), 282: 23867–23877;
272. Stead E., White J., Faast R., Conn S., Goldstone S., Rathjen J., Dhingra U., Rathjen P., Walker D. and Dalton S. Pluripotent cell division cycles are driven by ectopic Cdk2, cyclin A/E and E2F activities. *Oncogene* (2002), 21(54): 8320-8333;
273. Stearns T., Evans L. and Kirschner M. Gamma-tubulin is a highly conserved component of the centrosome, *Cell* (1991), 65: 825-836;
274. Subramanian A., Tamayo P., Mootha V. K., Mukherjee S., Ebert B. L., Gillette M. A. et al. Gene set enrichment analysis: a knowledge-based approach for interpreting genome-wide expression profiles. *Proc. Natl. Acad. Sci. U S A.* (2005), 102: 15545–15550;
275. Sugiyama K., Sugiura K., Hara T., Sugimoto K., Shima H., Honda K. et al. Aurora-B associated protein phosphatases as negative regulators of kinase activation. *Oncogene* (2002), 21: 3103–3111;
276. Takahashi K. and Yamanaka S. Induction of pluripotent stem cells from mouse embryonic and adult fibroblast cultures by defined factors. *Cell* (2006), 126: 663-676;
277. Tamrakar, S., Rubin, E. and Ludlow J. W. Role of pRB dephosphorylation in cell cycle regulation. *Front. Biosci.* (2000), 5: D121-D137;
278. Tanaka T. U., Rachidi N., Janke C., Pereira G., Galova M., Schiebel E., Stark M. J. and Nasmyth K. Evidence that the Ipl1-Sli15 (Aurora kinase-INCENP) complex promotes chromosome bi-orientation by altering kinetochore-spindle pole connections. *Cell* (2002), 108: 317– 329;
279. Tantin D. Oct transcription factors in development and stem cells: insights and mechanisms. *Development* (2013), 140: 2857-2866;
280. Taylor S. and Peters J. M. Polo and Aurora kinases: lessons derived from chemical biology. *Curr. Opin. Cell Biol.* (2008), 20: 77-84;
281. Terada, Y., Tatsuka M., Suzuki F., Yasuda Y., Fujita S. and Otsu M. AIM-1: a mammalian midbody- associated protein required for cytokinesis. *EMBO J.* (1998), 17: 667–676;
282. Tetzlaff M. T., Bai C., Finegold M., Wilson J., Harper J. W., Mahon K. A., Elledge S. J. Cyclin

F disruption compromises placental development and affects normal cell cycle execution. *Mol Cell Biol.* (2004), 24 (6): 2487-2498;
283. Tong W. M., Yang Y. G., Cao W. H., Galendo D., Frappart L., Shen Y et al. Poly(ADP-ribose) polymerase-1 plays a role in suppressing mammary tumourigenesis in mice. *Oncogene* (2007), 26: 3857–3867;
284. Trimarchi J. M and Lees J. A., Sibling rivalry in the E2F family. *Molecular cell biology* (2002), 3: 11-18;
285. Tsai L. L., Yu C. C., Chang Y. C., Yu C. H. and Chou M. Y. Markedly increased Oct4 and Nanog expression correlates with cisplatin resistance in oral squamous cell carcinoma. J. *Oral. Pathol. Med.* (2011), 40: 621-628;
286. Tsou A. P., Yang C. W., Huang C. Y., Yu R. C., Lee Y. C., Chang C. W., Chen B. R., Chung Y. F., Fann M. J., Chi C. W., Chiu J. H. and Chou C. K. Identification of a novel cell cycle regulated gene, HURP, overexpressed in human hepatocellular carcinoma. *Oncogene* (2003), 22: 298-307;
287. Tsukahara T., Tanno Y. and Watanabe Y. Phosphorylation of the CPC by Cdk1 promotes chromosome bi-orientation. *Nature* (2010), 467: 719–723;
288. Vader G., Kauw J. J., Medema R. H. and Lens S. M. Survivin mediates targeting of the chromosomal passenger complex to the centromere and midbody. *EMBO Rep*. (2006), 7: 85–92;
289. van der Horst A. and Lens S. M. A. Cell division: control of the chromosomal passenger complex in time and space. *Chromosoma* (2014), 123: 25–42;
290. van der Waal M. S., Hengeveld R. C., van der Horst A. and Lens S. M. Cell division control by the chromosomal passenger complex. *Exp. Cell Res.* (2012), 318: 1407–1420;
291. Van Eynde A., Nuytten M., Dewerchin M., Schoonjans L., Keppens S., Beullens M., Moons L., Carmeliet P., Stalmans W. and Bollen M. The nuclear scaffold protein NIPP1 is essential for early embryonic development and cell proliferation. *Mol. Cell Biol.* (2004), 24 (13): 5863-74;
292. Van Eynde A., Wera S., Beullens M., Torrekens S., Van Leuven F., Stalmans W. and Bollen M. Molecular Cloning of NIPP-1, a Nuclear Inhibitor of Protein Phosphatase-1, Reveals Homology with Polypeptides Involved in RNA Processing. *J. Biol. Chem.* (1995), 270 (47): 28068-28074;
293. van Harn T., Foijer F., van Vugt M., Banerjee R., Yang F., Oostra A., Joenje H., te Riele H. Loss of Rb proteins causes genomic instability in the absence of mitogenic signaling. *Genes Dev.* (2010), 24: 1377–1388;
294. Vang R., Shih I.-M. and Kurman R. J. Fallopian tube precursors of ovarian low- and high-grade serous neoplasms. *Histopathology* (2013), 62: 44–58;
295. Vasey P. A., Jayson G. C., Gordon A., Gabra H., Coleman R., Atkinson R., Parkin D., Paul J., Hay A., Kaye S. B. and the Scottish Gynaecological Cancer Trials Group. Phase III randomized trial of docetaxel-carboplatin versus paclitaxel-carboplatin as first-line chemotherapy for ovarian carcinoma. *J. Natl. Cancer Inst.* (2004), 96: 1682-1691;
296. Vathipadiekal V., Saxena D., Mok S. C., Hauschka P. V., Ozbun L. and Birrer M. J. Identification of a potential ovarian cancer stem cell gene expression profile from advanced stage papillary serous ovarian cancer. *PLoS One* (2012), 7: e29079;
297. Verdecia M. A., Huang H., Dutil E., Kaiser D. A., Hunter T. and Noel J. P. Structure of the human anti-apoptotic protein survivin reveals a dimeric arrangement. *Nature Struct. Biol.* (2000), 7: 602–608;
298. Vermeulen L., de Sousa e Melo F., Richel D. J. and Medema J. P. The developing cancer stem-cell model: clinical challenges and opportunities. *Lancet Oncol* (2012), 13 (2), e83-89;
299. Verschraegen C., Lounsbury K., Howe A. and Greenblatt M. Therapeutic implications for ovarian cancer emerging from the Tumor Cancer Genome Atlas. *Transl. Cancer Res.* (2015), 4 (1): 40-59;
300. Vietri M., Bianchi M., Ludlow J., Mittnacht S. and Villa-Moruzzi, E. Direct interaction between the catalytic subunit of protein phosphatase 1 and prb. *Cancer Cell Int.* (2006), 6: 3;
301. Vischioni B., Oudejans J. J., Vos W., Rodriguez J. A. and Giaccone G. Frequent overexpression of aurora B kinase, a novel drug target, in non–small cell lung carcinoma patients *Mol. Cancer Ther.* (2006), *5:* 2905-2913;
302. Wang F. Histone H3 Thr-3 phosphorylation by Haspin positions Aurora B at centromeres in mitosis. *Science* (2010), 330: 231–235;
303. Wang X. and Dai J. Concise review: isoforms of OCT4 contribute to the confusing stem cell biology. *Stem cells* (2010), 28: 885-893;
304. Wang X. Q., Ongkeko W. M., Chen L., Yang Z. F., Lu P., Chen K. K. et al. Octamer 4 (Oct4) mediates chemotherapeutic drug resistance in liver cancer cells through a potential Oct4-AKT-

ATP-binding cassette G2 pathway. *Hepathology* (Baltimore, Md) (2010), 52: 528-539;
305. Wang X., Zhao Y., Xiao Z., Chen B., Wei Z., Wang B., Zhang J., Han J., Gao Y., Li L., Zhao W., Lin H. and Dai J. Alternative translation of OCT4 by an internal ribosome entry site and its novel function in stress response. *Stem cells* (2009), 27 (6): 1265-1275;
306. Wang Y. D., Cai N., Wu X. L., Cao H. Z., Xie L. L. and Zheng P. S. OCT4 promotes tumorigenesis and inhibits apoptosis of cervical cancer cells by miR-125b/BAK1 pathway. *Cell Death Dis.* (2013), 4: e760;
307. Weaver B.A., Silk A.D., Montagna C., Verdier-Pinard P., Cleveland D.W. Aneuploidy acts both oncogenically and as a tumor suppressor. *Cancer Cell* (2007), 11: 25-36;
308. Weinberg R. A. The retinoblastoma protein and cell cycle control. *Cell* (1995), 81: 323–330;
309. Wheatley S. P., Carvalho A., Vagnarelli P. and Earnshaw W. C. INCENP is required for proper targeting of survivin to the centromeres and the anaphase spindle during mitosis. *Curr. Biol.* (2001), 11: 886–890;
310. Wheatley S. P., Henzing A. J., Dodson H., Khaled W. and Earnshaw W. C. Aurora-B phosphorylation *in vitro* identifies a residue of survivin that is essential for its localization and binding to inner centromere protein (INCENP) *in vivo*. *J. Biol. Chem.* (2004), 279: 5655–5660;
311. White J., Stead E., Faast R., Conn S., Cartwright P. and Dalton S. Developmental activation of the Rb-E2F pathway and establishment of cell cycle-regulated cyclin-dependent kinase activity during embryonic stem cell differentiation. *Mol. Biol. Cell.* (2005), 16 (4): 2018-2027;
312. Wu Y., Liu S., Xin H., Jiang J., Younglai E., Sun S. and Wang H. Up-regulation of microRNA-145 promotes differentiation by repressing OCT4 in human endometrial adenocarcinoma cells. *Cancer* (2011), 117 (17): 3989-98;
313. Yamagishi Y., Honda T., Tanno Y. and Watanabe Y. Two histone marks establish the inner centromere and chromosome bi-orientation. *Science* (2010), 330: 239–243;
314. Yang Z., Lončarek J., Khodjakov A. and Rieder C. L. Extra centrosomes and/or chromosomes prolong mitosis in human cells. *Nat. Cell Biol*. (2008), 10, 748-751;
315. Yin J. Y., Tang Q., Zhai L. L., Zhou L. Y., Qian J., Lin J., Wen X. M., Zhou J. D., Zhang X. W. and Deng Z. Q. High expression of OCT4 is frequent and may cause undesirable treatment outcomes in patients with acute myeloid leukemia. *Tumor Biol.* (2015), 36 (12): 9711-6;
316. Zeimet A. G., Reimer D., Sopper S., Boesch M., Martowicz A., Roessler J., Wiedemair A. M., Rumpold H., Untergasser G., Concin N., Hofstetter G., Muller-Holzner E., Fiegl H., Wolf F., Pesta M. and Hatina J. Ovarian cancer stem cells. *Neoplasma* (2012), 59 (6): 747-755;
317. Zhang J., Li Y. L., Zhou C. Y., Hu Y. T. and Chen H. Z. Expression of octamer-4 in serous and mucinous ovarian carcinoma. *J. Clin. Pathol.* (2010), 63: 879-883;
318. Zhang S., Balch C., Chan M. W., Lai H. C., Matei D., Schilder J. M., Yan P. S., Huang T. H. and Nephew K. P. Identification and characterization of ovarian cancer-initiating cells from primary human tumors. *Cancer Res.* (2008), 68 (11): 4311-20;
319. Zhang X., Han B., Huang J., Zheng B., Geng Q., Aziz F. et al. Prognostic significance of OCT4 expression in adenocarcinoma of the lung. *Jpn. J. Clin. Oncol.* (2010), 40: 961–6;
320. Zhao P.-P., Liu C.-X., Xu K., Zheng S.-B., Li H.-L., Xu Y.-W., Xu A., Li B. and Huang P. Expression of OCT4 protein in bladder cancer and its clinicopathological implications. *Nan Fang Yi Ke Da Xue Xue Bao = Journal of Southern Medical University* (2012), 32: 643-646.

ACKNOWLEDGMENTS

I would like to express my appreciation to my Principal Supervisor Dr. Roberta Benetti for her guidance and time dedicated to me in all these years, permitting me to complete my PhD project.

I would like to thank also the post doc of our lab Dr. Michele Scarola for the suggestions and help during the years spent to achieve my goal.

I am grateful to my parents and my family for the persistent support, patience and understanding. Finally, my gratitude to Stefano for the encouragement, comprehension and trust placed in me every day of this long journey. Without their support this project would not have been possible.

Thank you.